L'ÉCOLE DE TECHNOLOGIE SUPÉRIEURE
UNIVERSITÉ DU QUÉBEC

THESIS SUBMITTED TO
L'ÉCOLE DE TECHNOLOGIE SUPÉRIEURE

IN PARTIAL FULFILLMENT OF THE
REQUIREMENTS FOR THE
MASTER'S DEGREE IN MECHANICAL ENGINEERING
M.Eng.

BY
JIAN-HUA CHEN

DYNAMICS AND PARAMETER IDENTIFICATION OF A TRACTOR SEMITRAILER-DRIVER CLOSED-LOOP SYSTEM USING THE SIMULATED ANNEALING OPTIMIZATION APPROACH

MONTREAL, APRIL 30 2007

THIS THESIS HAS BEEN EVALUATED

BY THE FOLLOWING BOARD OF EXAMINERS

Zhaoheng Liu, Professor, Thesis Supervisor
Département de génie mécanique à l'École de technologie supérieure

Frédéric Laville, Professor, President of the Board of Examiners
Département de génie mécanique à l'École de technologie supérieure

Jean-Pierre Kenné, Professor, Member of the Board of Examiners
Département de génie mécanique à l'École de technologie supérieure

THIS THESIS HAS BEEN PRESENTED AND DEFENDED

BEFORE A BOARD OF EXAMINERS AND PUBLIC

À L'ÉCOLE DE TECHNOLOGIE SUPÉRIEURE

DYNAMICS AND PARAMETER IDENTIFICATION OF A TRACTOR SEMITRAILER-DRIVER CLOSED-LOOP SYSTEM USING THE SIMULATED ANNEALING OPTIMIZATION APPROACH

Jianhua Chen

SOMMAIRE

L'identification des paramètres et la dynamique du système camion lourd articulé/conducteur (camion semi-remorque) est l'objectif principal de ce mémoire. Un modèle de commande en boucle fermée est établi, comprenant les trois degrés de liberté (3 DDL) du modèle dynamique latéral du camion semi-remorque et le modèle de conducteur. Le déplacement et la vitesse latéraux, les angles et les vitesses de lacet du camion semi-remorque déterminent les variables d'état du modèle dynamique latéral. Le modèle de conducteur contrôle l'angle de braquage en fonction des variables d'état et d'un temps de réaction prescrit. Les paramètres du conducteur à identifier sont les gains du vecteur d'état, qui sont définis comme vecteur optimal de commande. Comme la recherche d'un vecteur de commande optimisé ne fait pas partie de la théorie de commande classique, la méthode de *Recuit Simulé* (RS) est employée pour déterminer ce vecteur de commande. Les simulations ont été réalisées avec une perturbation initiale de positionnement latéral du camion semi-remorque à un mètre de l'objectif. Pour chacune des configurations étudiées, la méthode de *Recuit Simulé* a permis d'obtenir les vecteurs de commande optimisés. Les réponses du camion semi-remorque illustrent ses caractéristiques dynamiques qui peuvent être employées pour améliorer la conduite du véhicule lourd. Plusieurs simulations ont été réalisées pour déterminer les meilleures méthodes de conduite importants et comparer les réponses dynamiques du camion semi-remorque à différentes vitesses, charges et temps de réaction du conducteur. Certains paramètres de contrôle ont été obtenus en comparant les réponses de deux camions semi-remorque différents. Enfin, un modèle de conducteur simplifié, dérivé du modèle complexe de conducteur, est employé pour déterminer la distance de visibilité sécuritaire. Les contributions de cette recherche consistent à proposer un nouveau système de contrôle en boucle fermée pour la dynamique des véhicules articulés et à identifier les paramètres d'un modèle de conducteur par une méthode d'optimisation sous le nom de Recuit Simulé. Cette nouvelle modélisation combinée par une méthode de solution optimale efficace ouvre une voie intéressante pour caractériser et comprendre les comportements dynamiques des véhicules et l'interaction conducteur/véhicule.

Mots-Clefs: Camion lourd articulé, contrôle latéral de véhicule, contrôle optimal, recuit simulé.

DYNAMICS AND PARAMETER IDENTIFICATION OF A TRACTOR SEMITRAILER-DRIVER CLOSED-LOOP SYSTEM USING THE SIMULATED ANNEALING OPTIMIZATION APPROACH

Jianhua Chen

ABSTRACT

Identifying the dynamics and parameters for an articulated heavy vehicle/driver (tractor semi-trailer/driver) system was the main objective of this thesis. The dynamic behaviour of the vehicle system was studied by setting up a closed-loop control model of a tractor semi-trailer/driver system that included a three-degree-of-freedom (3-DOF) tractor semi-trailer lateral dynamic model and a driver steering model. The tractor semi-trailer's lateral displacement, lateral velocity, yaw velocity and yaw angle were viewed as the state vector of the 3-DOF tractor semi-trailer lateral dynamic model. It was assumed that the driver-steering control model would respond to the state vector following a time delay. The inherent driver-steering parameters to be identified were the state vector's coefficients, here defined as an optimal control vector. The Simulated Annealing (SA) method was used to search this control vector, because the problem of searching optimal control vectors does not fall under classical control theory. When step lateral displacement was introduced, optimal control simulations were performed on the tractor semi-trailer vehicle using its own optimal control vector; this was searched using the SA method. The responses of the tractor semi-trailer vehicle illustrate its dynamic characteristics: these can be used to enhance the driver's steering performance. Other simulations were also conducted in order to discover optimal steering methods and the tractor semi-trailer's dynamic responses to various velocities, various loads and various human-reaction time delays. Some crucial control parameters were obtained by comparing the responses made by two different types of tractor semi-trailer vehicles. Lastly, a preview driver model derived from the complex driver model was used to search safe preview distance.

Keywords: articulated heavy vehicles, vehicle lateral control, optimal control, simulated annealing

RÉSUMÉ

Les camions semi-remorque jouent un rôle très important dans le secteur du transport des marchandises. Afin d'améliorer la sécurité de ces véhicules qui peuplent les autoroutes, beaucoup d'études ont été réalisées au cours des dernières années pour mieux comprendre l'influence de plusieurs paramètres. Par exemple, il est pertinent de considérer l'influence de la vitesse, la charge transportée, le temps de réaction du conducteur du véhicule à une excitation ou perturbation quelconque.

Les objectifs généraux de cette recherche sont d'identifier les paramètres d'un modèle de conducteur humain et d'étudier la réponse du système conducteur/camion semi-remorque à une excitation latérale en conduite à vitesse d'autoroute. Suite à une perturbation, le rôle du conducteur est de réduire le déplacement latéral. La réponse obtenue du système pourra ensuite être comparée avec des simulations comportant différentes variations des paramètres du système, telles que;

- Une variation de la vitesse du camion semi-remorque
- Différentes masses de semi-remorques
- Différents délais de réaction du conducteur

Le comportement dynamique latéral du véhicule est étudié avec le vecteur d'états de ce dernier; les caractéristiques inhérentes du conducteur humain sont définies en tant que vecteur optimal de commande. L'objectif principal de ce mémoire est d'identifier les paramètres du modèle optimal de commande et d'étudier le comportement dynamique du véhicule conduit par le conducteur optimal.

Le mémoire est présenté en six chapitres. Au chapitre 1, l'énoncé du problème et une revue de la littérature sont présentés. La conduite du camion semi-remorque par le

conducteur peut être considérée comme un problème de commande optimale de conducteur-véhicule en boucle fermée, qui inclue un modèle dynamique latéral du véhicule et un modèle de conducteur humain.

La revue de littérature couvre les modèles dynamiques de véhicule, les modèles de conducteur, les modèles d'interaction de pneu-route, les modèles de direction de puissance, les modèles de contrôle automatique et l'évaluation de paramètres. Cependant, seuls les modèles de véhicule, les modèles de conducteur et la méthode de résolution seront étudiés.

Le chapitre 2 présente les objectifs de cette étude et la méthodologie employée pour les atteindre. Les objectifs sont énumérés ci-dessous ;

1. Caractériser les paramètres du modèle de conducteur humain optimal.
2. Simuler la réponse dynamique du système composé du véhicule articulé et du modèle de conducteur optimal.
3. Simuler les comportements dynamiques du véhicule articulé pour diverses vitesses de véhicule, diverses charges de semi-remorque et plusieurs temps de réaction du conducteur humain avec les paramètres optimaux du modèle de conducteur.
4. Étudier l'effet de la distance de visibilité sur la réponse dynamique du véhicule en utilisant un modèle de conducteur simplifié.

Pour atteindre les objectifs ci-dessus, ce travail de recherche est divisé en plusieurs étapes. Différentes méthodes de modélisation et de résolution sont adoptées pour chaque étape ;

- Modélisation de la dynamique latérale de véhicule
- Modélisation du modèle de conducteur humain
- Méthode de résolution

Le chapitre 3 décrit les détails de dérivation du modèle de commande du camion semi-remorque et du conducteur. Dans le cadre de ce travail, l'étude du comportement conducteur/camion semi-remorque considère uniquement le déplacement latéral à vitesse longitudinale constante. Le camion semi-remorque est modélisé par le modèle *bicycle à deux corps rigides* avec trois degrés de liberté; la position latérale du camion, l'angle de lacet de ce dernier et l'angle de lacet de la remorque. Les équations du mouvement on été développées en utilisant la deuxième loi de Newton. Il est important de noter que les seules forces agissant sur le modèle dynamique sont les forces générées par l'angle de glissement des pneus.

Le modèle mathématique utilisé pour simuler le conducteur et générer l'angle de braquage est celui présenté par Garrott [44]. Ce modèle de conducteur est une fonction du vecteur d'états du véhicule, du vecteur de commande et du temps de réaction du conducteur. Le vecteur de commande H est basé sur six gains à déterminer, principalement en fonction des caractéristiques du camion semi-remorque, des perturbations et de la vitesse.

La dynamique du véhicule et la réaction du modèle de conducteur sont ainsi couplés pour former un système à boucle fermée. Le modèle de conducteur utilise les variables d'état retardées d'un temps de réaction ajustable comme entrée et génère une compensation sur l'angle de braquage. Le modèle du véhicule reçoit cet angle de braquage comme entrée et calcule les nouvelles variables d'état.

Les algorithmes numériques de la simulation pour les équations dynamiques retardées et l'optimisation des paramètres de conducteur sont présentés au chapitre 4. À cause du temps de réponse variable du conducteur, la méthode de *Runge-Kutta* modifiée est utilisée pour résoudre les équations dynamiques. Un des défis de cette recherche est d'obtenir les paramètres de commande H requis pour simuler le comportement du

conducteur/véhicule. Comme la théorie de commande classique ne permet pas de déterminer ces paramètres, on introduit une *fonction de coût J* qui est construite à partir des variables d'état et d'une matrice de gains. Il s'agit maintenant de déterminer les paramètres de commande *H* qui minimisent la *fonction de coût J*. Le processus utilisé pour calculer le vecteur *H* est le suivant;

1. Définir une valeur initiale arbitraire pour le vecteur de commande *H*.
2. Calculer le vecteur d'états à l'aide de la méthode de résolution d'équations différentielles modifiée de *Runge-Kutta*.
3. Calculer la *fonction de coût J* à partir des variables d'états.
4. Utiliser la méthode de *Recuit Simulé* pour chercher la *fonction de coût* minimale, puis obtenir le vecteur de commande *H*.

La méthode de *Recuit Simulé* (Simulated Annealing) est habituellement basée sur l'utilisation aléatoire de valeurs d'entrée et du calcul d'un nouveau vecteur de commande *H*. La *fonction de coût J* est ensuite comparée avec l'ancienne *fonction de coût* enregistrée, la plus petite des deux étant gardée. Cette méthode est très efficace pour minimiser une fonction qui possède plusieurs minimums locaux. Elle est valide à la fois pour un modèle de dynamique latérale linéaire et non-linéaire. Cependant, elle requiert un nombre élevé d'itérations à cause de son entrée aléatoire. Quelques étapes de calcul on été ajoutées afin d'améliorer la méthode de *Recuit Simulé* et c'est cette version améliorée qui a été utilisée pour résoudre le vecteur de commande *H* pour les simulations. Une étude de convergence de la méthode a été effectuée à partir de paramètres physiques d'un camion semi-remorque [46]. Dès les premières itérations de la méthode améliorée de *Recuit Simulé*, la *fonction de coût* diminue très rapidement pour se stabiliser après environ 200 itérations.

L'influence des différents paramètres du système conducteur/camion semi-remorque a été étudiée au chapitre 5. Désormais, les simulations peuvent être réalisées en calculant

un nouveau vecteur de commande H pour chaque cas. La perturbation pour toutes les simulations est une position initiale à y=1m et l'objectif du conducteur est de stabiliser le camion semi-remorque à y=0 afin de minimiser le déplacement latéral. Pour fins de comparaison entre les différents paramètres, la première simulation sera considérée comme la référence avec les paramètres suivants:

- Le véhicule roule à 100 km/h
- Le temps de réponse du conducteur est de 0.2 secondes

Le critère d'évaluation de sécurité du camion semi-remorque sera la réponse en déplacement du système conducteur/véhicule en boucle fermée.

La première simulation montre une oscillation avec dépassement de l'angle de braquage des roues par le conducteur pour stabiliser le véhicule. Le déplacement latéral, quant à lui, est une très bonne réponse qui stabilise le véhicule en moins de 7 secondes, sans dépassement. La vitesse latérale du véhicule lors de la manœuvre est maximale à environ une seconde et ne dépasse pas 1m/s. Les légères oscillations de la vitesse latérale du véhicule, comparativement à la position latérale, démontrent que le conducteur est plus apte à détecter la position latérale du véhicule que sa vitesse latérale. Dans le cas du tracteur et de la semi-remorque, les angles de lacet et vitesses de lacet sont bien contrôlé.

L'influence de la vitesse longitudinale du véhicule sur la stabilité du camion semi-remorque est maintenant étudiée. Les mêmes paramètres de véhicule et temps de réponse ont été conservés, cependant deux autres vitesses longitudinales du véhicule ont été ajoutées: 80 et 100 km/h. Les vecteurs de commande H sont calculés pour ces différentes vitesses. Pour des vitesses réduites, l'angle de braquage maximal est légèrement supérieur aux vitesses élevées. En effet, à faible vitesse, la réaction du véhicule face à un angle de braquage est moins importante qu'à haute vitesse. Pour

toutes les vitesses, le déplacement latéral est équivalent, alors que la vitesse latérale est légèrement plus élevée pour les faibles vitesses. On remarque les mêmes tendances pour les angles de lacet du tracteur et de la semi-remorque. Pour les vitesses de 80 à 120 km/h, par incrément de 10 km/h, la *fonction de coût* a été calculée pour chacun des cas en régime permanent. Cette étude démontre une légère augmentation de la *fonction de coût* presque proportionnelle avec l'augmentation de la vitesse du véhicule. Ainsi, la vitesse longitudinale a un impact sur la réponse dynamique du camion semi-remorque.

La réponse du système conducteur/camion semi-remorque est maintenant étudiée pour différentes charges de semi-remorque. La charge est variée de 5 à 25 tonnes par incrément de 5. Les résultats montrent que l'angle de braquage, la vitesse latérale et les angles de lacet pour toutes les charges sont sensiblement les mêmes. Les charges simulées de la semi-remorque n'affectent donc pas la réponse dynamique du camion semi-remorque. Dans ces conditions, la *fonction de coût* a aussi été calculée pour chacun des cas en régime permanent. On remarque une légère augmentation de la *fonction de coût* proportionnellement avec l'augmentation de la charge.

La prochaine variable qui a été modifiée est le délai de réaction du conducteur. Originalement à .2 secondes, le délai est étudié de 0.2 à 1 seconde par intervalle de 0.1 seconde. L'angle de braquage en fonction du temps montre une importante augmentation du temps de stabilisation du véhicule, stabilisation qui n'est jamais complète pour les temps de réaction près d'une seconde. Le déplacement latéral témoigne de ces difficultés à stabiliser le véhicule pour les longs délais de réaction, cependant quoique l'angle de braquage soit en constante oscillation, le véhicule se stabilise avec peu de dépassement. Tel qu'observé précédemment, la *fonction de coût* augmente proportionnellement avec l'augmentation du délai de réponse du conducteur, mais d'une manière beaucoup plus importante que lors d'une augmentation de charge ou de vitesse longitudinale. Le temps de réaction du conducteur a donc un effet très prononcé sur le comportement et la stabilité du véhicule.

Deux types de camions semi-remorque ont été comparés afin d'évaluer l'impact des différences de design sur la stabilité du système.

Le chapitre 6 présente un modèle de conducteur simplifié pour évaluer la distance de visibilité sécuritaire pour le système de camion semi-remorque/conducteur. Le modèle de conducteur simplifié est obtenu en évaluant l'importance du vecteur de commande H. Le système de commande du camion semi-remorque/conducteur a été transposé dans le domaine de Laplace. Dans le domaine de Laplace, le gain K et le délai T_a sont définis. La distance L de visibilité est présentée pour évaluer le degré de sécurité du camion semi-remorque. Les mêmes conclusions qu'au chapitre 5 peuvent être tirées concernant la sécurité. En particulier quand la distance de visibilité est réduite, par exemple en cas de mauvais temps, le conducteur doit réduire la vitesse longitudinale pour conduire le véhicule de façon sécuritaire.

Les principales contributions de cette recherche sont ;

- Application de la méthode de *Recuit Simulé* (RS) améliorée pour étudier le système de commande du camion semi-remorque/conducteur.
- Étude de la réponse dynamique du système du camion semi-remorque/conducteur afin d'améliorer le comportement de conduite.
- Évaluation de l'importance des éléments de commande pour établir un modèle de conducteur simplifié et trouver la distance sécuritaire de visibilité d'un camion semi-remorque.

La prochaine étape de ce travail serait d'analyser le système du camion semi-remorque/conducteur dans le domaine de Laplace pour étudier la stabilité du véhicule. Les bénéfices de ces travaux futurs sont de permettre l'analyse théorique du système du camion semi-remorque/conducteur.

ACKNOWLEDGMENTS

I would like to thank my advisor, Dr. Zhaoheng Liu, for his invaluable guidance and excellent assistance during the course of this research. Working with him has been rewarding in many ways that include and go beyond this research project.

I am deeply grateful to all the professors who have so generously provided information and the assistance I required during my course of study and during this research project. Without their help, this work would not have been possible.

My thanks also go to the expert reviewers who took time to examine and critique the work in manuscript form.

Very special thanks go to my parents. I have been greatly influenced by them and their attitudes have always played an important role in my life.

TABLE OF CONTENTS

LIST OF TABLES

LIST OF FIGURES

NOMENCLATURE

Body 1	Tractor
Body 2	Semi-trailer
$O_1X_1Y_1$	The tractor's body-fixed coordinate system
$O_2X_2Y_2$	The semi-trailer's body-fixed coordinate system
OXY	Global reference coordinate system
Axis OX	Road straight line
δ	The tractor's steering angle
u	The tractor's constant forward velocity
ε_i	Heading angle
ϕ_1	The tractor's heading angle
ϕ_2	The semi-trailer's heading angle
y_1	The tractor's lateral deviation
y_2	The semi-trailer's lateral deviation
v_1	The tractor's lateral velocity (in $O_1X_1Y_1$)
v_2	The semi-trailer's lateral velocity (in $O_2X_2Y_2$)
r_1	The tractor's yaw velocity ($r_1 = \dot{\phi}_1$)
r_2	The semi-trailer's yaw velocity ($r_2 = \dot{\phi}_2$)
I	Unit matrix
I_{z1}	Principal yaw moment of inertia for the tractor's mass
I_{z2}	Principal yaw moment of inertia for the semi-trailer's mass
Q	Joint articulation point between tractor and semi-trailer
Q_w	Weighting matrix
a_1	Distance between the tractor's front axle and centre of mass
b_1	Distance between the tractor's rear axle and centre of mass

b_2	Distance between the semi-trailer's rear axle and centre of mass
c_1	Distance between joint point Q and the tractor's centre of mass
c_2	Distance between joint point Q and the semi-trailer's centre of mass
t	Simulation time
Tr	Time delays
M_I	Symmetric positive definite matrix
N_I	Damping matrix
K	Closed-loop gain
H	Optimal control vector
A	Mass matrix in (3.38)
B	Damping matrix in (3.38)
C	Stiffness matrix in (3.38)
D	Coefficient vector of steering angle in (3.38)
F_{Qy}	Force at articulated point
F_{f1}	Lateral force of the tractor's front wheels
F_{r1}	Lateral force of the tractor's rear wheels
F_{r2}	Lateral force of the semi-trailer's rear wheels
C_{f1}	Tire characteristics for the tractor's front tires
C_{r1}	Tire characteristics for the tractor's rear tires
C_{r2}	Tire characteristics for the semi-trailer's rear tires
α_{f1}	Side slip angle of the tractor's front tires
α_{r1}	Side slip angle of the tractor's rear tires
α_{r2}	Side slip angle of the semi-trailer's rear tires
J	Cost function
$RK2$	Second-order Runge-Kutta method
SA	Simulated annealing method

INTRODUCTION

Over the last few decades, the lateral dynamics and performance characteristics of articulated vehicle systems have been extensively studied, especially with regard to heavy-duty tractor semi-trailer vehicles, for the following reasons: firstly, tractor semi-trailer vehicles play a significant role in transportation; secondly, there have been increasing concerns on how highway safety is affected by these heavy-duty tractor semi-trailer vehicles. This thesis explores the identification of lateral dynamics and parameters for tractor semi-trailer/driver systems under conditions of straight-line driving at a constant forward speed. The study of lateral dynamics focuses on modeling the tractor semi-trailer's lateral and yaw motions; parameter identification centers around recognizing the characteristics inherent in the human driver model. From a driver/vehicle closed-loop point of view, the human operator always tries to reduce lateral displacement caused by external disturbances such as road irregularities or wind gusts, according to the vehicle's directional responses to the driver's delays in perception and reaction. Lateral dynamic responses are here defined as the vehicle's state vector: this consists of displacements and velocities. The inherent characteristics of human drivers are defined as parameters involving an optimal control model. The main goals of this thesis are to identify parameter vectors in an optimal control model and to study the dynamic behaviour of the vehicle system as driven by a predetermined optimal driver. Multi-body vehicle system equations are developed using Newton's second law; interaction between the vehicle and the road surface is modeled using a linear tire model for its lateral dynamics. A closed-loop system is achieved by combining the vehicle model and an optimal driver model with unknown parameter values. To identify the characteristics of these driver parameters, a numerical algorithm is used for searching optimal parameters while minimizing cost function. To illustrate the behaviour of the driver-vehicle system, simulations are performed using optimal control vectors under various steering conditions. In addition, a preview driver model is deduced from the

optimal driver model in order to demonstrate the importance of visibility distance for safe driving under a variety of driving conditions.

The chapters are organized as follows: Chapter 1 states the problem and reviews the literature. Chapter 2 defines this study's goals and the methodology used to achieve them. Chapter 3 describes details on how to derive the tractor semi-trailer/driver control model. The numerical algorithms used for simulating delayed dynamic equations and an optimization method for determining optimal driver parameters are presented in Chapter 4. Chapter 5 demonstrates simulation results under various driving conditions. Chapter 6 introduces a preview driver model for evaluating safe visibility distance for the tractor semi-trailer/driver system. The Conclusion summarizes this project's main contributions and makes recommendations for further study.

CHAPTER 1

STATEMENT OF THE PROBLEM AND LITERATURE REVIEW

1.1 Statement of the problem

A tractor semi-trailer is a typical heavy articulated vehicle that plays a very important role in today's long-distance highway transportation. When a tractor semi-trailer is driven following a straight line at a constant forward speed, certain undefined lateral disturbances, such as wind gusts, may cause the tractor semi-trailer to stray from its straightforward direction. In such a case, the driver must guide his tractor semi-trailer back to its previous course as soon as possible by adjusting the steering wheel. The process of driving may be considered as a closed-loop driver-vehicle optimal control problem including the lateral dynamic vehicle model and the human driver model. Figure 1 demonstrates a closed-loop optimal control model, where the vehicle's input is the steering angle and the output is the tractor semi-trailer's states (displacement, speed and acceleration).

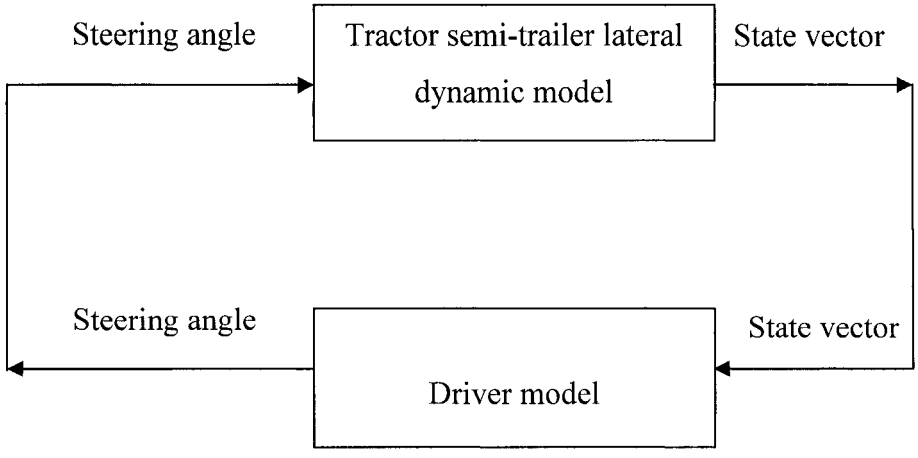

Figure 1 A closed-loop driver-vehicle model

Optimal control of the tractor semi-trailer is determined not only by various tractor semi-trailer designs and operating factors, but also by the driver's interactions with the tractor semi-trailer. These interactions reveal how the driver's behaviour and the responses of the tractor semi-trailer affect one another. An excellent driver can adapt to a tractor semi-trailer and improve his performance rapidly. The behaviour of an excellent driver may be characterized as a set of inherent parameters. Thus, Figure 1's closed-loop driver-vehicle optimal control model can be expressed by a driver-parameter input model, as shown in Figure 2.

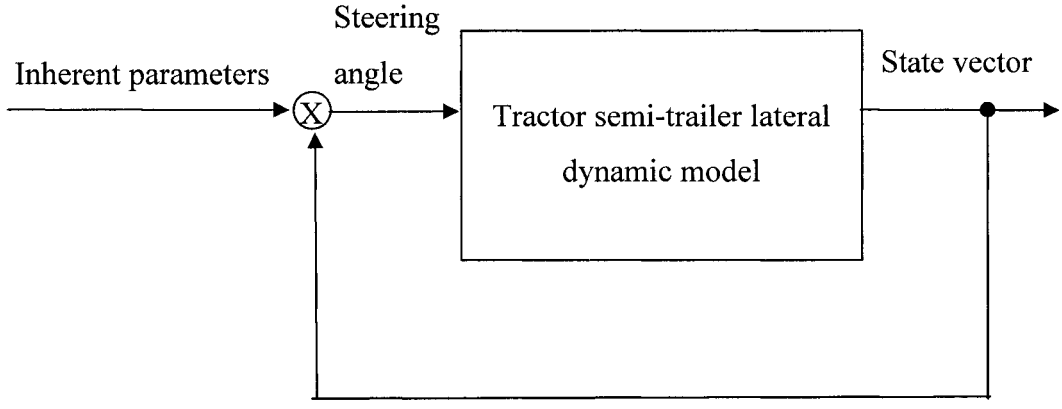

Figure 2 Driver-parameter input model

In this research project, focus has been placed on identifying lateral dynamics and parameters for a tractor semi-trailer/driver system. As shown in Figure 2, this problem does not fall under the classical framework of linear quadratic optimal control theory, because the input parameters are unknown and require identification. The Simulated Annealing algorithm is employed to search input parameters while minimizing cost function. This is achieved via large-scale searching without using a gradient method. The adopted algorithm is also well suited to both linear and nonlinear vehicle lateral dynamic models.

1.2 Literature review

In recent years, extensive research has been conducted in areas such as creating vehicle dynamic models [1-6]; driver models [7-15]; tire-road interaction models [16-19]; power steering models [20, 21]; automatic control models [22-32] and parameter estimations [33-35]. In this section of the thesis, we describe vehicle models, driver models and the solution method.

1.2.1 Vehicle models

The "bicycle model" is a well-known dynamic model for simulating vehicle kinetics [38]. In this model, a vehicle with four wheels and two axles is modeled as a one-track vehicle with two wheels (front and rear) with double lateral stiffness. J. P. Wideberg [1] has presented a simplified method for evaluating the lateral behaviour of a heavy vehicle using the bicycle model. Wideberg's results show that during simulations, dynamic effects worsen when flexible vehicle frames are taken into account.

Der Ho Wu *et al.* [4] have proposed a three-degree-of-freedom vehicle model, using the following assumptions:

- Nonlinearities in the springs; the dampers' behaviours are not taken into account;
- The cornering force produced by a given tire is a linear function of the slip angle;
- The influence of wheel camber on lateral force generation and aligning moment are not taken into account;
- The tractor's forward speed remains constant.

In addition, in [4] the system is considered to be stable if it returns to a state of equilibrium within a finite time following a disturbance.

Chien Chen *et al.* [3] have proposed a complex vehicle model for the tractor semi-trailer. In their project, the results of the open loop experiment following a field test are compared with the results of simulating the complex vehicle model. The results of this comparison yield a linear model as follows:

$$M_1\ddot{q}(t) + N_1\dot{q}(t) + E(\dot{q}(t), q(t)) + Lq(t) = \delta \tag{1.4}$$

Two properties are observed in this linear model:

- M_1 is a symmetric positive definite matrix containing the vehicle system's inertial information. δ is the steering angle. L is a matrix.
- The N_1 matrix can be interpreted as a damping matrix. Each element of the E matrix contains tire-cornering stiffness. If the cornering stiffness is small, the vehicle system will become lightly damped and more oscillatory. For example, if the vehicle is operated on an icy road, its stability will decrease.

In work done by M.Tai *et al.* [2], a heavy vehicle is considered as a system of interconnected rigid-bodies interacting with the environment. In their simple model, only planar translational motion, the tractor's yaw motion, and the semi-trailer's yaw motion are considered. This model simplifies the complex model by setting certain modes at zero. By applying Newton's second law, M. Tai *et al.* set up the following dynamic equations:

$$\begin{aligned} F_{yu1}^{total} &= \sum_{i=1}^{n}((\sum_{j=1}^{4} F_{txj}^{i})\sin(\varepsilon_i - \varepsilon_1) + (\sum_{j=1}^{4} F_{tyj}^{i})\cos(\varepsilon_i - \varepsilon_1)) \\ F_{xu1}^{total} &= \sum_{i=1}^{n}((\sum_{j=1}^{4} F_{txj}^{i})\cos(\varepsilon_i - \varepsilon_1) - (\sum_{j=1}^{4} F_{tyj}^{i})\sin(\varepsilon_i - \varepsilon_1)) \end{aligned} \tag{1.5}$$

where F is force, ε_i is heading angle

1.2.2 Driver models

Human-driver lateral control behaviour resembles a situation where a driver repeatedly tries to minimize lateral position and/or orientation tracking errors. This effort is constrained by the driver's physical limitations.

X. Yang *et al.* [7] have proposed a single-loop and a multi-loop driver directional control model in order to study driver/vehicle interaction. During the directional control process, the driver acts as both sensor and controller. The driver's feedback information may include the tractor unit's path and orientation errors as well as both units' lateral accelerations, yaw rates, roll angles and roll rates. These variables may be detected by the driver directly and indirectly while formulating his directional control strategy.

In [7], the considerations and assumptions associated with studying a driver's directional control behaviour include the following:

- The previewed path is expressed by a low-order polynomial function, since it includes primarily low-frequency components;
- The vehicle's path is previewed with respect to the body fixed co-ordinate system of the lead or trailing unit;
- The driver's control actions are always directed towards minimizing the cost function.

A.Y. Ungoren *et al.*[8] have proposed an adaptive lateral-preview human-driver model. Their driver model is developed using the adaptive predictive control (APC) framework. The following key features characterize this APC framework:

- Use of preview information;
- Internal model identification;
- Weight adjustment to simulate different driving styles.

In this model, the driver uses predicted vehicle information in a future window to determine optimal steering action. A tunable matrix is defined in order to assign relative importance to lateral displacement, lateral velocity, yaw angle and yaw velocity in the cost function to be optimized. In this paper [8], a weighting matrix Q_w is introduced in order to evaluate relative importance.

According to T. Legouis *et al.* [36], the mathematical models for driver steering control have progressed along three dimensions:

- *Quasi-linear*; where the human operator is represented by a function with a frequency-dependent gain and phase;
- *Predictive,* leading to a better physical interpretation. It is assumed that the driver focuses on a fictitious point ahead in the vehicle's direction and reacts only to the vehicle's apparent lateral displacement;
- *Optimal control*, generated by a linear feedback loop resulting from the cascade combination of a Kalman filter and a minimum mean squared predictor.

In studying a closed-loop system for a passenger car [36], the steering model is written as

$$\delta(t) = h_1 \dot{y}(t - T_r) + h_2 r(t - T_r) + h_3 y(t - T_r) + h_4 \phi(t - T_r) \tag{1.6}$$

where the constants h_1, h_2, h_3 and h_4 are real numbers determined experimentally from the vehicle's characteristics, speeds, and the disturbances. ϕ is heading angle. r is yaw velocity. y is lateral displacement.

1.2.3 Solution method

T. Legouis *et al.* [36] have proposed an optimal-approach method with time delay in order to solve the problem of driver-vehicle control. This problem does not fall under the

classical framework of linear quadratic optimal control theory, even without time delay. To solve this problem, the authors have devised an alternative numerical method. They begin by considering cost function to be a function of the control vector. The cost function's gradient is then expressed by the state vector and its derivative. To solve the state vector's derivative, an adjoint state equation is defined. After integrating the adjoint state equation in reverse order, from the simulation's end to its beginning, it becomes possible to evaluate the gradient. The cost function's minimum value is determined in the direction opposite to this gradient by means of a one-dimensional optimization algorithm yielding a new control vector. This algorithm must integrate the state equations, adjoint state equations, and the introduction of a one-dimensional optimization algorithm. It is limited by simulation time and step size.

M. Heinkenschloss *et al.*[39] have proposed an interface between the application problem and the proposed nonlinear optimization algorithm in order to solve the numerical solution of distributed optimal control problems. By using this interface, numerical optimization algorithms can be designed to take advantage of inherent problem features: for instance, splitting variables into states, controls, and scaling inherited from functional scalar products.

S. Nahar *et al.* [40] used the Simulated Annealing method to solve the problem of combinatorial optimization. Later, P. P. Mutalik *et al.* [41] proposed a parallel Simulated Annealing method for solving a similar problem involving combinatorial optimization.

P. Siarry *et al.* [42] have proposed a new global optimization algorithm for functions containing many continuous variables. Their new global optimization algorithm, derived from the basic Simulated Annealing method, can deal with high-dimensionality minimization problems that are often difficult to solve by all known minimization methods, with or without gradients.

CHAPTER 2

OBJECTIVES AND METHODOLOGY

2.1 Objectives

The general objectives are to identify the model parameters inherent in an optimal human driver and to study the behaviour of a tractor semi-trailer vehicle system for a typical lateral regulation task following an external disturbance during high-speed driving. The specific objectives are:

1. Characterizing the model parameters inherent in an optimal human driver;
2. Simulating the articulated vehicle's dynamic responses using the predetermined optimal driver model;
3. Simulating the articulated vehicle's dynamic behaviour at various vehicle speeds, vehicle loads and human-driver reaction delays using optimal-driver model parameters;
4. Evaluating the effect of visibility distance on the vehicle's dynamic response using a simplified driver model.

2.2 Methodology

To achieve these objectives, research is divided into several steps; various modeling and solution methods were adopted for each step.

2.2.1 Modeling the vehicle's lateral dynamics

Using the bicycle model ([38] and [1]), the tractor semi-trailer is studied as a "two-rigid-body bicycle model" consisting of the bicycle model and its "trailer model" connected at

point Q (the fifth wheel). The lateral dynamics of both the tractor unit and the semi-trailer unit are studied together, using a two-rigid-body bicycle model, since both units have the same lateral velocity at point Q. Newton's second law is used to arrive at the articulated vehicle's lateral dynamic equations, as used in [2], using the linear tire force along with some assumptions such as those found in **[4]**. The variables used for the articulated vehicle's lateral dynamic equations are the tractor's lateral displacement and the yaw angles for both the tractor and semi-trailer units. The driver's steering angle is unknown.

2.2.2 Modeling the human driver model

Modeling the human driver involved extending to the 3-DOF mathematical driver-steering model used by T. Legouis *et al.* [36], which is a 2-DOF driver-steering-angle model (2.1).

$$\delta(t) = h_1 \dot{y}(t - T_r) + h_2 r(t - T_r) + h_3 y(t - T_r) + h_4 \phi(t - T_r) \tag{2.1}$$

The articulated vehicle/driver model (2.1), possessing single-loop [7] and lateral-preview [8] aspects, is here defined as the function of the vehicle's state vector *q(t)*, control vector *H* and time delay *Tr*. To suit the 3-DOF tractor semi-trailer dynamic equations, equation (2.1) has been extended as follows:

$$\delta(t) = h_1 \dot{y}_1(t - T_r) + h_2 r_1(t - T_r) + h_3 r_2(t - T_r) + h_4 y_1(t - T_r) + h_5 \phi_1(t - T_r) + h_6 \phi_2(t - T_r) \tag{2.2}$$

where y_1 is lateral displacement of the tractor, $\dot{y}_1$ is lateral velocity of the tractor, ϕ_1 is the tractor's yaw angle and $r_1 = \dot{\phi}_1$ is the tractor's yaw velocity, ϕ_2 is the semi-trailer's yaw angle and $r_2 = \dot{\phi}_2$ is the semi-trailer's yaw velocity

2.2.3 Solution method

The closed-loop tractor semi-trailer system has been set up using a vehicle lateral dynamic model and a driver steering model. The lateral dynamic equations include the vehicle's state vector with time delay and control vector H, as yet unidentified. Improvements are made to the Runge-Kutta method [45] in order to solve the problem of time delay in the dynamic equations. To identify control vector H, the cost function proposed by T. Legouis *et al.* [36] is introduced, consisting of the state vector and the weight matrix. In general, the weight matrix is considered to be equivalent to the unit matrix. Although the value of the initial state vector is known, cost function J cannot be calculated, because the state vector is known to be a function of control vector H and the previous state vector. This problem does not fall under classical control theory. The gradient method by T. Legouis *et al.* [36] proposed for solving this problem is limited by the linear equation. P. Siarry *et al.* [42] recommend the introduction of a modified Simulated Annealing algorithm to solve such problems in this type of research. Using a form of the Simulated Annealing algorithm enhanced by utilizing a fixed-search step size, we are able to seek the optimal control vector by minimizing cost function J.

CHAPTER 3

FORMULATING THE VEHICLE / DRIVER CONTROL MODEL

In this chapter we propose a tractor semi-trailer lateral dynamic model and a driver model. For our purposes, the tractor semi-trailer's input is the steering angle, whereas the tractor semi-trailer model's output is the state vector. As for the input of the driver model, this is the state vector a human driver can detect following a certain time delay; the output of the human driver model is the steering angle. In this way, a closed-loop tractor semi-trailer/driver control system with time delay can be created.

3.1 The tractor semi-trailer vehicle dynamic model

An articulated vehicle such as a tractor semi-trailer consists of the tractor unit and a semi-trailer unit. These are assumed to be rigid bodies with fixed centre of gravity. A five-axle tractor semi-trailer is the type of heavy articulated vehicle used in this thesis. We chose a tractor unit with a single driving axle and rear twin-axle, linked by a wheel coupling to a twin-axle trailer unit. Figure 3 shows a typical five-axle tractor semi-trailer running on a highway.

In order to study the vehicle's dynamics, we used a coordinate system; this was attached to the vehicle in order to describe the vehicle's motion. The tractor semi-trailer's motion was described within an x-y inertial reference frame. The extended bicycle model for automobiles was used to analyze the tractor semi-trailer's motion. The tractor semi-trailer vehicle was considered to be moving along a straight line at a constant forward speed with a small angular deviation in heading. The suspension and brakes were ignored. Following Newton's second law and after applying some simplifications, it was then possible to set up a three-degree-of-freedom (3-DOF) tractor semi-trailer vehicle dynamic model.

Figure 3 Five-axle tractor semi-trailer [37]

3.1.1 The tractor in an inertial coordinate system

The first analysis we performed concerned the motion of the tractor that can be described within an x-y inertial reference frame. Figure 4 shows a view of the tractor as seen from above. The coordinates x and y locate the centre of mass of the tractor with respect to the ground; ϕ is the angle between the centerline of the tractor and a line on the ground parallel to the x-axis. The x-y axes are presumed to be neither accelerating nor rotating. The parameters of the tractor are a_1 and b_1 or the distance from the centre of mass to the front and rear axles respectively; m_1 is the mass, and I_{z1} is the moment of inertia surrounding the centre of mass, with respect to the vertical axis.

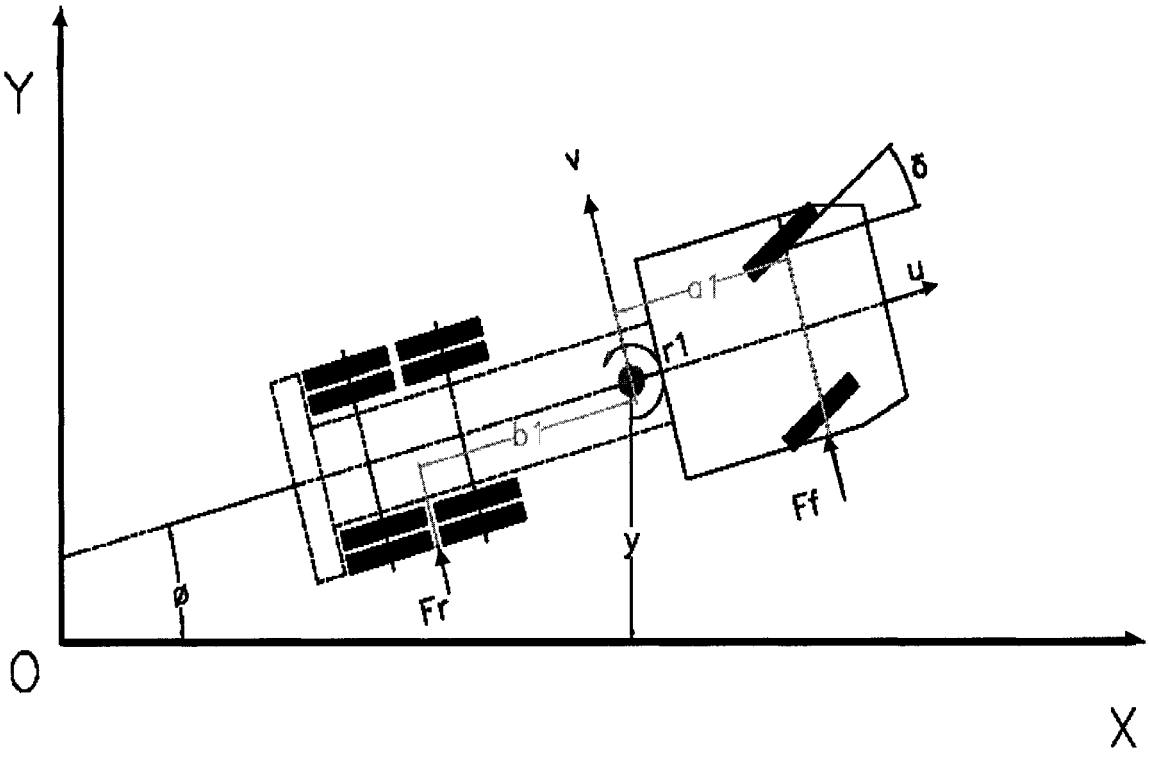

Figure 4 Tractor yaw motion

Normal motion is considered to have a constant speed u along the x-axis; the variables needed to describe the lateral motion are therefore primarily $y(t)$ and $\phi(t)$. Although $x(t)$ is also required, generally speaking, under conditions of normal and disturbed motion, it is here assumed that $\dot{x} \approx u$ is a constant; therefore, *x(t)=ut+constant*. Thus speed, u, plays the role of a parameter in the analysis. In normal motion, because there is no lateral disturbance, $y, \dot{y}, \phi$ and $\dot{\phi}$ all vanish, and the rigid body proceeds along the x-direction at a constant speed u.

When motion is disturbed, $\dot{y}$ is assumed to be small as compared to the constant speed u; values ϕ and $\dot{\phi}$ are also small. The speed, $b\phi$ is therefore small compared to the constant speed u. This means that the small angle approximations $\cos\phi \approx 1$ and $\sin\phi \approx \phi$ may be used when taking disturbed motion into account. The kinematic equations can therefore be written as

$$\frac{d\phi}{dt} = r \tag{3.1}$$

$$\frac{dy}{dt} = v + u\phi \tag{3.2}$$

where y is the lateral displacement, ϕ is the yaw angle, r is the yaw velocity, v is the lateral speed, and u is the constant forward speed.

The side forces are determined to be F_f and F_r. Of course, vertical forces at both axles are necessary in order to support the weight of the body; however, these forces play no role in the body's lateral dynamics. Three equations of motion can be written easily, because the tractor is described in an inertial coordinate system and is undertaking a plane motion. The force equations are arrived at by multiplying mass by acceleration in two directions; the moment is found to be equal to the rate of changing of angular momentum around the z-axis. The angle ϕ is assumed to be very small for the disturbed motion; the equations for the disturbed motion are

$$m\dot{u} = 0 \tag{3.3}$$

$$m(\dot{v} + ur) = F_f + F_r \tag{3.4}$$

$$I_z\dot{r} = aF_f - bF_r \tag{3.5}$$

where u is the constant forward speed of the vehicle, m is the total mass of the vehicle, v is its lateral speed, and r is its yaw velocity.

3.1.2 Tractor semi-trailer dynamic system

The second analysis takes into account the motion of both the tractor and the semi-trailer, connected at point Q. These are also described within an x-y inertial reference frame. Figures 5 and 6 show a view of the tractor semi-trailer. The global coordinates x and y located at the centres of mass of the tractor and semi-trailer (ϕ_1 and ϕ_2 respectively) are

the angles between the centreline of the tractor semi-trailer and a line on the ground that is parallel to the x-axis. The x-y axes are presumed to be neither accelerating nor rotating.

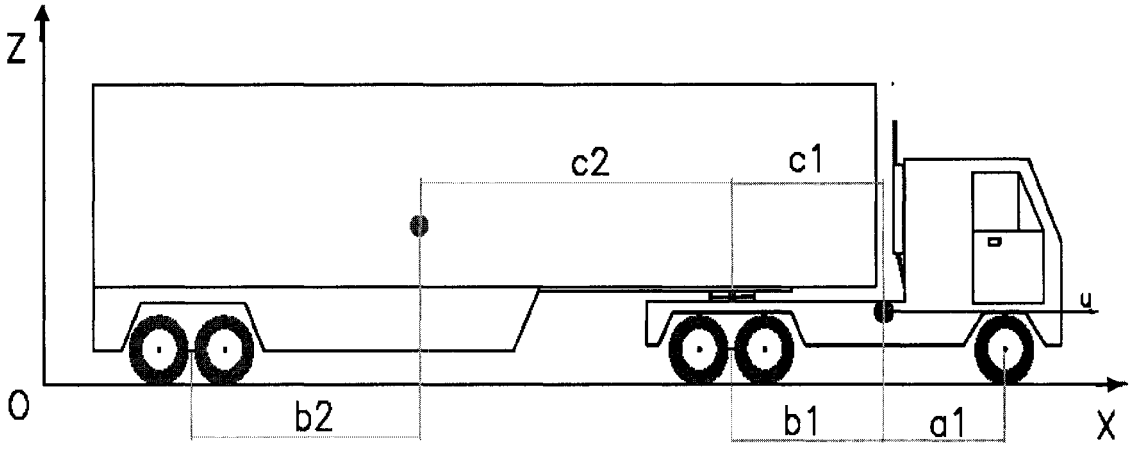

Figure 5 The tractor semi-trailer

The parameters of the tractor are a_1 and b_1; the distance from the centre of mass to the front and rear axles, c_1 (or the distance between joint point Q and the centre of mass); m_1 is the mass, and I_{z1}, the moment of inertia surrounding the centre of mass with respect to the vertical axis. The parameters for the semi-tractor are b_2, the distance from the centre of mass to the rear axles; c_2, the distance between joint point Q and the mass centre; m_2, the mass, and I_{z2}, the moment of inertia surrounding the centre of mass with respect to the vertical axis. The distance between the two tires, which are fixed on the same side of the axle, is not taken into account. Lateral forces for both tires are taken to be twice that for a single tire.

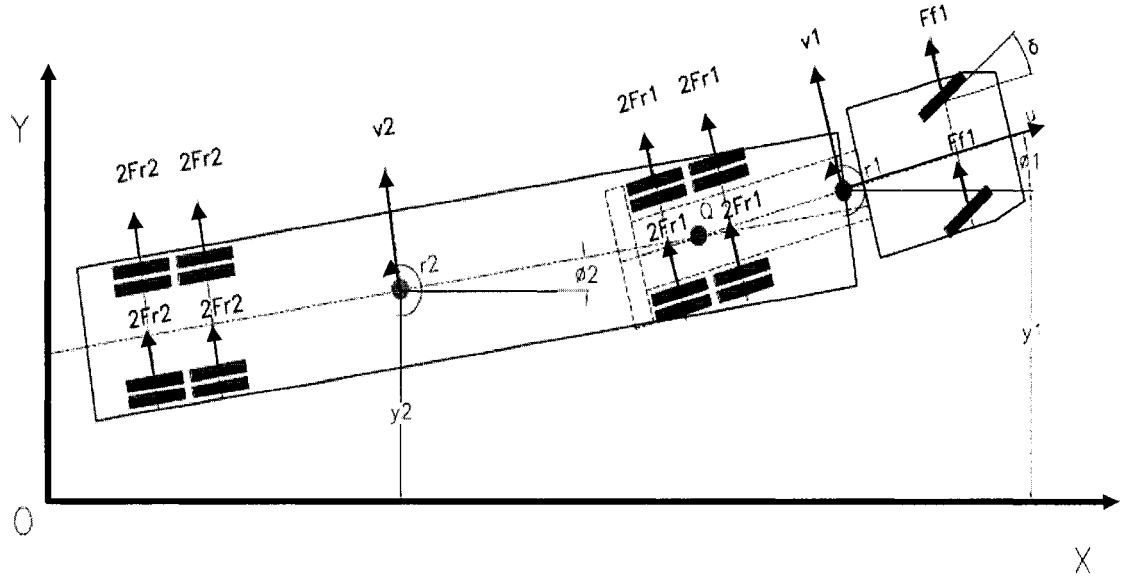

Figure 6 Yaw motion of the tractor semi-trailer

When some approximations are applied with respect to the tractor semi-trailer, such as disregarding the distance between the tractor's two rear axles, this yields a bicycle model of the tractor semi-trailer, as shown in Figure 7.

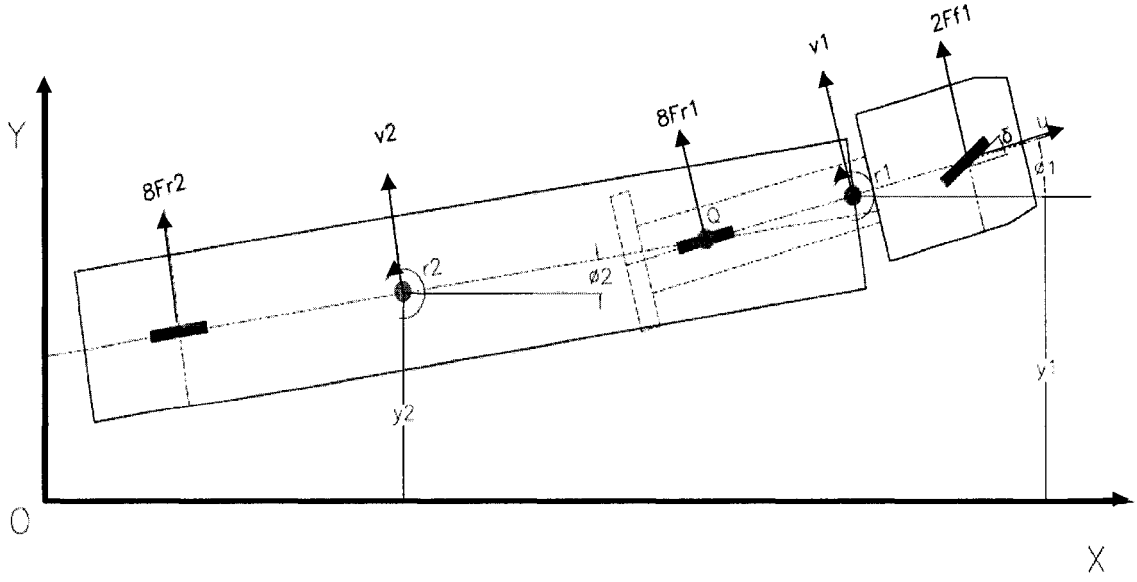

Figure 7 Bicycle model of the tractor semi-trailer

According to the tractor dynamics analyzed in subsection 3.1.1, two kinematic equations can be arrived at for the tractor when motion is disturbed:

$$\frac{d\phi_1}{dt} = r_1 \tag{3.6}$$

$$\frac{dy_1}{dt} = v_1 + u\phi_1 \tag{3.7}$$

According to the tractor dynamics analyzed in subsection 3.1.1, two kinematic equations can also be written for the semi-trailer in the event of disturbed motion:

$$\frac{d\phi_2}{dt} = r_2 \tag{3.8}$$

$$\frac{dy_2}{dt} = v_2 + u\phi_2 \tag{3.9}$$

For the tractor, the side forces are $2F_{f1}$ and $8F_{r1}$ for the front wheel and the rear wheel, respectively. F_{Qy} is the side force generated by the semi-trailer. The above analysis shows that equations of motion for the tractor unit can be expressed as follows:

$$m_1(\dot{v}_1 + ur_1) = 2F_{f1} + 8F_{r1} - F_{Qy} \tag{3.10}$$

$$I_{z1}\dot{r}_1 = 2a_1F_{f1} - 8b_1F_{r1} + c_1F_{Qy} \tag{3.11}$$

For the semi-trailer, the side forces are $8F_{r2}$ for the rear wheel. F_{Qy} is the side force generated by the tractor. The analysis above shows that equations of motion for the semi-trailer unit can be expressed as follows:

$$m_2(\dot{v}_2 + ur_2) = 8F_{r2} + F_{Qy} \tag{3.12}$$

$$I_{z2}\dot{r}_2 = c_2 F_{Qy} - 8b_2 F_{r2} \tag{3.13}$$

The tractor's lateral velocity at joint articulation point Q can be represented as:

$$v_Q = u\phi_1 + v_1 - c_1 r_1 \tag{3.14}$$

The semi-trailer's lateral velocity at joint articulation point Q can be represented as:

$$v_Q = u\phi_2 + v_2 + c_2 r_2 \tag{3.15}$$

Because the tractor and semi-trailer are connected at joint articulation point Q, they have the same lateral velocity at this point:

$$v_Q = u\phi_1 + v_1 - c_1 r_1 = u\phi_2 + v_2 + c_2 r_2 \tag{3.16}$$

Thus, the lateral velocity of the semi-trailer at point Q can be written as:

$$v_2 = u(\phi_1 - \phi_2) + v_1 - c_1 r_1 - c_2 r_2 \tag{3.17}$$

Based on the derivative in (3.17), the lateral acceleration of the semi-trailer can be written as:

$$\dot{v}_2 = u(r_1 - r_2) + \dot{v}_1 - c_1 \dot{r}_1 - c_2 \dot{r}_2 \tag{3.18}$$

Based on equation (3.12) and equation (3.18), the force, F_{Qy} can be written as:

$$F_{Qy} = m_2(\dot{v}_2 + ur_2) - 8F_{r2} = m_2(\dot{v}_1 - c_1\dot{r}_1 - c_2\dot{r}_2 + ur_1) - 8F_{r2} \tag{3.19}$$

The resulting dynamic equations for the tractor semi-trailer system are obtained by displacing force F_{Qy} by equation (3.19). Equation (3.10) can then be written as:

$$m_1(\dot{v}_1 + ur_1) = 2F_{f1} + 8F_{r1} + 8F_{r2} - m_2(\dot{v}_1 - c_1\dot{r}_1 - c_2\dot{r}_2 + ur_1)$$

After simplification, the above equation is expressed by the state vector and the tire forces.

$$(m_1 + m_2)\dot{v}_1 + (m_1u + m_2u)r_1 - m_2c_1\dot{r}_1 - m_2c_2\dot{r}_2 = 2F_{f1} + 8F_{r1} + 8F_{r2} \tag{3.20}$$

Equation (3.11) can be written as:

$$I_{z1}\dot{r}_1 = 2a_1F_{f1} - 8b_1F_{r1} - 8c_1F_{r2} + c_1m_2(\dot{v}_1 - c_1\dot{r}_1 - c_2\dot{r}_2 + ur_1)$$

After simplification, the above equation is expressed by the state vector and the tire forces.

$$-c_1m_2\dot{v}_1 - c_1m_2ur_1 + (I_{z1} + c_1^2m_2)\dot{r}_1 + c_1c_2m_2\dot{r}_2 = 2a_1F_{f1} - 8b_1F_{r1} - 8c_1F_{r2} \tag{3.21}$$

Equation (3.13) can be written as:

$$I_{z2}\dot{r}_2 = -8b_2F_{r2} - 8c_2F_{r2} + c_2m_2(\dot{v}_1 - c_1\dot{r}_1 - c_2\dot{r}_2 + ur_1)$$

After simplification, the above equation is expressed by the state vector and the tire forces.

$$-c_2m_2\dot{v}_1 - c_2m_2ur_1 + c_1c_2m_2\dot{r}_1 + (I_{z2} + c_2^2m_2)\dot{r}_2 = -8(b_2 + c_2)F_{r2} \tag{3.22}$$

The equations of motion (3.20),(3.21),(3.22) corresponding to 3 DOF consist of the dynamic equations presented in terms of lateral tire force.

3.1.3 Tire forces

Accurate nonlinear mathematical models of tire-road interaction, verified by experiment, have been developed for use in computer simulations of vehicle dynamics [38]. These models are useful for simulating complex vehicle models that are in turn utilized for predicting the response of proposed vehicle designs. Generally, simple linear models of tire force generation are used to analyze vehicle dynamics under the influence of small disturbances away from a basic state of motion. Slip angle and the cornering coefficients are used to describe tire-road interaction.

3.1.3.1 Slip angle and the cornering coefficient

Because the wheel supports the load, a normal force exists between the road's surface and the tire's contact patch. If a small lateral force is then applied to the wheel, a corresponding lateral force will arise in the contact patch between the tire and the road surface due to friction. Although the lateral force may be too small to cause the tire to slide sideways over the surface, the wheel will no longer continue to move in the direction in which it has been pointed. Rather, it will acquire a sideways or lateral velocity in addition to its forward velocity. Thus, the total velocity vector of the wheel will point in a different direction than the direction of the wheel's centre plane. This angle between the wheel and the direction in which the wheel moves when a lateral force is applied is called the slip angle, α . [43] An example of a slip angle is shown in Figure 8.

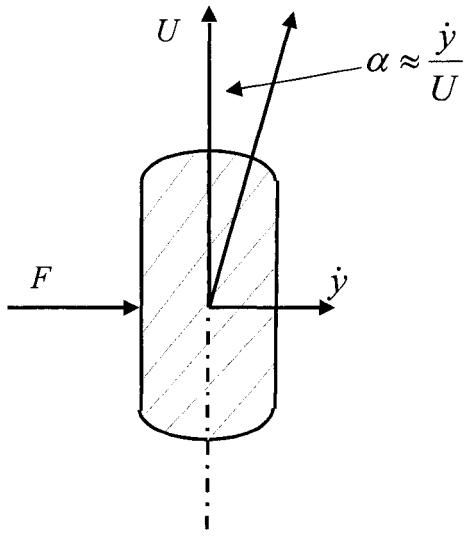

Figure 8 The slip angle

When analyzing the stability of vehicles using pneumatic tires, it is common to use a linear model showing the relationship between the lateral force generated by the tire, F, and the slip angle, α.

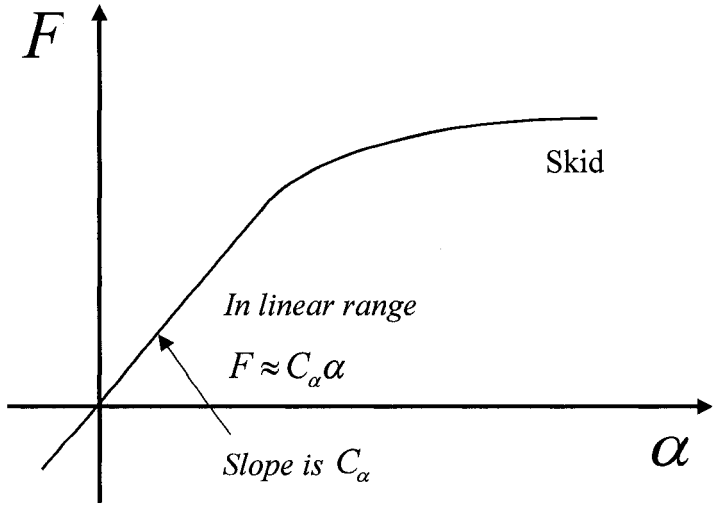

Figure 9 A tire model

Figure 9 shows that over a certain range, lateral force and the slip angle are found to be nearly proportional to each other. The linear tire force model will apply in an approximate way for small values of the lateral force and for small values of the slip angle. As long as the lateral force remains small enough so that the tire does not begin to skid, the slip angle remains quite small. For small slip angles, a proportionality constant, the cornering coefficient C_α, can be defined as the slope of the line that relates lateral force to slip angle. This means that the lateral force can be expressed as:

$$F = C_\alpha \alpha \tag{3.23}$$

At large slip angles, the tire begins to skid and the force-vs-slip-angle relationship becomes significantly nonlinear. At a certain slip angle, the lateral force reaches a maximum.

3.1.3.2 Lateral force of the tractor semi-trailer

When a disturbance is slight, the linear tire model is used to analyze the tire force generated by the tractor semi-trailer. The tractor's front-tire force can be expressed as:

$$F_{f1} = -C_{f1}\alpha_{f1}$$

where

$$\alpha_{f1} = \frac{v_1 + a_1 r_1}{u} - \delta$$

δ is the front steering angle.

Front-tire force is then expressed using lateral velocity, yaw velocity, constant forward speed, vehicle parameters and steering angle.

$$F_{f1} = -C_{f1}(\frac{v_1 + a_1 r_1}{u} - \delta) \tag{3.24}$$

The tractor's rear-tire force can be expressed as

$$F_{r1} = -C_{r1}\alpha_{r1}$$

where

$$\alpha_{r1} = \frac{v_1 - b_1 r_1}{u}$$

Rear-tire force is then expressed using lateral velocity, yaw velocity, constant forward speed and vehicle parameters.

$$F_{r1} = -C_{r1}(\frac{v_1 - b_1 r_1}{u}) \tag{3.25}$$

The semi-trailer's rear tire force can be expressed as

$$F_{r2} = -C_{r2}\alpha_{r2}$$

where

$$\alpha_{r2} = \frac{v_2 - b_2 r_2}{u}$$

The semi-trailer's rear-tire force is expressed using lateral velocity, yaw velocity, constant forward speed, and vehicle parameters.

$$F_{r2} = -C_{r2}(\frac{v_2 - b_2 r_2}{u}) \tag{3.26}$$

3.1.4 Final equations for the vehicle's dynamic system

From equations (3.24), (3.25) and (3.26), tire forces for the tractor semi-trailer can be expressed in terms of vehicle parameters, state variables and tire-cornering coefficients. Substituting the tire force into the tractor semi-trailer dynamic equations yields the equations for the tractor semi-trailer's dynamic system.

$$\begin{aligned}&(m_1 + m_2)\dot{v}_1 + (m_1 + m_2)ur_1 - m_2 c_1 \dot{r}_1 - m_2 c_2 \dot{r}_2 = \\ &-2C_{f1}(\frac{v_1 + a_1 r_1}{u} - \delta) - 8C_{r1}(\frac{v_1 - b_1 r_1}{u}) - 8C_{r2}(\frac{v_2 - b_2 r_2}{u})\end{aligned} \tag{3.27}$$

$$\begin{aligned}&-c_1 m_2 \dot{v}_1 - c_1 m_2 u r_1 + (I_{z1} + c_1^2 m_2)\dot{r}_1 + c_1 c_2 m_2 \dot{r}_2 = \\ &-2a_1 C_{f1}(\frac{v_1 + a_1 r_1}{u} - \delta) + 8b_1 C_{r1}(\frac{v_1 - b_1 r_1}{u}) + 8c_1 C_{r2}(\frac{v_2 - b_2 r_2}{u})\end{aligned} \tag{3.28}$$

$$-c_2 m_2 \dot{v}_1 - c_2 m_2 u r_1 + c_1 c_2 m_2 \dot{r}_1 + (I_{z2} + c_2^2 m_2)\dot{r}_2 = 8(b_2 + c_2)C_{r2}(\frac{v_2 - b_2 r_2}{u}) \tag{3.29}$$

In equations (3.27), (3.28) and (3.29), there are four variables: v_1, v_2, r_1, r_2; however, a 3-DOF dynamic model has only three independent equations. Using equation (3.11), v_2 is eliminated and the equations become:

$$\begin{aligned}&(m_1 + m_2)\dot{v}_1 + (m_1 + m_2)ur_1 - m_2 c_1 \dot{r}_1 - m_2 c_2 \dot{r}_2 = -2C_{f1}(\frac{v_1 + a_1 r_1}{u} - \delta) \\ &-8C_{r1}(\frac{v_1 - b_1 r_1}{u}) - 8C_{r2}(\frac{u(\phi_1 - \phi_2) + v_1 - c_1 r_1 - c_2 r_2 - b_2 r_2}{u})\end{aligned} \tag{3.30}$$

and

$$
\begin{aligned}
&- c_1 m_2 \dot{v}_1 - c_1 m_2 u r_1 + (I_{z1} + c_1^2 m_2)\dot{r}_1 + c_2 c_1 m_2 \dot{r}_2 \\
&= -2a_1 C_{f1}\left(\frac{v_1 + a_1 r_1}{u} - \delta\right) + 8 b_1 C_{r1}\left(\frac{v_1 - b_1 r_1}{u}\right) \\
&+ 8 c_1 C_{r2}\left(\frac{u(\phi_1 - \phi_2) + v_1 - c_1 r_1 - c_2 r_2 - b_2 r_2}{u}\right)
\end{aligned} \tag{3.31}
$$

and

$$
\begin{aligned}
&- c_2 m_2 \dot{v}_1 - c_2 m_2 u r_1 + c_1 c_2 m_2 \dot{r}_1 + (I_{z2} + c_2^2 m_2)\dot{r}_2 \\
&= 8(b_2 + c_2) C_{r2}\left(\frac{u(\phi_1 - \phi_2) + v_1 - c_1 r_1 - c_2 r_2 - b_2 r_2}{u}\right)
\end{aligned} \tag{3.32}
$$

Following calculation and simplification:

$$
\begin{aligned}
&(m_1 + m_2)\dot{v}_1 - m_2 c_1 \dot{r}_1 - m_2 c_2 \dot{r}_2 + \left(\frac{2C_{f1} + 8C_{r1} + 8C_{r2}}{u}\right) v_1 \\
&+ \left((m_1 + m_2)u + \frac{2a_1 C_{f1} - 8b_1 C_{r1} - 8c_1 C_{r2}}{u}\right) r_1 \\
&- \frac{8C_{r2}(b_2 + c_2)}{u} r_2 + 8C_{r2}\phi_1 - 8C_{r2}\phi_2 = 2C_{f1}\delta
\end{aligned} \tag{3.33}
$$

and

$$
\begin{aligned}
&- c_1 m_2 \dot{v}_1 + (I_{z1} + c_1^2 m_2)\dot{r}_1 + c_1 c_2 m_2 \dot{r}_2 + \left(\frac{2a_1 C_{f1} - 8b_1 C_{r1} - 8c_1 C_{r2}}{u}\right) v_1 \\
&+ \left(\frac{2a_1^2 C_{f1} + 8b_1^2 C_{r1} + 8c_1^2 C_{r2}}{u} - c_1 m_2 u\right) r_1 + \frac{8c_1(b_2 + c_2)C_{r2}}{u} r_2 \\
&- 8c_1 C_{r2}\phi_1 + 8c_1 C_{r2}\phi_2 = 2a_1 C_{f1}\delta
\end{aligned} \tag{3.34}
$$

and

$$
\begin{aligned}
&- c_2 m_2 \dot{v}_1 + c_1 c_2 m_2 \dot{r}_1 + (I_{z2} + c_2^2 m_2)\dot{r}_2 - \frac{8(b_2 + c_2)C_{r2}}{u} v_1 \\
&+ \left(\frac{8c_1(b_2 + c_2)C_{r2}}{u} - c_2 m_2 u\right) r_1 + \frac{8(b_2 + c_2)^2 C_{r2}}{u} r_2 \\
&- 8(b_2 + c_2)C_{r2}\phi_1 + 8(b_2 + c_2)C_{r2}\phi_2 = 0
\end{aligned} \tag{3.35}
$$

From equation (3.2), the relative equation of $\dot{y}_1$ and v_1 is obtained:

$$v_1 = \dot{y}_1 - u\phi_1 \tag{3.36}$$

After differentiation, the relative equation of $\ddot{y}_1$ and $\dot{v}_1$ is obtained:

$$\dot{v}_1 = \ddot{y}_1 - u\dot{\phi}_1 = \ddot{y}_1 - ur_1 \tag{3.37}$$

Lastly, the tractor semi-trailer's dynamic equations, which are expressed by the state vector, can be written as follows:

$$\begin{bmatrix} A_{11} & A_{12} & A_{13} \\ A_{21} & A_{22} & A_{23} \\ A_{31} & A_{32} & A_{33} \end{bmatrix} \begin{bmatrix} \ddot{y}_1 \\ \dot{r}_1 \\ \dot{r}_2 \end{bmatrix} + \begin{bmatrix} B_{11} & B_{12} & B_{13} \\ B_{21} & B_{22} & B_{23} \\ B_{31} & B_{32} & B_{33} \end{bmatrix} \begin{bmatrix} \dot{y}_1 \\ r_1 \\ r_2 \end{bmatrix} + \begin{bmatrix} C_{11} & C_{12} & C_{13} \\ C_{21} & C_{22} & C_{23} \\ C_{31} & C_{32} & C_{33} \end{bmatrix} \begin{bmatrix} y_1 \\ \phi_1 \\ \phi_2 \end{bmatrix} = \begin{bmatrix} D_{11} \\ D_{21} \\ D_{31} \end{bmatrix} \delta \tag{3.38}$$

where

δ = Steering angle of the tractor

ϕ_1 = Heading angle of the tractor

ϕ_2 = Heading angle of the semi-trailer

y_1 = Lateral deviation of the tractor

r_1 = Yaw velocity of the tractor ($r_1 = \dot{\phi}_1$)

r_2 = Yaw velocity of the semi-trailer ($r_2 = \dot{\phi}_2$)

$A_{11} = m_1 + m_2$
$A_{12} = -m_2 c_1$
$A_{13} = -m_2 c_2$
$A_{21} = -c_1 m_2$
$A_{22} = c_1^2 m_2 + I_{z1}$

$$A_{23} = c_1 c_2 m_2$$

$$A_{31} = -c_2 m_2$$

$$A_{32} = c_1 c_2 m_2$$

$$A_{33} = c_2^2 m_2 + I_{z2}$$

$$B_{11} = \frac{2c_{f1} + 8c_{r1} + 8c_{r2}}{u}$$

$$B_{12} = \frac{2a_1 c_{f1} - 8b_1 c_{r1} - 8c_1 c_{r2}}{u}$$

$$B_{13} = -8(\frac{b_2 + c_2}{u})c_{r2}$$

$$B_{21} = \frac{2a_1 c_{f1} - 8b_1 c_{r1} - 8c_1 c_{r2}}{u}$$

$$B_{22} = \frac{2a_1^2 c_{f1} + 8b_1^2 c_{r1} + 8c_1^2 c_{r2}}{u}$$

$$B_{23} = 8c_1(\frac{b_2 + c_2}{u})C_{r2}$$

$$B_{31} = -\frac{8(b_2 + c_2)}{u}C_{r2}$$

$$B_{32} = \frac{8(b_2 + c_2)c_1 c_{r2}}{u}$$

$$B_{33} = \frac{8(b_2 + c_2)^2 c_{r2}}{u}$$

$$C_{11} = 0$$

$$C_{12} = -2c_{f1} - 8c_{r1}$$

$$C_{13} = -8c_{r2}$$

$$C_{21} = 0$$

$$C_{22} = -2a_1 c_{f1} + 8b_1 c_{r1}$$

$$C_{23} = 8c_1 c_{r2}$$

$$C_{31} = 0$$

$$C_{32} = 0$$

$$C_{33} = 8(b_2 + c_2)c_{r2}$$

$$D_{11} = 2c_{f1}$$

$$D_{21} = 2a_1 c_{f1}$$

$$D_{31} = 0$$

3.2 Driver model with time delay

When a human driver detects a disturbance in the tractor semi-trailer, he will guide the tractor back to its straightforward direction by adjusting the steering angle. Because there is some time delay in both human and mechanical reactions, the driver must adjust the steering angle successively in order to decrease lateral displacement, lateral velocity, yaw velocity and lateral accelerations. The graph trace appears similar to that of a damped oscillation. The driver model simulates two aspects of driving behaviour:

1. First, the steering angle is adjusted according to the state vector. This step in the mathematic driver model is denoted by the state vector's coefficients: when an optimal coefficient is found, only the state vector can change the steering angle. If the state vector increases, the steering angle will tend to minimize the state vector's augmentation. Should the state vector be reduced to zero, the steering angle also decreases to zero; at this moment, the tractor semi-trailer will return to its straightforward direction.

2. Secondly, the time delay induced by the driver's physical limitations must be taken into account, because it takes time to detect the driver's - and the sensors' - state vector. The human driver adjusts the steering angle only by using the previous state vector; as a result, the mathematical driving model must include the time delay.

The mathematical model for the human driver model includes both aspects of the human driver's behaviours as proposed by Garrott [44] and based on the quasi-linear model presented in equation (1.6) . For our research, we have written the steering angle as

$$\delta(t) = h_1 \dot{y}_1(t-T_r) + h_2 r_1(t-T_r) + h_3 r_2(t-T_r) + h_4 y_1(t-T_r) + h_5 \phi_1(t-T_r) + h_6 \phi_2(t-T_r) \tag{3.39}$$

where the constants $h_1, h_2, h_3, h_4, h_5, h_6$ are real numbers determined mainly by the tractor semi-trailer's characteristics, disturbances, and the tractor's speed. The steering angle can be expressed by two vectors: H as a control vector, and $q(t)$ as a state vector.

$$\delta(t) = Hq(t - T_r) \tag{3.40}$$

Where $H = [h_1, h_2, h_3, h_4, h_5, h_6]$

$$q(t - T_r) = [\dot{y}_1(t - T_r), r_1(t - T_r), r_2(t - T_r), y_1(t - T_r), \phi_1(t - T_r), \phi_2(t - T_r)]^T$$

3.3 The tractor semi-trailer control system with time delay

Figure 10 shows the total tractor semi-trailer/driver control model, in which the driver detects the state vector $q(t)$ as well as the disturbances, then adjusts the steering angle $\delta(t)$. The steering angle $\delta(t)$ is the input of the tractor semi-trailer; the state vector is the output of the tractor semi-trailer.

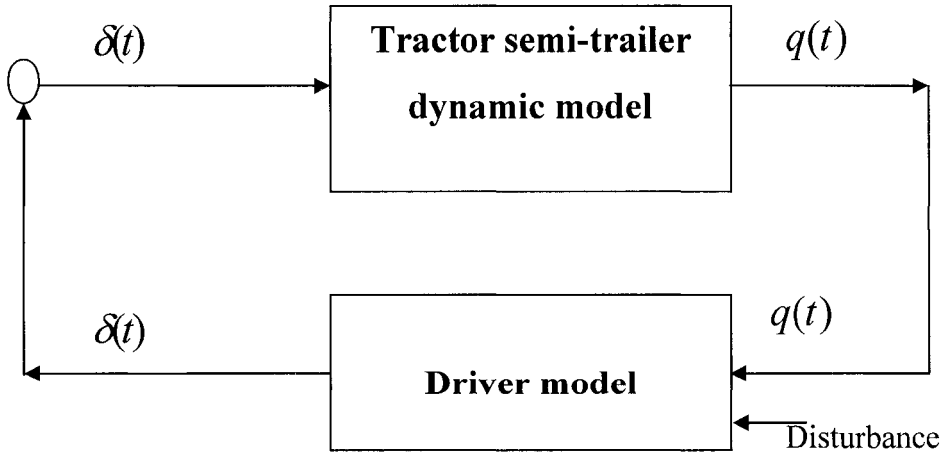

Figure 10 Tractor semi-trailer/driver control model

After some transformations, the tractor semi-trailer dynamic model (3.38) can be written as $q(t)$. The resulting equation is expressed as follows:

$$M\dot{q}(t) + Nq(t) = P\delta(t) \tag{3.41}$$

where

$$q(t) = [\dot{y}_1, r_1, r_2, y_1, \varphi_1, \varphi_2]^T$$

$$M = \begin{bmatrix} A & B \\ 0 & I \end{bmatrix}$$

$$N = \begin{bmatrix} 0 & C \\ -I & 0 \end{bmatrix}$$

$$P = \begin{bmatrix} D \\ 0 \end{bmatrix}$$

Substituting (3.40) into (3.41) yields the tractor semi-trailer control system:

$$\begin{aligned} M\dot{q}(t) + Nq(t) &= PHq(t - T_r) && 0 \le t \le T \\ q(t) &= 0 && -T_r \le t \le 0 \end{aligned} \tag{3.42}$$

From equation (3.42), vector H is the optimal control value. Identifying the tractor semi-trailer/driver system's parameters involves searching optimal control vector H : this causes state vector *q(t)* to revert to zero as quickly as possible.

3.4 Summary

In this chapter, we have investigated the tractor unit's lateral dynamics by using the bicycle model with linear tire force, as introduced in [38]. The semi-trailer unit is then attached to the tractor unit at point Q (the fifth wheel). From the viewpoint of the whole tractor semi-trailer unit, the lateral velocity of semi-trailer v_2 can be expressed using the

tractor's lateral velocity, yaw velocity and vehicle parameters, taking into account that the tractor and semi-trailer units both have the same lateral velocities at point Q. Thus, the 3-DOF lateral dynamic equations can take form. The driver steering model can also be extended to the 3-DOF model from the 2-DOF model used by T. Legouis *et al.* [36]. We obtained the closed-loop tractor semi-trailer lateral dynamic equations by using the lateral dynamic model and the driver model. From the closed-loop tractor semi-trailer lateral dynamic equations, we found that optimal control vector H is the parameter needing identification.

CHAPTER 4

SOLUTION METHOD FOR SOLVING TIME-DELAYED SYSTEM AND OPTIMAL CONTROL PROBLEM

In this chapter, a numerical integration method and an optimization method are proposed with a view to solving optimal control vector H, given in (3.40). A cost function defined by the state vector and a constant matrix is used to determine optimal driving parameters. The cost function has previously been used by T. Legouis *et al.* [36]. The form of the cost function is

$$J(H) = \frac{1}{2}\int_0^T (q^T(t) Q_w q(t))dt \tag{4.1}$$

where Q_w is a given 6×6 weighting matrix; $q(t)$ is the state vector; And T is the simulation time.

Vector H is calculated as follows:

1. An arbitrary initial value is defined for control vector H and weighting matrix Q_w with regard to $0 \le t \le T$;
2. The state vector $q(t)$ is computed by using a modified Runge-Kutta method to solve the differential equations (3.42).
3. The cost function is computed with the state vector $q(t)$.
4. The Simulated Annealing method is used to search the minimum cost function, after which optimal control vector H can be determined.

4.1 Modified Runge-Kutta (RK) method for solving the differential-equation system with time delay

For the purpose of solving the differential equation (3.42) using the Runge-Kutta method, the differential equation (3.42) is written as follows:

$$\dot{q}(t) = M^{-1}(PHq(t-T_r) - Nq(t)) \qquad 0 \le t \le T \qquad (4.2)$$
$$q(t) = 0 \qquad -T_r \le t \le 0$$

The numerical Runge-Kutta method is often used to solve differential equations without time delay. Time delay does exist in the tractor semi-trailer/driver system. For the purpose of solving the time delay problem, the differential equation (4.2) can be divided into two parts. Where $0 \le t \le T_r$, $q(t-T_r)$ is zero; where $T_r \le t \le T$, $q(t-T_r)$ is the previous $q(t)$. Consequently, the time-delay problem can be solved, and the differential equation (4.2) written in this way:

$$\dot{q}(t) = -M^{-1}Nq(t) \qquad 0 \le t \le T_r \qquad (4.2a)$$
$$\dot{q}(t) = M^{-1}(PHq(t-T_r) - Nq(t)) \qquad T_r \le t \le T \qquad (4.2b)$$

The procedure for using the RK method is as follows:

Given vector q_{n-1} as an approximation to $q(x_{n-1})$, where q satisfies the differential equation system:

$$\dot{q}(t) = f(q(t)) \qquad (4.3)$$

the approximation q_n to $q(t_n)$ is computed by evaluating equations (4.4), for $i = 1,2,...,s$,

$$F_i = f(Y_i) \qquad (4.4)$$

where $Y_1, Y_2, ..., Y_s$ are given by

$$Y_i = q_{n-1} + h\sum_{j<i} a_{ij} F_j \tag{4.5}$$

We must then evaluate

$$q_n = q_{n-1} + h\sum_{j=1}^{s} b_j F_j \tag{4.6}$$

The quantities $Y_1, Y_2, ..., Y_s$, as given by (4.5), are approximations to solution values $q(t)$ for t ranging through various values near t_{n-1}. Also, from (4.4), we see that $F_1, F_2, ..., F_s$ are approximations to $\dot{q}(t)$ at the same values. Specifically, because the sum in (4.5) is empty when $i = 1$, $Y_i = q_{n-1}$ is therefore an approximation to $q(x_{n-1})$ and F_i is an approximation to $\dot{q}(t_{n-1})$. The integer s represents the number of evaluations of f per step equals s. The set of numbers $a_{21}, a_{31}, a_{32}, ..., a_{s,s-1}$, $b_1, b_2, ..., b_s$ are constants characterizing any particular method of this type.

4.2 The Simulated Annealing (SA) algorithm for an optimal control system

The Simulated Annealing algorithm refers to a physical process that establishes different crystalline structures, each of which can be associated with a different minimum potential energy. Figure 11 demonstrates the Annealing process. These crystalline structures move with high energy at high temperatures. When temperature is reduced, the kinetic energy drifts towards low energy. At the end of the process, different crystalline structures will become stagnant and converge into a global minimum potential energy. This process is completed by the reheating and cooling of the materials/metals while controlling the rate of cooling. Based on the use of statistical mechanics, this algorithm establishes thermal equilibrium in a collection of atoms. The term itself is more representative of the process of cooling materials, particularly metals, after raising their temperature to achieve a definite crystalline state. But the extension to optimization is mainly heuristic [47].

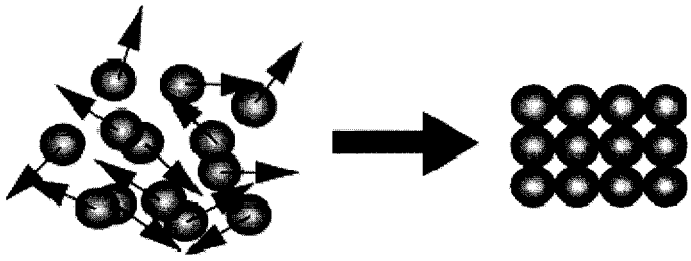

Figure 11 The annealing process

4.2.1 Normal simulated annealing algorithm for a vehicle/driver dynamic system

The normal way of using the Simulated Annealing algorithm is to generate a new control value H via random selection, and then evaluate a new value H using a cost function: this will result in the acceptance or rejection of the new value H. The present algorithm uses a rate that accepts a value that is not optimal, even in cases where the new value H is rejected. This rate will prevent a value from being trapped within a local optimal value. The Simulated Annealing algorithm for the vehicle/driver dynamic system is presented below:

Step 1: Choose a starting design x_0 and calculate the cost function $J_0=f(x_0)$
(requirements: stopping criteria, initial temperature)

Step 2: Choose a random point on the surface of a unit n-dimensional hyper sphere to establish a search direction S (the sphere is in n-dimensions)

Step 3: Using a random step size A, calculate
$J_1=f(x0+AS)$, $\Delta J = J_0 - J_1$

Step 4: If $\Delta J \le 0$,then $p=1$, otherwise, $p = \exp(-\beta \cdot \Delta J)$

Step 5: A random number r ($0<r<1$) is generated.

If $r \le p$, then the step is accepted and the design vector is updated.

Otherwise, no change is made to the design.

Step 6: Temperature is dropped with a ratio α ; go back to Step 2.

Implementing the algorithm will trigger a larger number of iterations in order to drift the solution towards a global minimum. Through careful observation, α and β are seen to be important parameters for the algorithm. Therefore, the selection of α and β is essential for maintaining the accuracy of the calculation.

Generally speaking, parameter β can be related to the Boltzmann probability distribution. In statistical mechanics it is expressed as –k/T: T is considered to be the annealing temperature, and k is the Boltzmann constant. It dictates the conditional probability that a worse solution can be accepted. For the algorithm to be effective, it is recommended that the acceptance ratio r lie within in the $0.5<r<0.9$ range.

The following ideas are apparent in the algorithm:

- the algorithm is heuristic;
- the algorithm is suggestive of a biased random walk;
- decrease in the function is directly accommodated;
- directions that increase the value of the function are sometimes permitted. This is important in order to escape a local optimum. It represents the potential for discovering the global optimum by means of the algorithm.

4.2.2 Solving the optimal control problem using improved Simulated Annealing (SA)

To solve the tractor semi-trailer/driver control system, some calculation steps have been taken in order to improve the performance of the Simulated Annealing algorithm. If we use random step size to generate the new control vector, it will be very difficult to obtain an accurate solution, because solving the control problem is not the same as solving a combination problem such as one involving *Travel Salesman Problem* (TSP). The difference between these two problems is that the combination problem has very large, though finite, solution space; the solution space for a control problem is infinite, because

the solution space belongs to all real numbers (R). In order to use the Simulated Annealing algorithm, we should define its precision in calculation, so that the solution space becomes finite. In the improved Simulated Annealing method, we have chosen this calculation precision as a fixed-step size.

Figure 12 illustrates the improved Simulated Annealing (SA) method for solving the tractor semi-trailer/driver control system. At the beginning of the program, the initial control vector H, initial temperature T, and the search step are given. The initial cost function J_0 can be obtained using equation (4.1). The new control vector is generated by adding the search step to the first element of the control vector. The new cost function J can be obtained using equation (4.1). Comparing the initial cost function J_0 with the new cost function J will lead to the acceptance of the new control vector. If J is smaller than J_0, J will take the place of cost function J_0; if J is greater than J_0, however, this means that the new control vector and search direction are poor and cannot generate the most accurate control. A change in search direction is then required in order to generate a new control vector H. A new cost function J is thus obtained. Then, when the initial cost function J_0 is compared with the new cost function J, if J is smaller than J_0, this means that the new control vector has been accepted and will update cost function J_0 by J; if J is still greater than J_0, an acceptance rate β is introduced in order to decide whether to accept the new cost function or not. The acceptance rate can help the program to jump out of the local optimal solution. The program then returns to the second step and generates a new control vector, using the same step to decide whether or not to accept the new control vector. After a sufficient number of iterations, the cost function becomes stable and then accepts the current H as the optimization control vector.

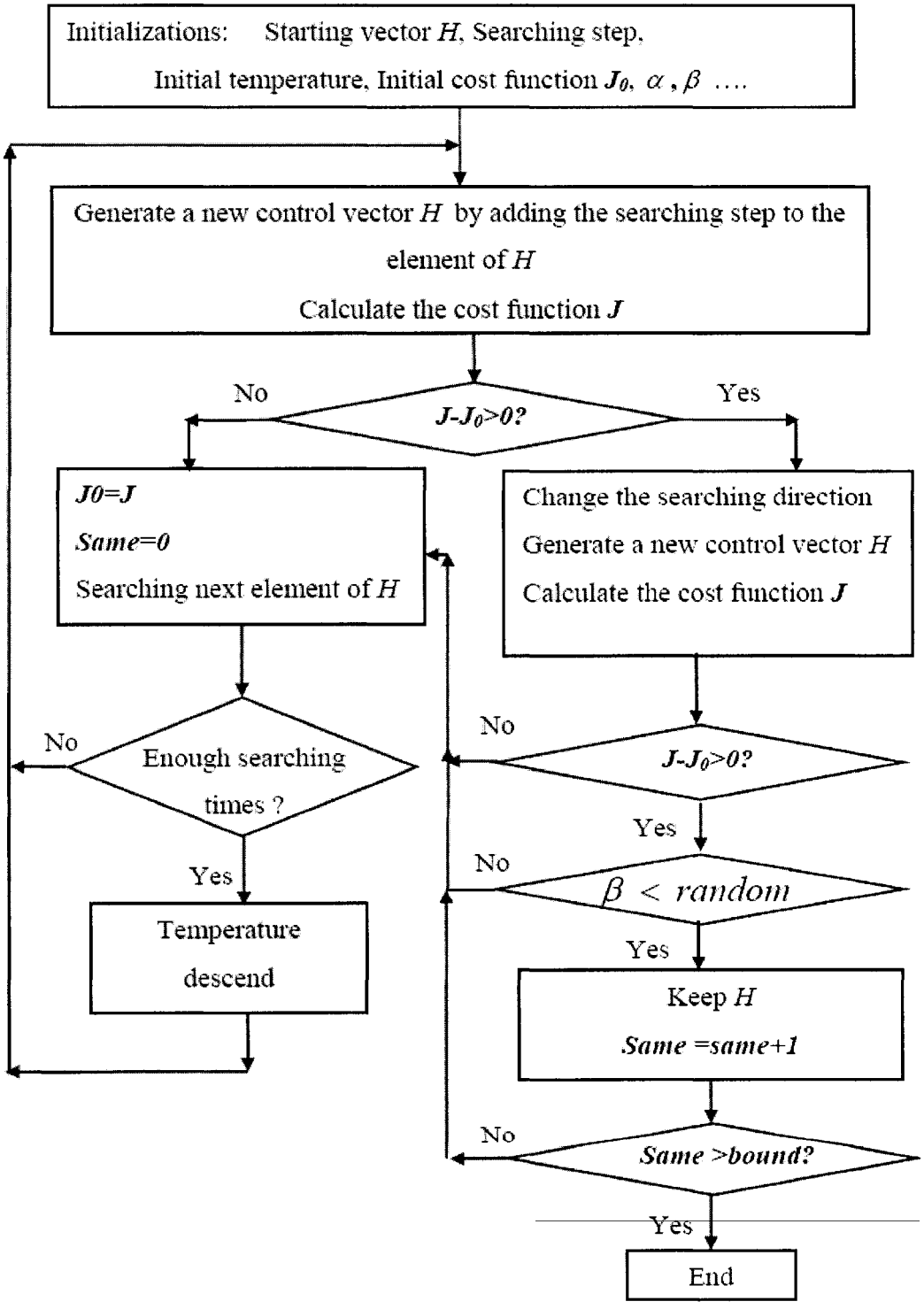

Figure 12 Improved SA method for solving the tractor semi-trailer/driver system

4.2.3 Parameter settings for the SA algorithm

Parameter settings for the SA method are determined by trial and error, based on results and computing time. Here, the tractor semi-trailer's parameters, which have been taken from a paper by *Tai et al.*[46], are listed in Table I in order to set parameters for the SA method.

Table I

Parameters for the tractor semi-trailer

	Tractor semi-trailer
m_1 (Kg)	7956
m_2 (Kg)	10682
I_{z1} (Kg×m^2)	32000
I_{z2} (Kg×m^2)	482790
a_1 (m)	1.68
b_1 (m)	3.67
b_2 (m)	7.32
c_1 (m)	3.56
c_2 (m)	2.9
C_{af} (N/rad)	177678
C_{r1} (N/rad)	710713.5
C_{r2} (N/rad)	710713.5

After some trial and error, the parameters of the SA method are set as follows:

- Initial temperature $T=800$
- Temperature decrease rate $\alpha = 0.9$
- Initial control vector $H=[0\ 0\ 0\ 0\ 0\ 0]$
- Search step $h=0.001$
- Boundary times $bound=2000$
- Times unchanged by the control vector = *Same*
- Number of iterations at each temperature $times=500$

The SA method will stop under two conditions: firstly, when the final temperature reaches 10; secondly, when control vector H has remained unchanged for 2000 iterations. The optimal control problem has no accurate solution, only a global optimal solution. In consequence, very small variations in cost function exist according to various control vectors H. These small variations affect acceptance of the control vector. Thus, a boundary value of acceptance of the control vector is defined as 0.00003 if the descending cost function is less than the boundary value. The cost function is considered unchanged and control vector H is not updated.

4.2.4 Results of parameter setting

Using the parameter values determined in 3.2.3, control vector H can be computed. Figure 13 illustrates variations in control vector H. The y-axis shows the values of each element in the control vector, and the x-axis shows the number of iterations. At first, all elements of the control vector are zero. After a few iterations, the elements become steady and the control vector remains the same, reaching a steady state. Figure 13 shows that the elements affect one another for the purpose of minimizing the cost function. At the end of the process, the cost function becomes stable, and an optimal control vector H is obtained.

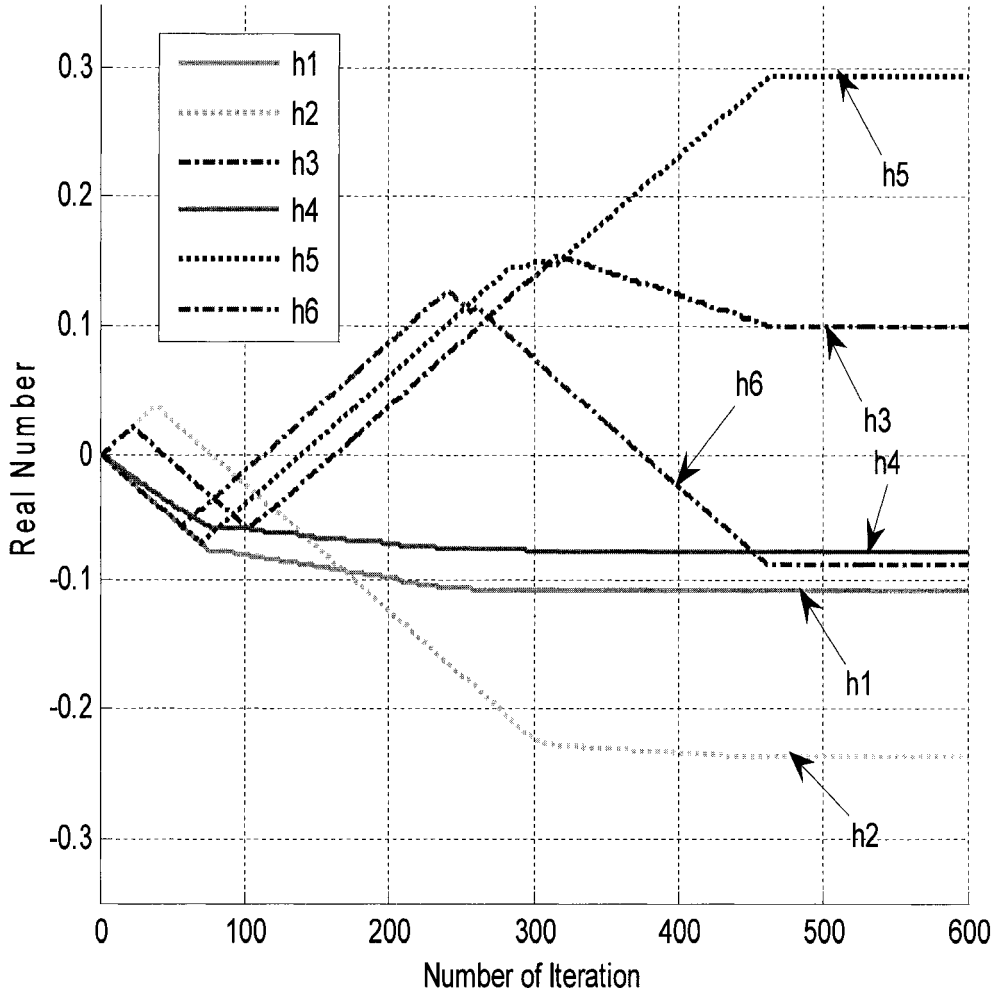

Figure 13 Variation of control vector H as a function of the number of iterations

Figure 14 shows the convergence of the cost function. As the iterations begin, the cost function decreases rapidly, reaching a steady state very soon. This demonstrates that the parameter setting is suitable, and that the SA method is well suited for solving the tractor semi-trailer optimal control system.

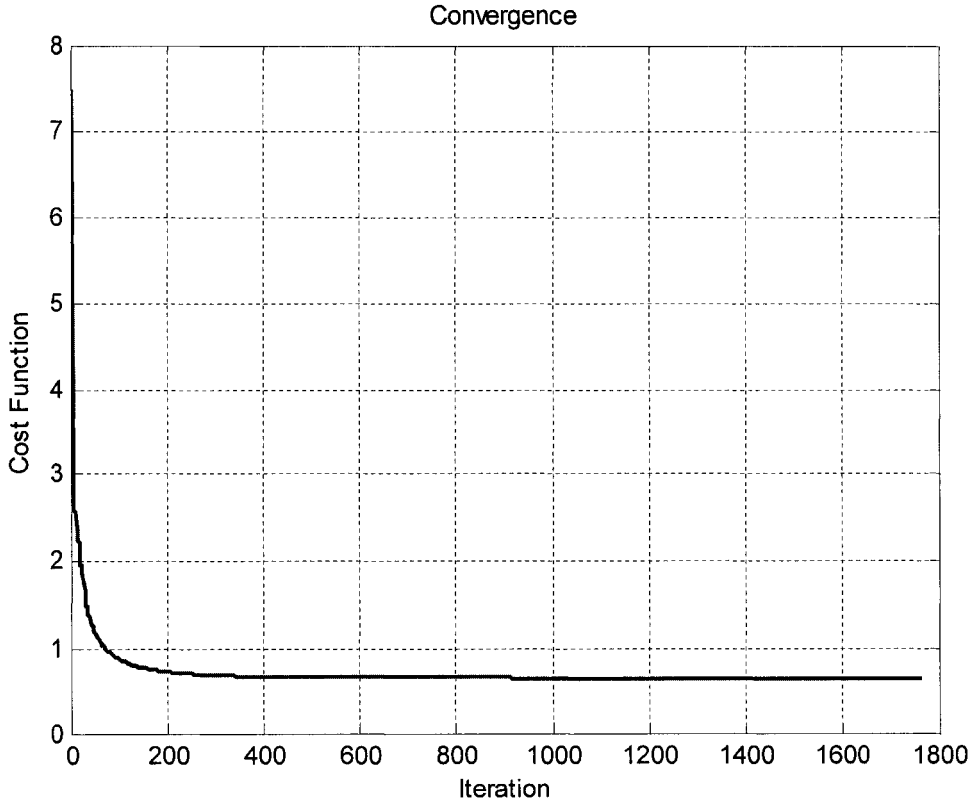

Figure 14 Convergence of cost function in terms of iterations

Figure 15 illustrates the annealing speed. The x-axis represents the acceptance times and the y-axis, the anneal values. Along the y-axis, negative values illustrate that the new cost function is smaller than the old cost function; on the other hand,, positive values reveal that the new cost function is greater than the old cost function. At each update, both negative and positive values are accepted. The SA method can accept some poor values: this demonstrates that the SA method can avoid falling into local optimization.

Figures 13, 14 and 15 demonstrate that the parameters of Simulated Annealing are set suitably and exactly; using these parameters, the Simulated Annealing method can perform well.

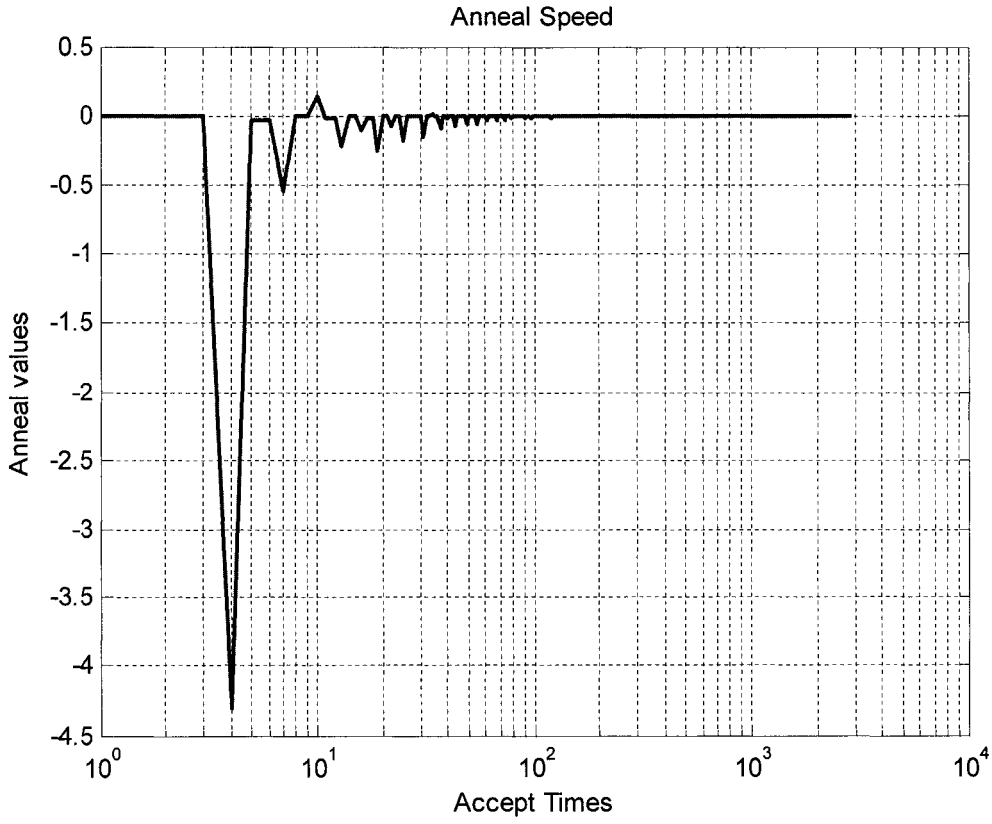

Figure 15 Anneal speed

4.3 Summary

This chapter has proposed a modified Runge-Kutta method for solving differential equations with time delay as well as an improved SA method for searching an optimal control vector *H*. Using a set of tractor semi-trailer parameters, the improved SA method has been applied in order to seek optimal control vector *H*. The convergence of the cost function and anneal speed enables us to conclude that the improved SA method is adequate for seeking optimal control vector *H*.

CHAPTER 5

SIMULATION RESULTS

This chapter begins by introducing the tractor semi-trailer's dynamic responses. The second section emphasizes velocity, trailer loads and time delay as factors affecting the tractor semi-trailer's dynamic behaviour. A second type of tractor semi-trailer is then introduced in order to compare how the tractor semi-trailer's parameters affect its dynamic behaviour.

5.1 Dynamic responses of the tractor semi-trailer in cases of lateral disturbance

In considering the tractor semi-trailer's response to a lateral-force input equivalent to a response to step lateral displacement, the free motion of response may be considered as the basis upon which the tractor semi-trailer's degree of safety should be assessed. In order to evaluate the tractor semi-trailer's degree of safety, some assumptions are introduced, as follows:

- an initial step lateral displacement $y = 1\,m$, $(t = 0)$
- no external forces other than road-tire forces;
- constant forward speed is $u = 100\ km/h$;
- lag time $T_r = 0.2\,s$;
- the aim of the optimization control is to steer the tractor semi-trailer back to its initial course; $y = 0$
- the tractor semi-trailer's parameters and the parameter setting for the SA method have been presented in Chapter 3.

5.1.1 Control vector *H* and steering angle response

It has been proposed that the steering angle be expressed by control vector *H* and the state vector. Table II shows control vector *H,* which is searched by the SA method for a step lateral displacement.

Table II

Optimal control vector *H*

H	h_1	h_2	h_3	h_4	h_5	h_6
	-0.109	-0.269	-0.063	-0.077	0.754	-0.55

Figure 16 illustrates the steering angle as a function of time. The steering angle is the input of the tractor semi-trailer/driver control system, while the optimal steering angle shows the behaviour of a well-trained human driver. Figure 16 shows once again that the tractor semi-trailer/driver control system is well controlled.

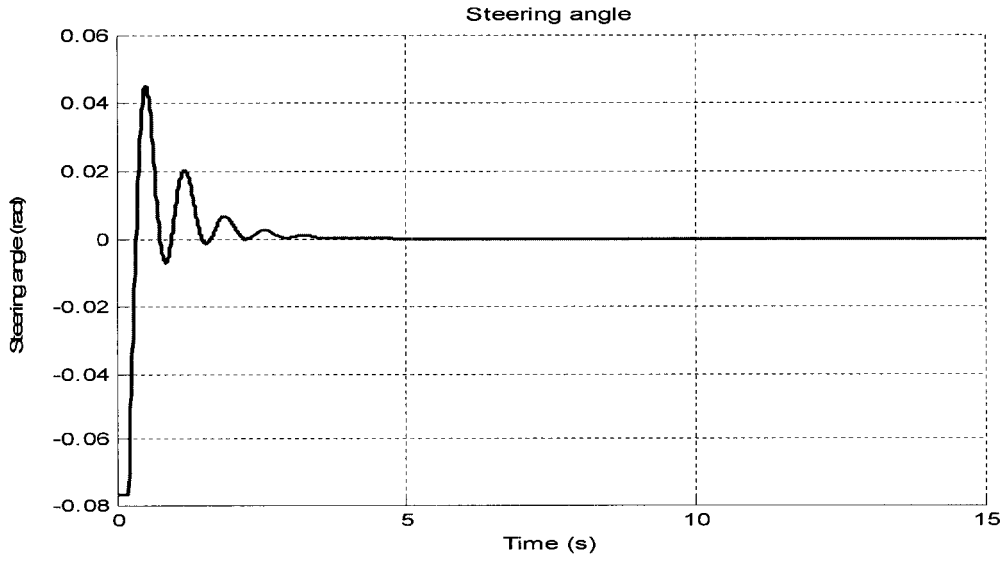

Figure 16 Steering angle for step lateral displacement

5.1.2 Responses to lateral displacement and lateral velocity

A human driver can more easily detect lateral displacement than lateral velocity. The human driver can guide his tractor semi-trailer back to its previous course simply by adjusting the steering wheel. Figure 17 shows the response of lateral displacement as a function of time. From the tractor semi-trailer's trajectory, we observe that the human driver always tries to minimize lateral displacement. The tractor semi-trailer returns to its previous course rapidly and smoothly, without oscillation. The tractor semi-trailer/driver system is considered to be stable.

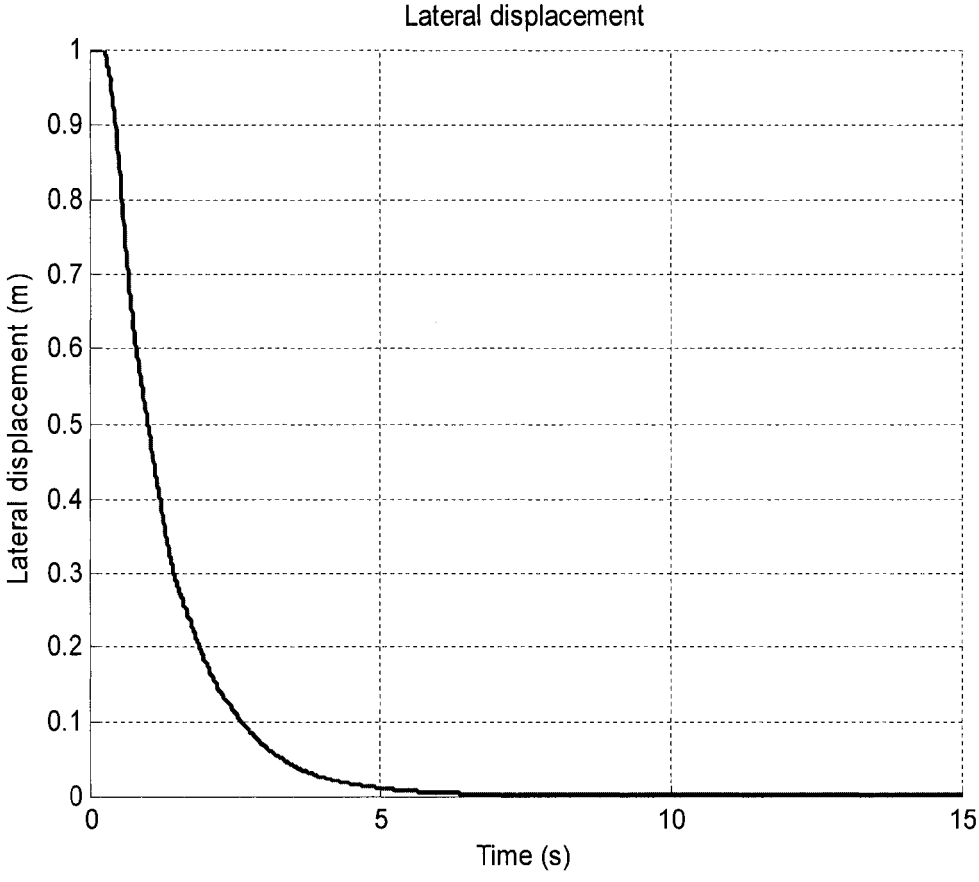

Figure 17 Lateral displacement

Figure 18 shows the response of lateral velocity as a function of time. Maximal lateral velocity is less than 1 m/s, and lateral velocity returns to zero in just under 5 seconds. In Figure 18, the disturbances before the fifth second are mainly caused by the driver's disability to detect lateral velocity directly; therefore, lateral velocity cannot be controlled completely.

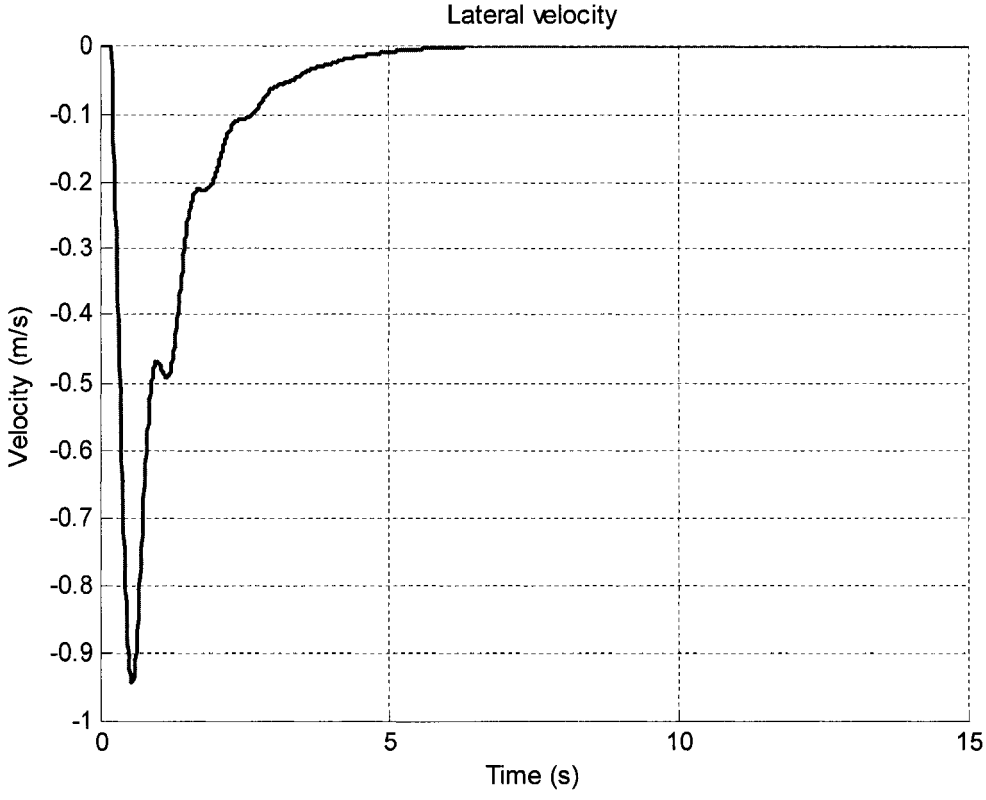

Figure 18 Lateral velocity

5.1.3 Responses to yaw angle and yaw velocity

Figure 19 illustrates the tractor's yaw velocities and yaw angles as a function of time. For the tractor semi-trailer combination, the trailer's motion states may further affect the driver's directional control in a complex manner. The tractor's yaw angle values are

therefore of relatively greater importance than are its yaw velocities. Figure 19 shows some small disturbances in the yaw angles: these are generated by the semi-trailer.

Figure 20 illustrates the semi-trailer's yaw velocity and yaw angle as a function of time. Because there are two forms of instability that lead to jack-knife and lateral oscillations of the trailer, the trailer's yaw angle values hold relatively greater importance than does yaw velocity. Figure 20 demonstrates that the semi-trailer is well controlled.

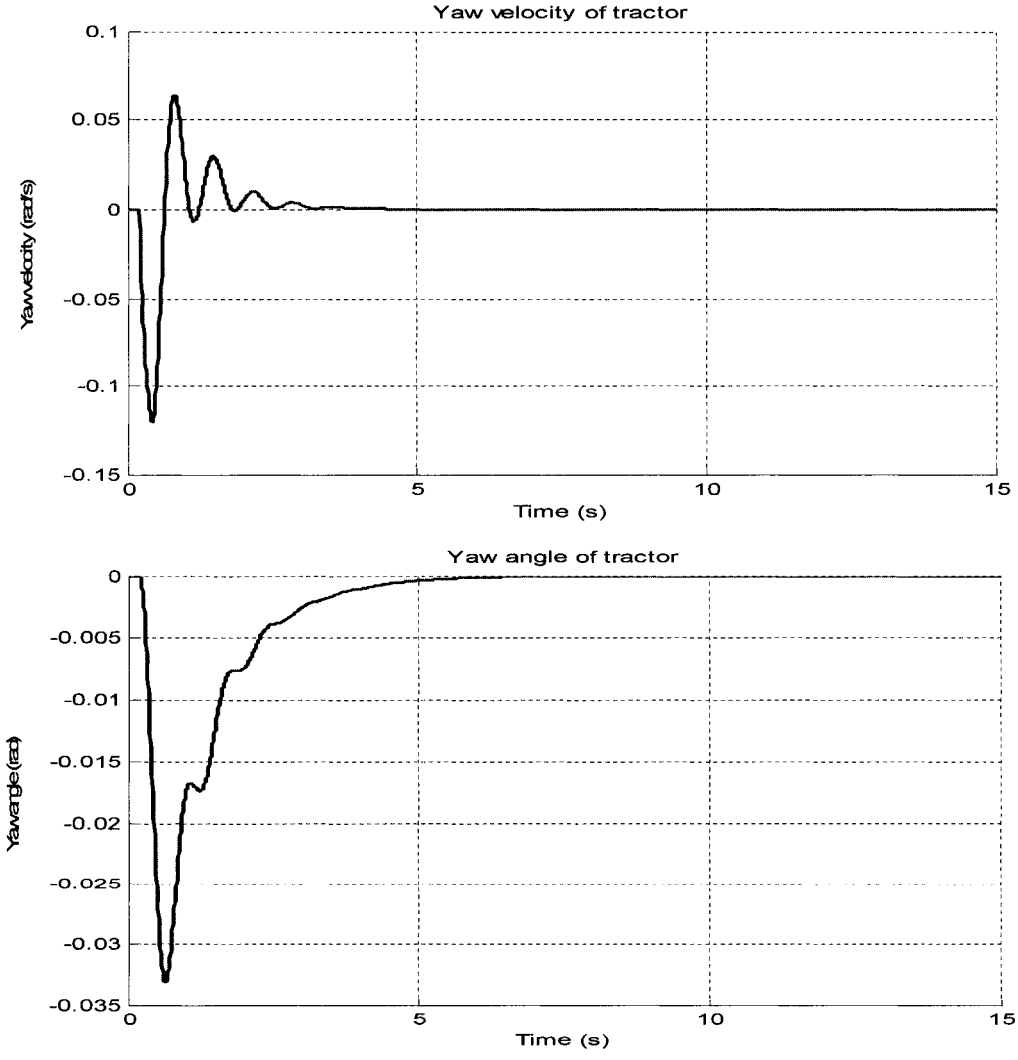

Figure 19 Yaw velocity and yaw angle of the tractor

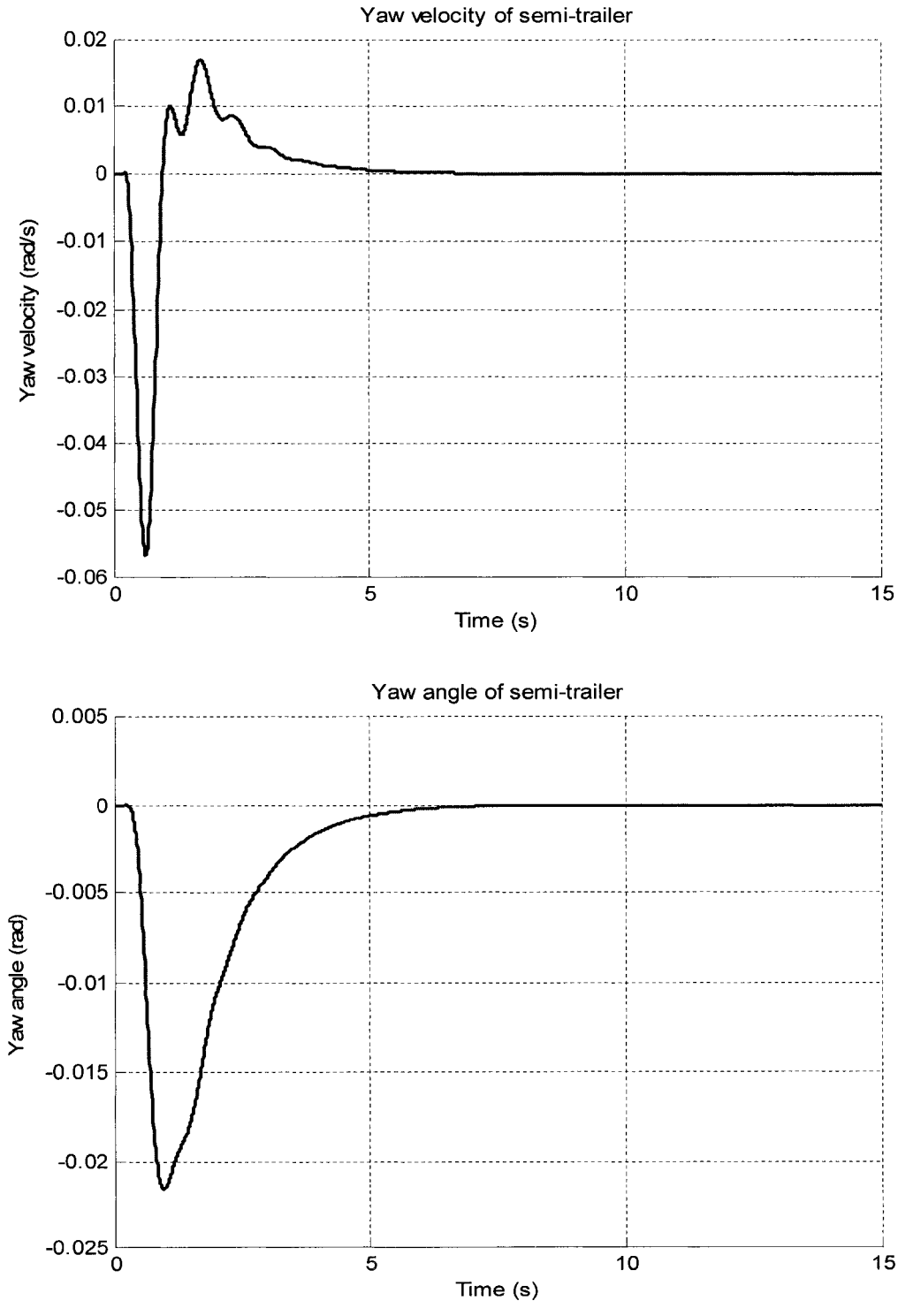

Figure 20 Yaw velocity and yaw angle of the semi-trailer

5.2 Responses to various forward speeds

This section of the thesis focuses on how forward speed affects the tractor semi-trailer's stability while it operates at high speeds on a highway. For the purpose of simulating the tractor semi-trailer's response to various forward speeds, some assumptions are made as follows:

- testing the constant forward speed u from 80 km/h to 120 km/h;
- the other conditions are the same as in **5.1.**

5.2.1 Control vector *H* and steering angle response

Table III illustrates control vector H at various forward speeds. During the forward speed of 80 km/h to 100 km/h, the elements h_1 and h_4 of control vector H remain almost stable, while elements h_3 and h_4 change more than the others.

Table III

Control vector H at various forward speeds

Speed\H	h_1	h_2	h_3	h_4	h_5	h_6
80km/h	-0.114	-0.191	0.006	-0.084	0.394	-0.332
90km/h	-0.111	-0.225	0.023	-0.08	0.443	-0.313
100km/m	-0.109	-0.269	-0.063	-0.077	0.754	-0.55
110km/h	-0.106	-0.286	-0.022	-0.074	0.678	-0.423
120km/h	-0.103	-0.29	0.038	-0.071	0.501	-0.194

Figure 21 illustrates the tractor semi-trailer's steering angles at various forward speeds. Steering-angle responses simulate the ways in which a human driver adjusts the steering wheel. Figure 21 shows that at a lower forward velocity, steering is relatively wider than it is in other cases. In the case of a relative lower forward velocity, the sensitivity of the tractor semi-trailer is relatively lower, and the human driver will have more time in which to steer his tractor semi-trailer vehicle.

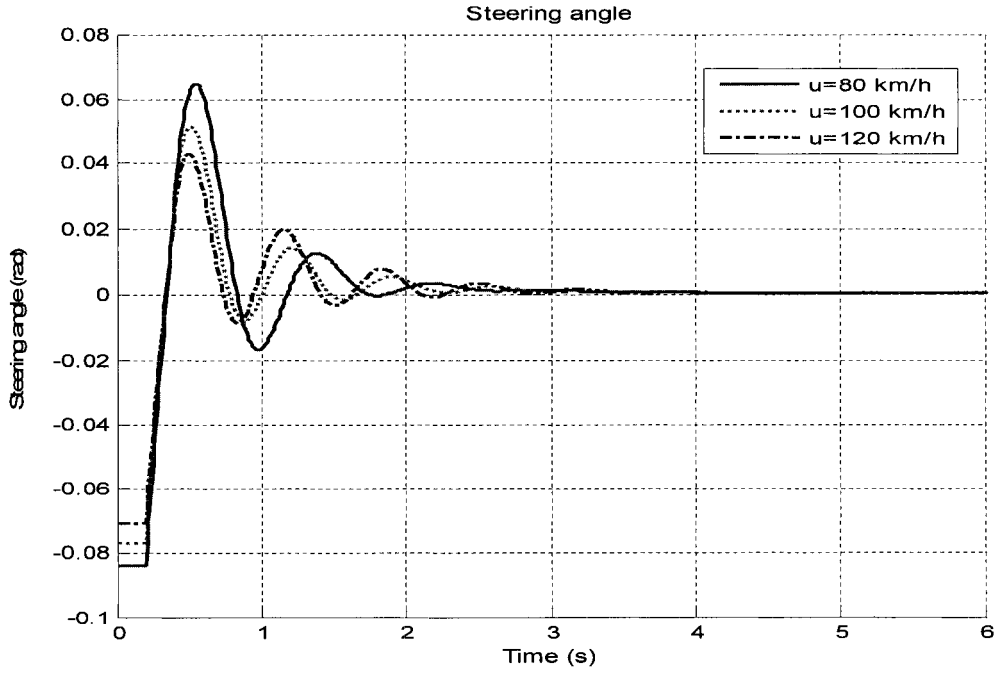

Figure 21 Steering angle at various forward speeds

5.2.2 Cost function at various forward speeds

Figure 22 illustrates values for cost function at various forward speeds. Cost function becomes greater as forward speed is increased. This means that forward speed affects the tractor semi-trailer's dynamic characteristic response. The tractor semi-trailer becomes more difficult to manipulate at higher forward speeds. At a critical forward speed, the tractor semi-trailer will go out of control: the tractor semi-trailer is no longer

stable. This phenomenon explains the need for speed limits on highways, for security reasons.

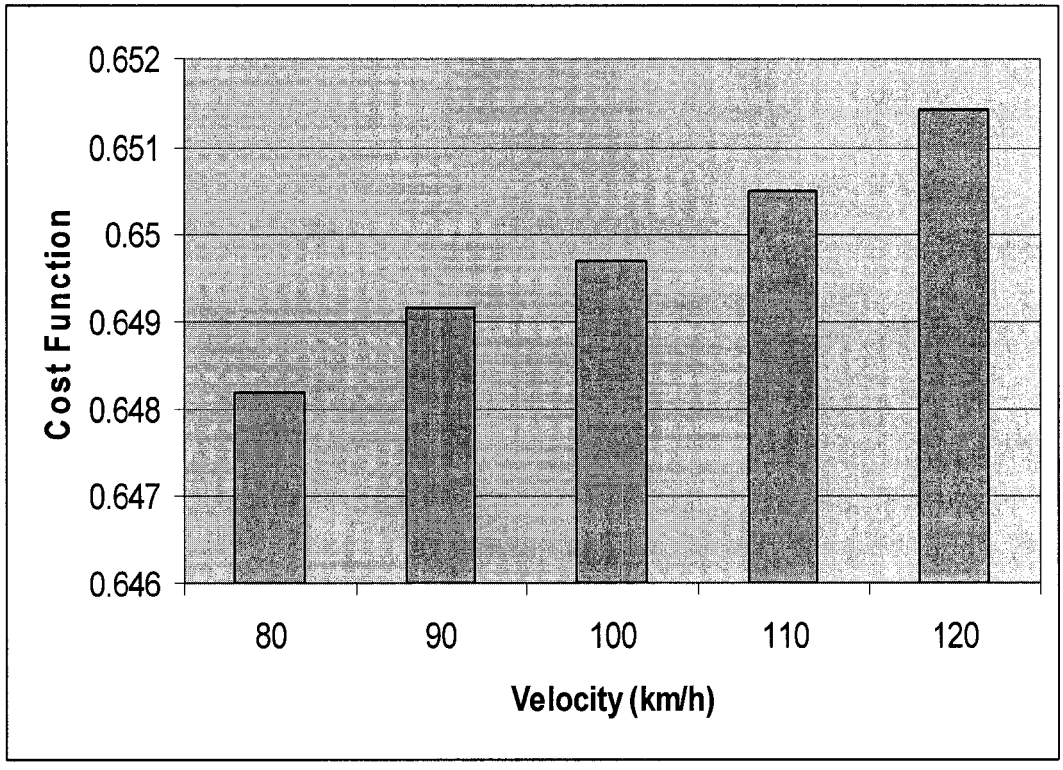

Figure 22 Cost function at various forward speeds

5.2.3 Responses to lateral displacement and lateral velocity at various forward speeds

Figure 23 illustrates values for lateral displacement at various forward speeds as a function of time. Responses to lateral displacement are similar at various forward speeds. The figure shows that there is little difference between the responses at *u=80 km/h* and *u=120 km/h*. At a latter stage, these responses reach a steady state at the same time. In consequence, we may consider that the tractor semi-trailer's responses are similar to lateral displacement within a certain range of forward speeds.

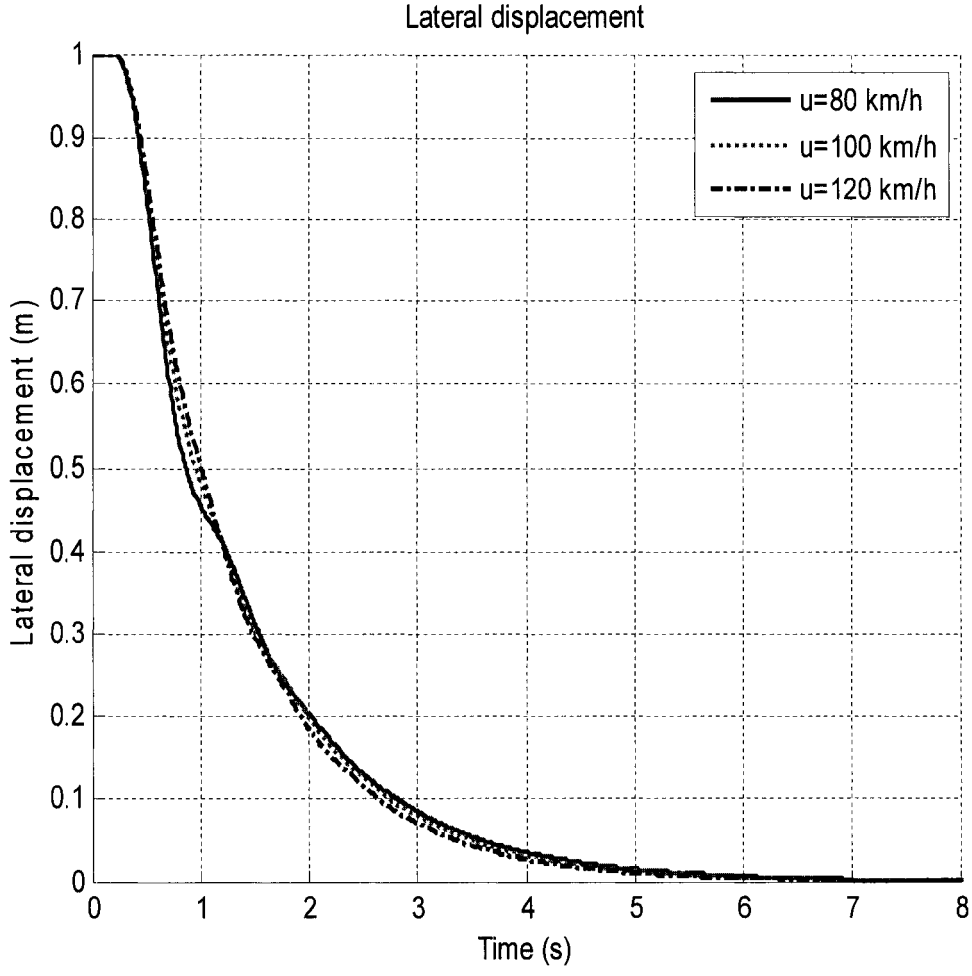

Figure 23 Lateral displacement at various forward speeds

Figure 24 illustrates lateral velocity at various forward speeds as a function of time. There are obvious differences between the responses to various forward speeds. When forward velocity *u=80 km/h*, lateral velocity is relatively lower than that of *u=100km/h*. It can thus be assumed that when the tractor semi-trailer moves at a relatively lower forward velocity, its driver can control lateral velocity easily.

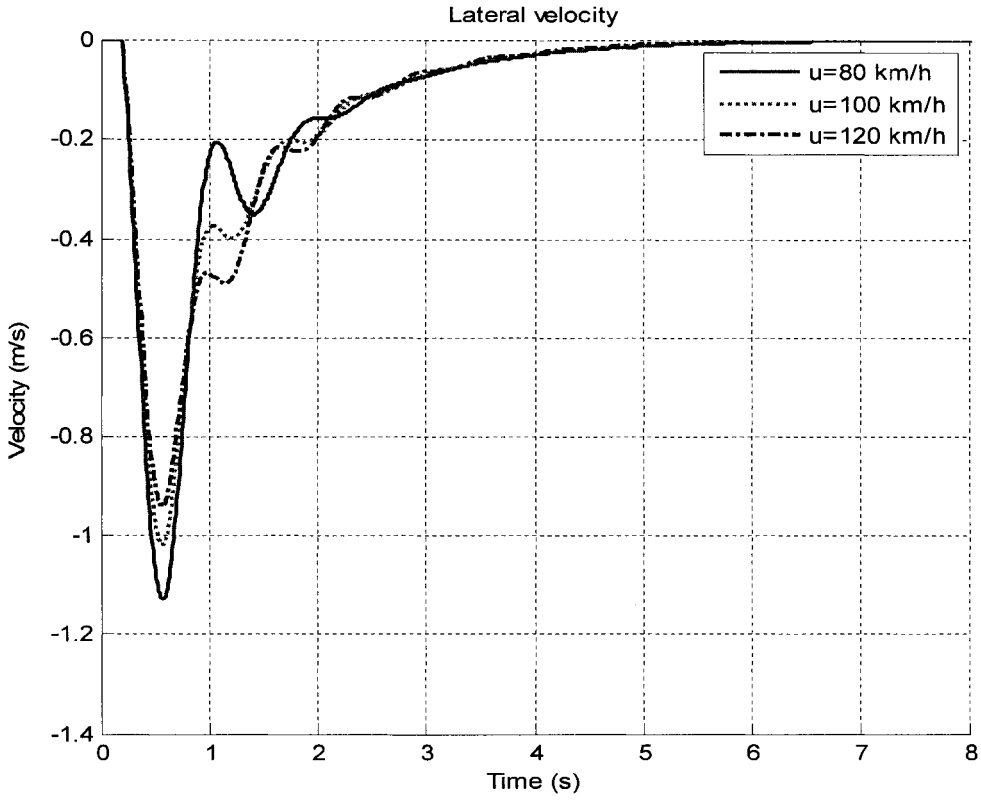

Figure 24 Lateral velocity at various forward speeds

5.2.4 Responses to yaw angles and yaw velocities at various forward speeds

Figures 25 and 26 illustrate the tractor semi-trailer's yaw velocities and yaw angles at various forward speeds. Figure 25 shows that when forward speed is lower, the tractor also has a smaller yaw angle. At a lower velocity, the tractor is easy to control. Figure 26 shows that the semi-trailer is more manageable as forward speed decreases. Figure 25 and Figure 26 demonstrate that within a certain range of forward speeds, the tractor semi-trailer has similar dynamic responses. This particular range of forward speeds may be called a "safe forward speed."

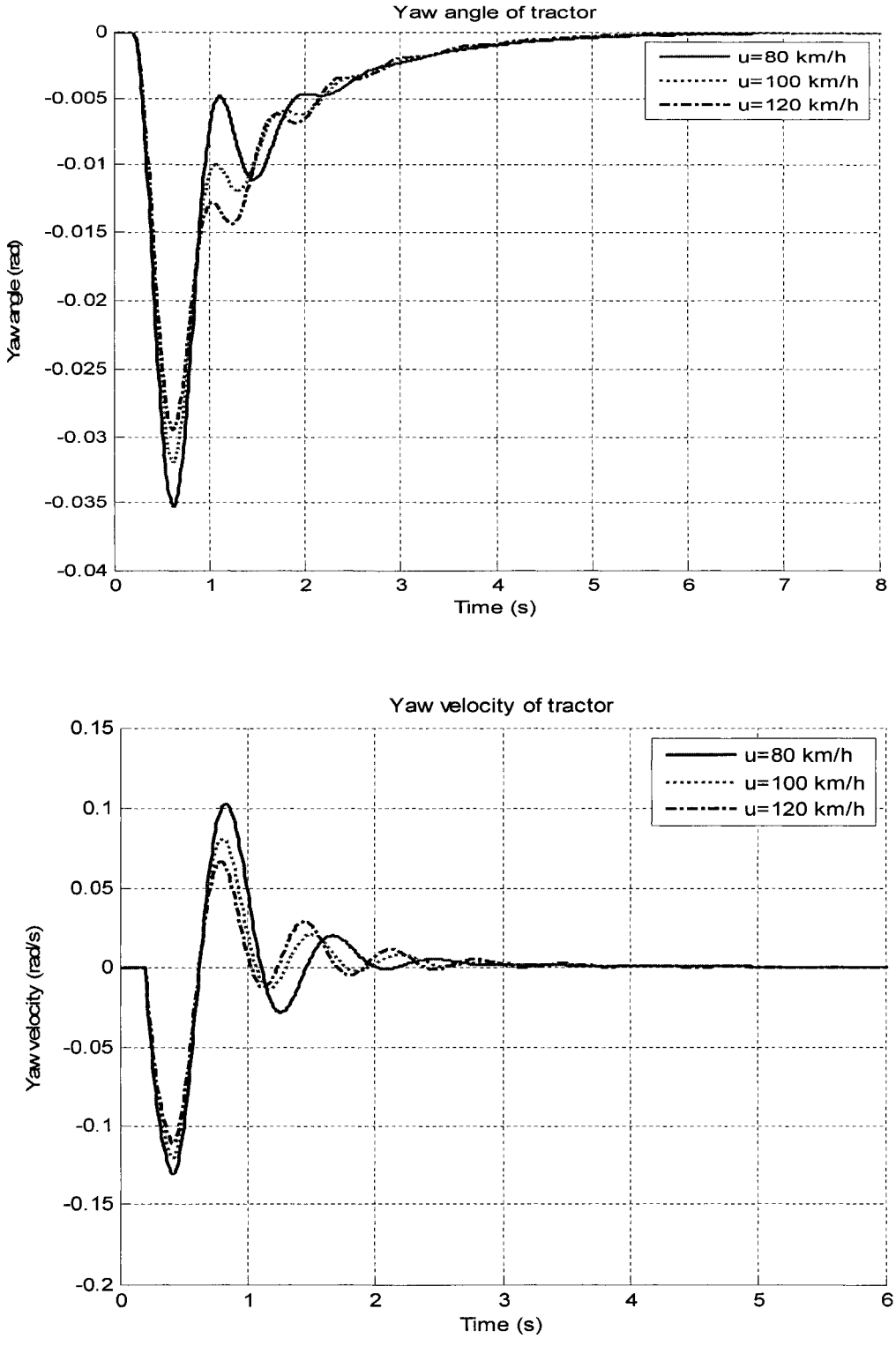

Figure 25 The tractor's yaw angle and yaw velocity at various forward speeds

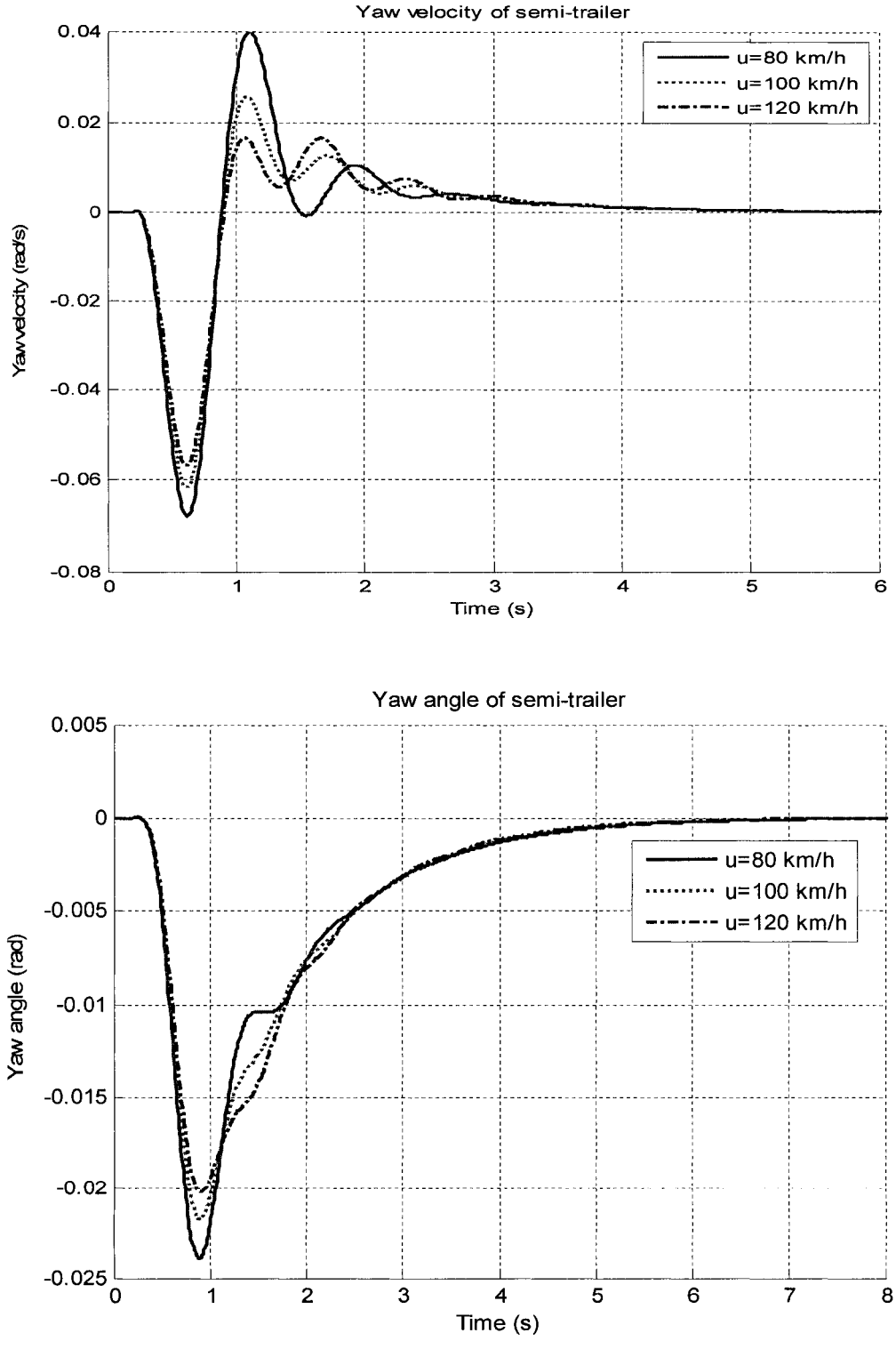

Figure 26 The semi-trailer's yaw angle and yaw velocity at various forward speeds

5.3 Responses to various semi-trailer loads

A tractor semi-trailer is often fully loaded and sometimes even overloaded. Load capacity is a crucial factor in the tractor semi-trailer's stability. In order to simulate a situation showing the effects of loads on a tractor semi-trailer's dynamic responses, some assumptions are made as follows:

- semi-trailer loads are tested from *5* to *25 tons*;
- the other conditions are the same as for **5.1**

5.3.1 Control vector *H* and steering angles at various loads

Table IV illustrates control vector *H* at various loads on the semi-trailer. During semi-trailer loads of from 5 to 25 tons, elements h_1 and h_4 of control vector *H* are almost identical: elements h_3 and h_6 change more than do the others.

Table IV

Control vector *H* at various loads on the semi-trailer

Loads\H	h_1	h_2	h_3	h_4	h_5	h_6
5T	-0.109	-0.233	0.061	-0.076	0.341	-0.105
10T	-0.109	-0.228	0.031	-0.076	0.335	-0.095
15T	-0.111	-0.222	0.006	-0.077	0.351	-0.085
20T	-0.111	-0.216	-0.025	-0.077	0.347	-0.078
25T	-0.111	-0.212	-0.059	-0.077	0.351	-0.085

Figure 27 illustrates the tractor semi-trailer's steering angles under various semi-trailer loads. Steering angle responses simulate the ways in which human drivers adjust the steering wheel. Figure 27 illustrates that within a safe load range, the steering angles are same. This also means that the semi-trailer's loads do not affect the tractor semi-trailer's dynamic responses within the range of the rated loads.

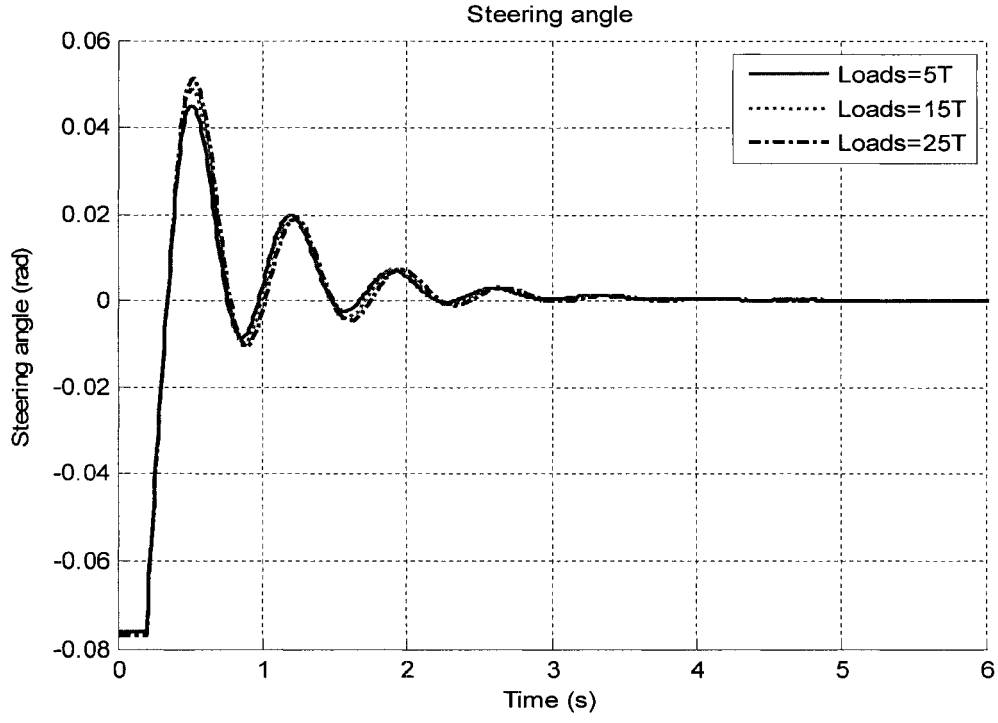

Figure 27 Steering angle for various loads

5.3.2 Cost function for various loads

Figure 28 illustrates cost function at various semi-trailer loads. The cost function becomes greater as semi-trailer loads become greater. This means semi-trailer loads affect the tractor semi-trailer's dynamic characteristic responses. With an overloaded semi-trailer, the tractor semi-trailer becomes harder to control. At critical semi-trailer loads, the tractor semi-trailer will go out of control. The tractor semi-trailer is no longer stable. Figure 28 explains, however, that cost function does not change much more. This

means that for the semi-trailer, within the 5-25 ton range, the tractor semi-trailer's dynamic responses will not change much either.

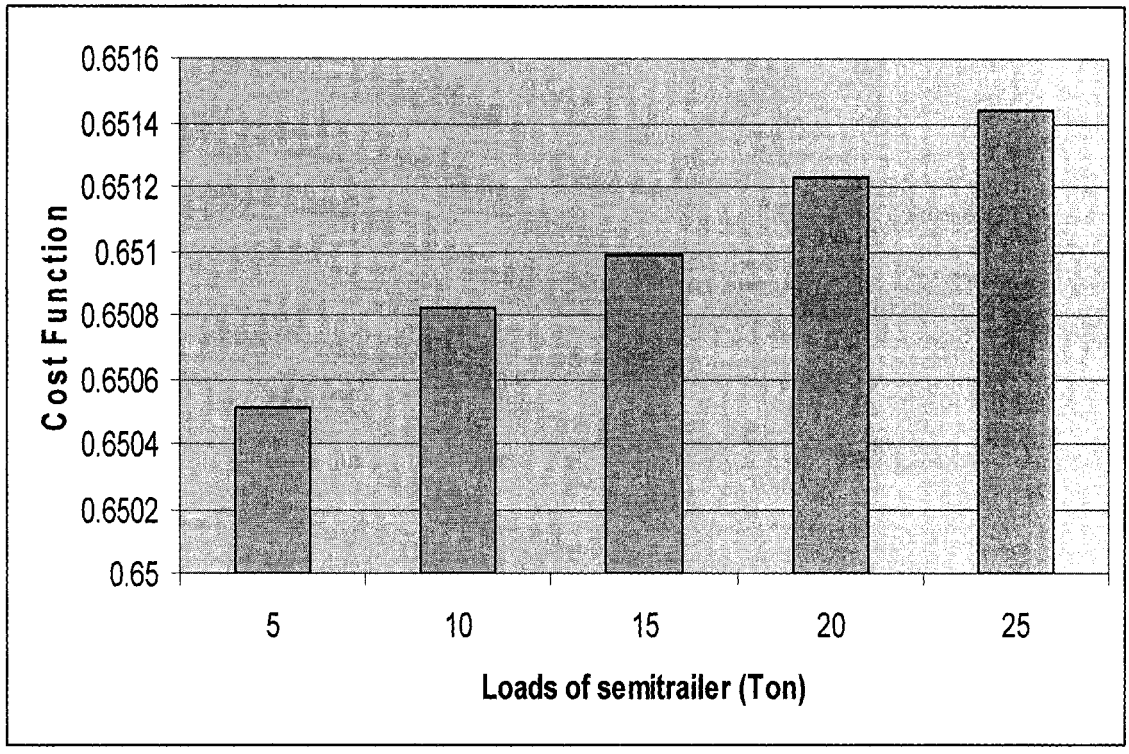

Figure 28 Cost function for various loads

5.3.3 Dynamic responses of the tractor semi-trailer at various loads on the semi-trailer

Figures 29, 30, 31 and 32 illustrate the tractor's lateral displacement, lateral velocity, yaw velocity and yaw angle, and the semi-trailer's yaw velocity and yaw angle, all at various semi-trailer loads. The tractor semi-trailer responds to various loads in exactly the same way. These figures show the same result as in Figure 28, where the tractor semi-trailer has identical dynamic responses to loads ranging from 5-25 tons. The range of safe loads is usually called the "rated load."

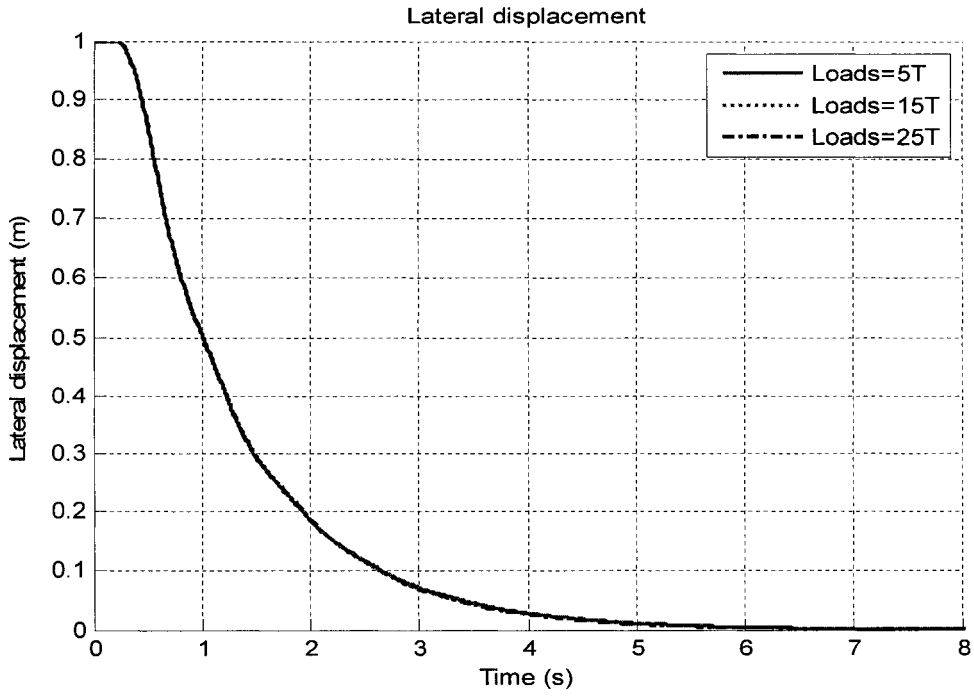

Figure 29 Lateral displacement at various loads

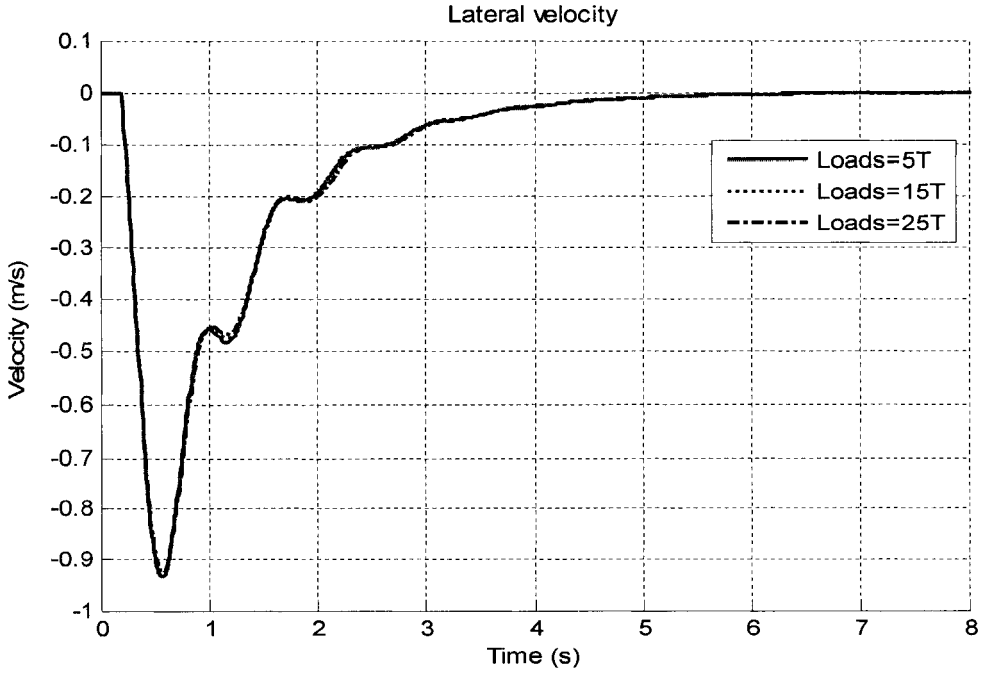

Figure 30 Lateral velocity at various loads

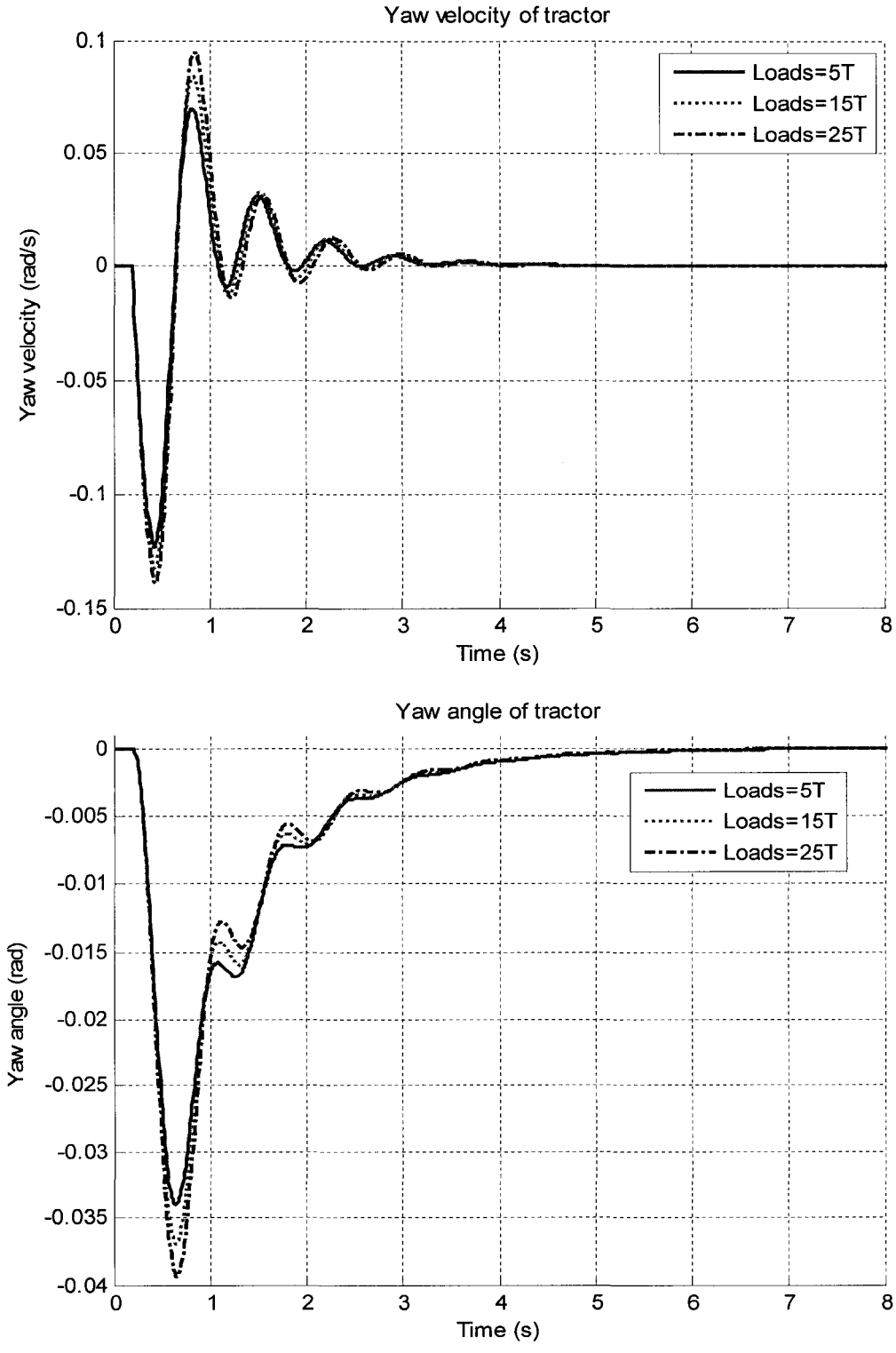

Figure 31 Yaw velocity and yaw angle of the tractor at various loads

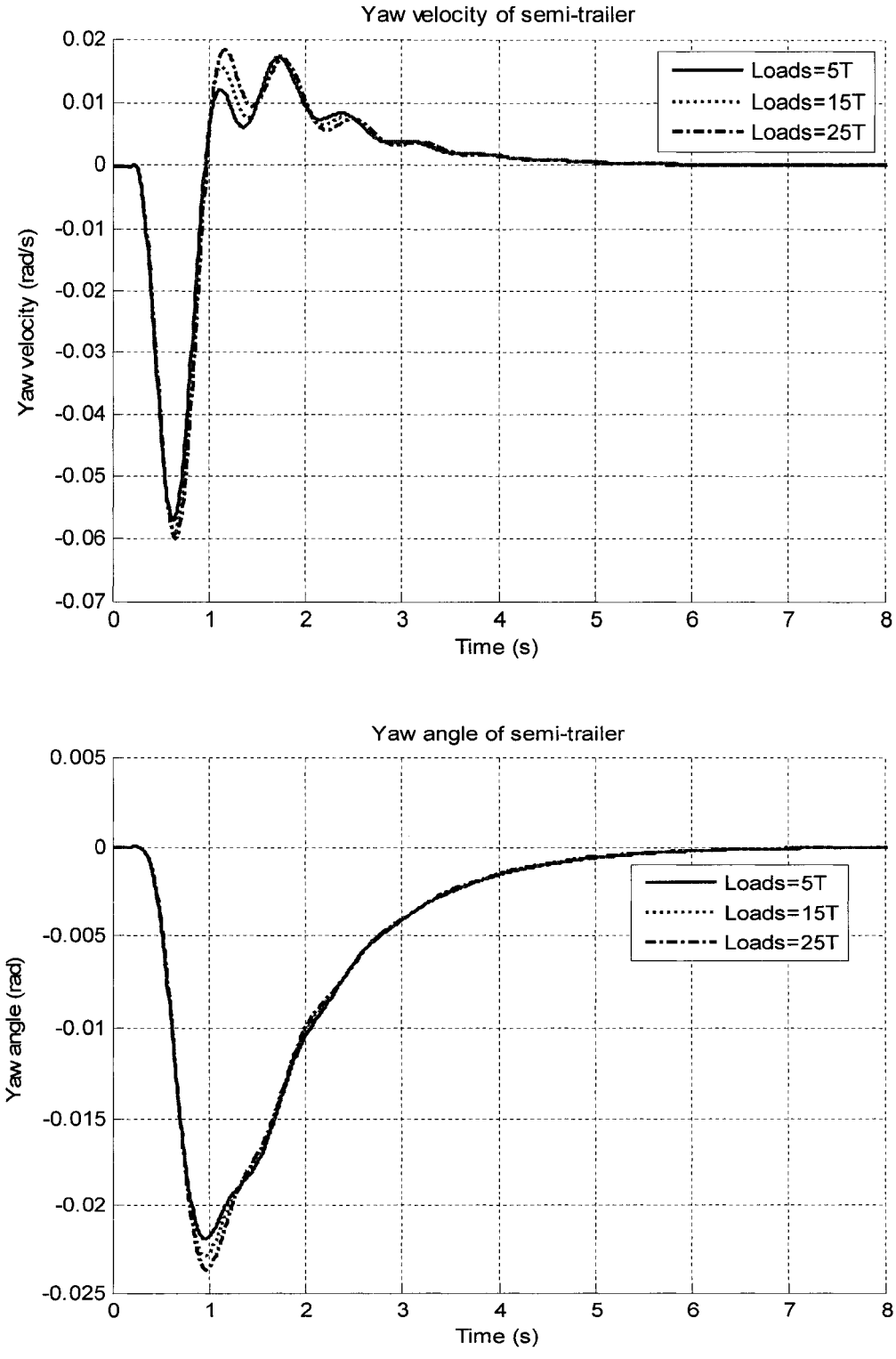

Figure 32 Yaw velocity and yaw angle of the semi-trailer at various loads

5.4 Responses to various time delays

The tractor semi-trailer/driver control system is also affected by human driver limitations. In order to simulate a situation demonstrating the impact of a human driver's time delay on the tractor semi-trailer's dynamic response, some assumptions are made as follows:

- testing the lag time T_r from *0.2 s* to *1 s*;
- the other conditions are same as in **5.1.**

5.4.1 Control vector *H* and the steering angle at various time delays

Table V illustrates control vector *H* at various time delays, and shows that control parameters vary considerably for time delays ranging from 0.1 s to 1 s.

Table V

Control vector *H* at various time delays

Delay/H	h_1	h_2	h_3	h_4	h_5	h_6
0.2s	-0.109	-0.269	-0.063	-0.077	0.754	-0.55
0.3s	-0.08	-0.302	0.05	-0.05	0.466	-0.303
0.4s	-0.062	-0.358	0.082	-0.037	0.325	-0.286
0.5s	-0.049	-0.411	0.115	-0.029	0.175	-0.258
0.6s	-0.04	-0.43	0.25	-0.023	-0.239	0.096
0.7s	-0.035	-0.466	0.274	-0.019	-0.271	0.122
0.8s	-0.031	-0.506	0.292	-0.016	-0.271	0.114
0.9s	-0.028	-0.554	0.323	-0.014	-0.283	0.112
1s	-0.025	-0.584	0.335	-0.012	-0.288	0.111

Figure 33 illustrates values for the steering angle at various time delays as a function of time. As the human driver reacts with a lengthy time delay, the tractor semi-trailer falls into an unstable state: the driver becomes incapable of steering the tractor semi-trailer back to its initial course.

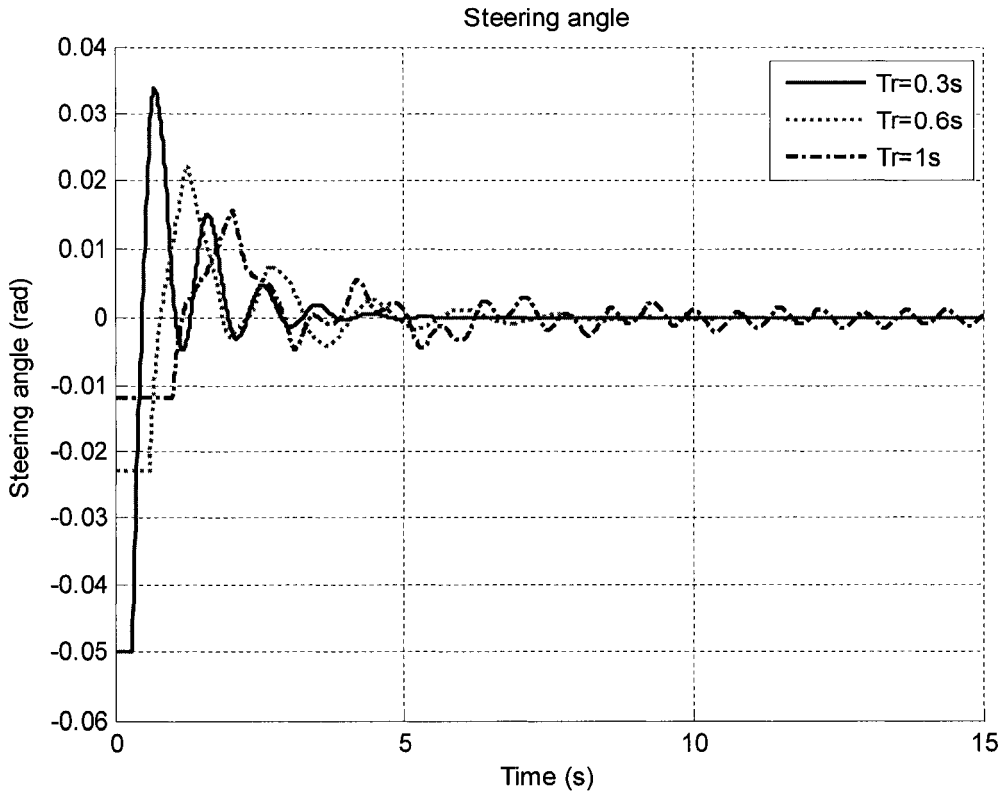

Figure 33 Steering angle at various time delays

5.4.2 Cost function at various time delays

Figure 34 illustrates cost function at various time delays. The cost function increases when time delays increase: time delays affect the tractor semi-trailer's dynamic characteristic responses. With lengthy time delays, such as 0.6 second, the tractor semi-trailer becomes harder to control. At critical time delays, such as 1 second, the tractor semi-trailer will go out of control: the tractor semi-trailer is no longer stable and the

human driver cannot guide the tractor semi-trailer back to its previous course by adjusting the steering wheel.

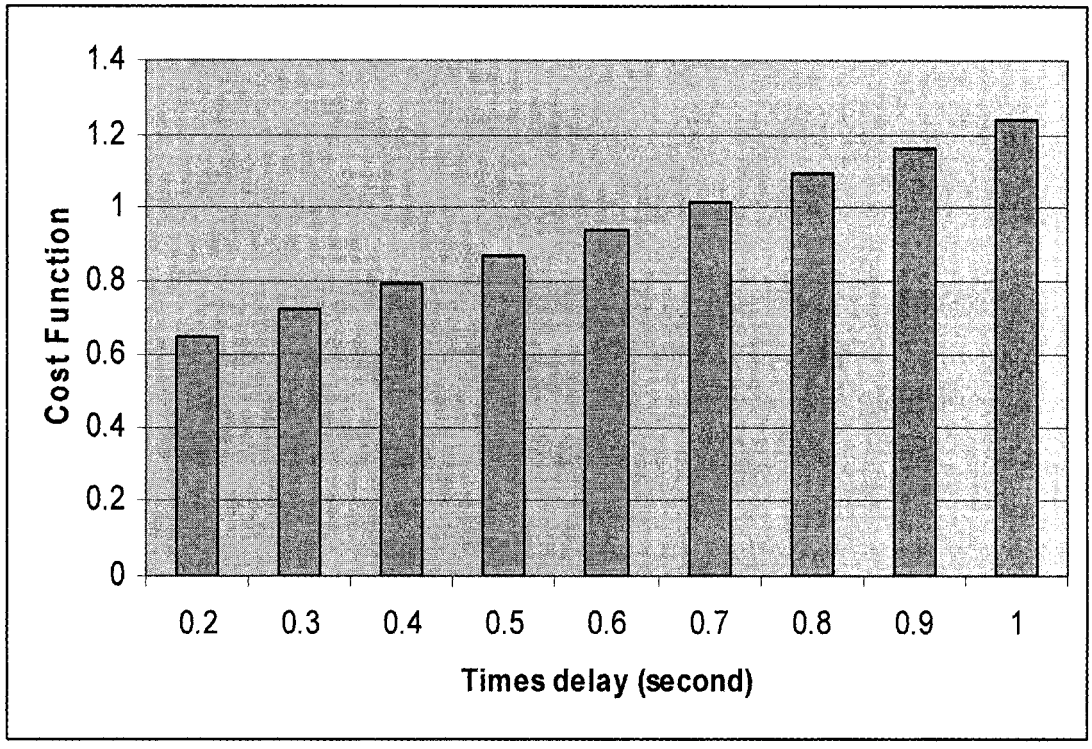

Figure 34 Cost function at various time delays

5.4.3 Lateral displacement and lateral velocity at various time delays

Figure 35 illustrates lateral displacement at various time delays as a function of time. With increases in time delay, the tractor semi-trailer's lateral displacement begins to oscillate. When the time delay is 0.3 second, the tractor semi-trailer is still under control, as during the previous stage. When the time delay is 0.6 second, however, the tractor semi-trailer is harder to control. When time delay reaches 1 second, the tractor semi-trailer goes out of control: time delay can also be considered as affecting tractor semi-trailer stability to a large extent, and the tractor semi-trailer will be controllable only within a certain range.

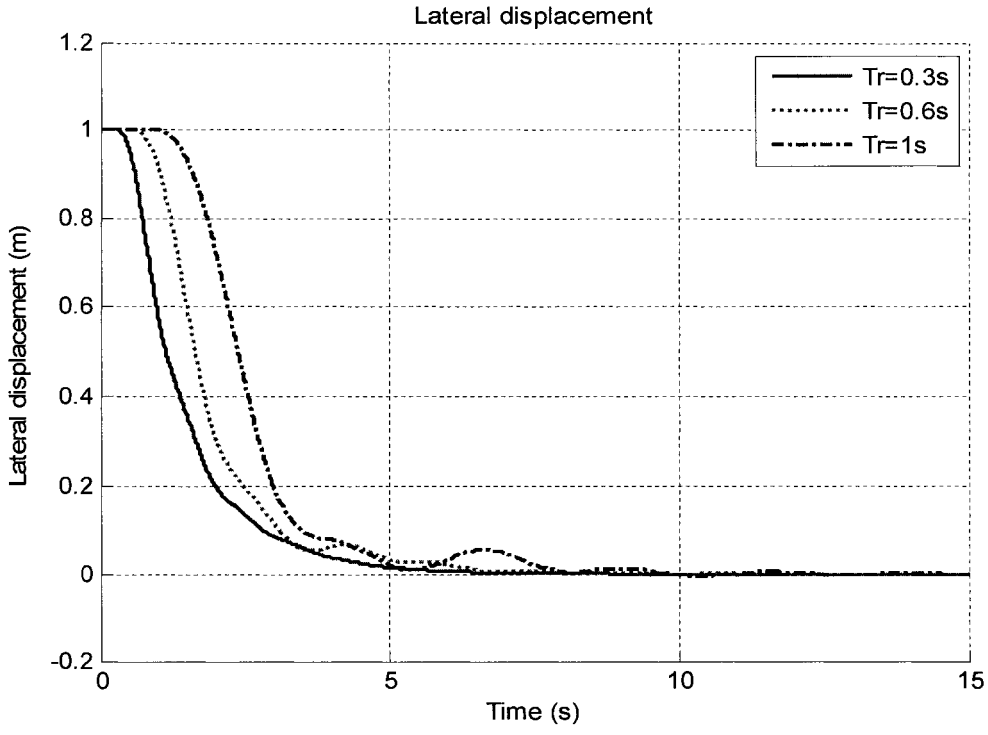

Figure 35 Lateral displacement at various time delays

Figure 36 illustrates values for lateral velocity at various time delays as a function of time. With increases in time delay, the tractor semi-trailer's lateral velocity begins to oscillate. The driver of the tractor semi-trailer cannot minimize lateral velocity to zero, and the tractor semi-trailer vehicle is no longer stable. A greater time delay may be induced by tires, a disability on the part of the human driver, or for other reasons. This analysis illustrates that a longer time delay in the driver model will decrease the vehicle's stability.

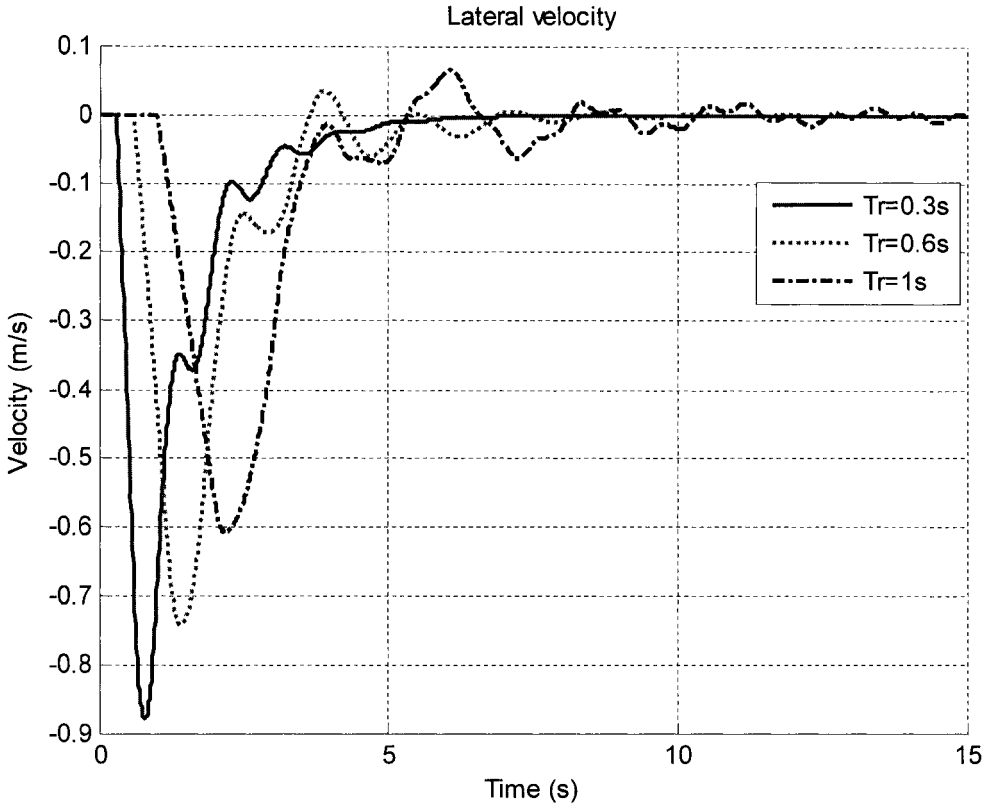

Figure 36 Lateral velocity at various time delays

5.4.4 Responses to yaw angle and yaw velocity at various time delays

Figures 37 and 38 illustrate the tractor's yaw velocity and yaw angle and the semi-trailer's yaw velocity and yaw angle at various semi-trailer time delays. The dynamic responses of the tractor semi-trailer to various time delays vary. Observably, when the time delay reaches 1 second, both tractor and semi-trailer go into oscillation. The tractor and semi-trailer interact with each other. When this happens, the human driver is incapable of guiding the tractor semi-trailer back to its initial course.

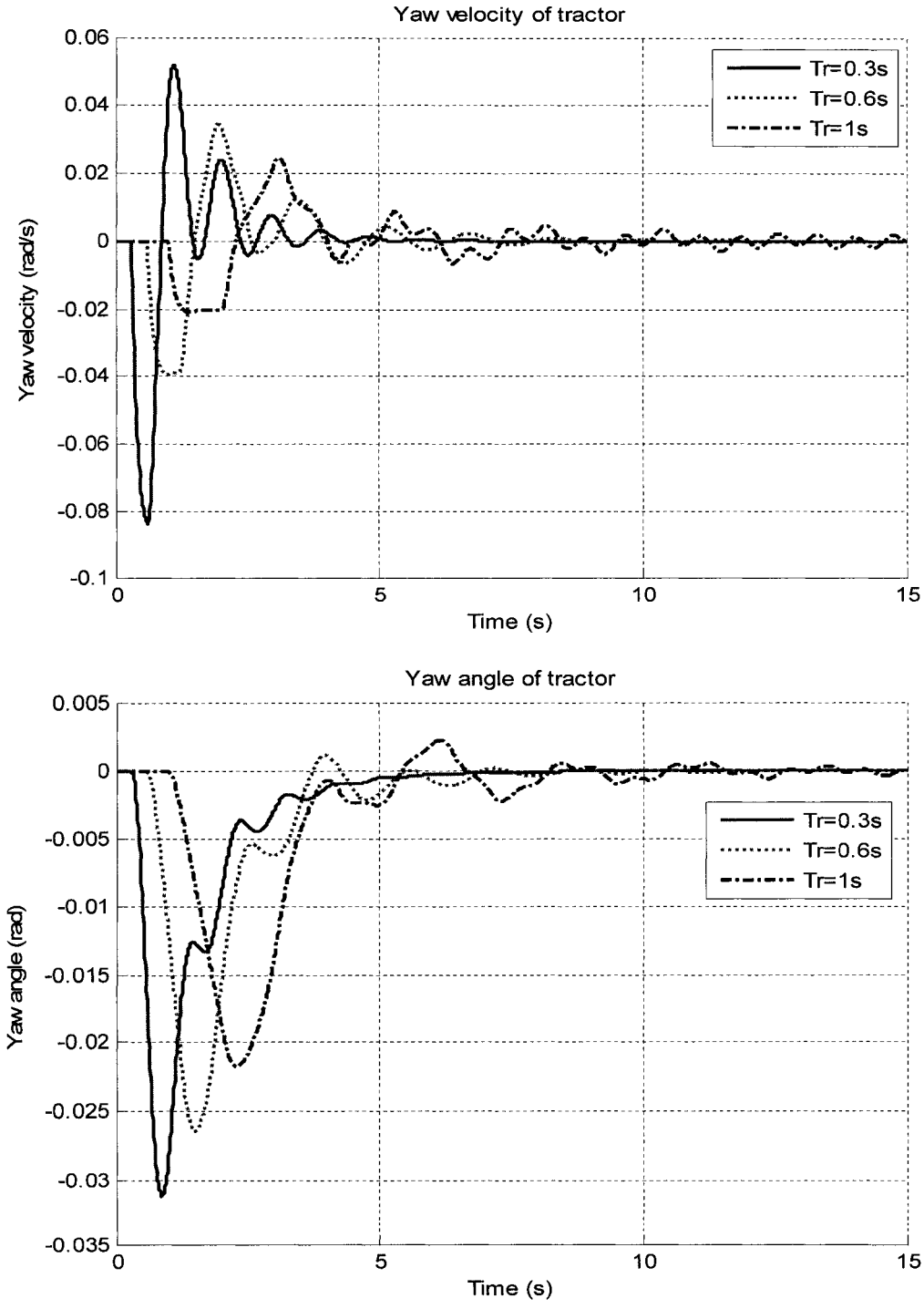

Figure 37 Yaw angle and yaw velocity of the tractor at various time delays

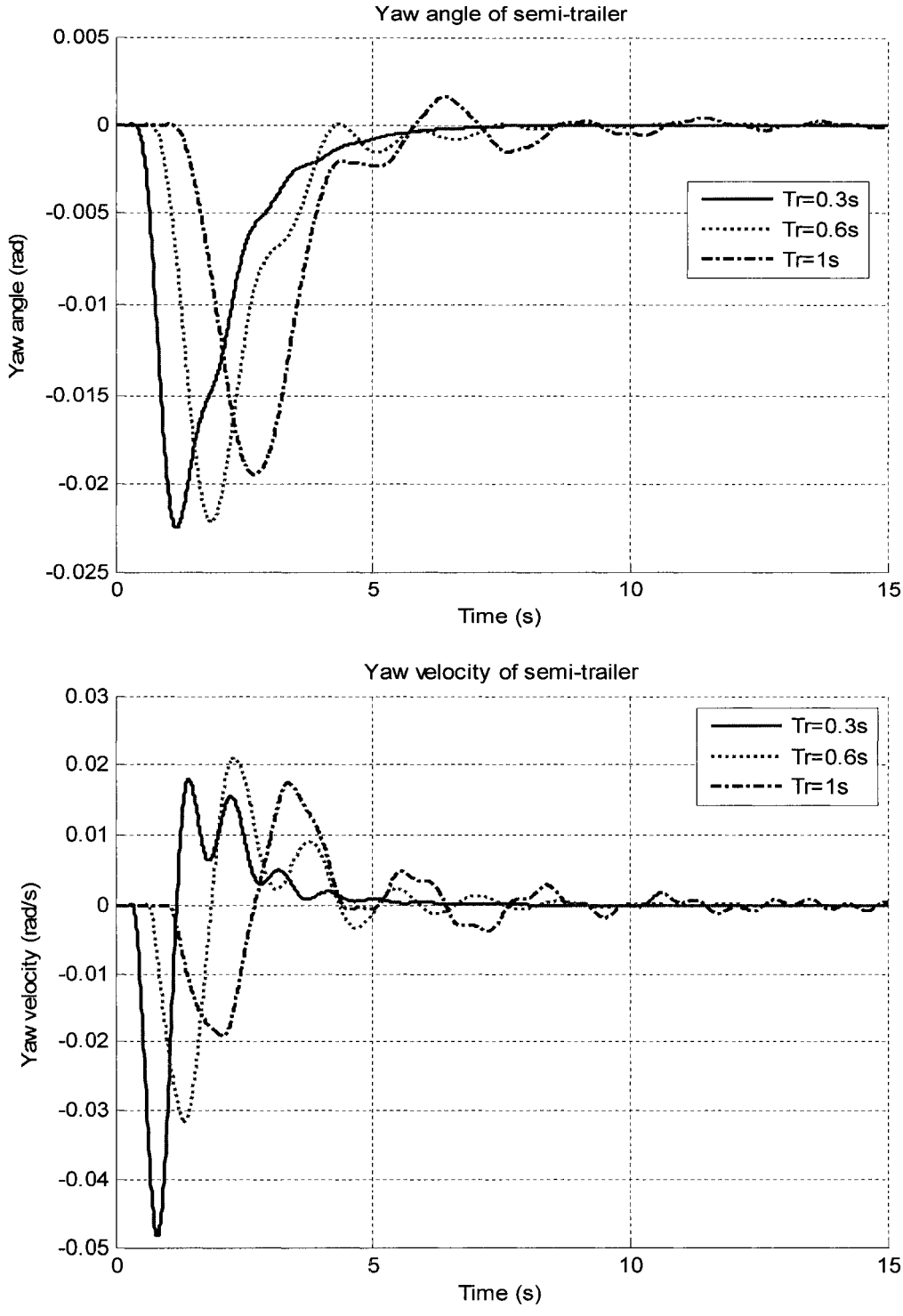

Figure 38 Yaw angle and yaw velocity of the semi-trailer at various time delays

5.5 Comparison of two kinds of tractor semi-trailer

Generally, each type of tractor semi-trailer has its own dynamic characteristics. The driver must adapt to his tractor semi-trailer and improve his own driving performance. This means that each tractor semi-trailer/driver system has its own optimization control characteristics. In the tractor semi-trailer/driver system model, the optimization control characteristics are represented by an optimal control vector (H). This optimal control vector is applied to the tractor semi-trailer vehicle which has the best control performance. We will now compare two tractor semi-trailers under the same conditions as in **5.1,** except that the simulation time is now set at 10 seconds.

5.5.1 Parameters for two types of tractor semi-trailer vehicle

The parameters for two types of tractor semi-trailers (described in two papers by [46],[3] and here labeled ***T1*** and ***T2***), are listed in Table VI.

Table VI

Parameters for the two tractor semi-trailers

	T1	***T2***
m_1 (Kg)	7956	8444
m_2 (Kg)	10682	23472
I_{z1} (Kg×m^2)	32000	65734.6
I_{z2} (Kg×m^2)	482790	181565.5
a_1 (m)	1.68	2.59
b_1 (m)	3.67	3.29
b_2 (m)	7.32	5.45
c_1 (m)	3.56	3.06
c_2 (m)	2.9	4.2
C_{af} (N/rad)	177678	143330
C_{r1} (N/rad)	710713.5	143330
C_{r2} (N/rad)	710713.5	80312

Table VI shows the parameters for both types of tractor semi-trailer. Although the masses of both tractors are nearly identical, the other parameters for the two tractor semi-trailers are quite different. Given the masses of the two semi-trailers, the moments of inertia and dimensions between the axes and centers of gravity, we can deduce that tractor semi-trailer 1 (*T1*) is smaller than tractor semi-trailer 2 (*T2*). From the tire characteristics of both tractor semi-trailers, it would appear that tractor semi-trailer 1 (*T1*) uses the same tires on the rear axles of its tractor and semi-trailer, while tractor semi-trailer 2 (*T2*) uses the same tires on the axes of its tractor only. The above characteristics confirm that tractor semi-trailer 1 (*T1*) and tractor semi-trailer 2 (*T2*) are different types of tractor semi-trailer vehicles, and that they differ substantially in design.

5.5.2 Control vector H and steering angle

Table VII shows the control vector for the two tractor semi-trailers. These two control vectors are totally different, thus demonstrating that each vehicle company has its own control characteristics.

Table VII

Control vectors for the two vehicles

Vehicle\H	h_1	h_2	h_3	h_4	h_5	h_6
T1	-0.116	-0.457	-1.129	-0.082	3.7959	-3.5449
T2	-0.145	0.446	-0.505	-0.102	1.212	-1.029

The steering angle shows the driver how to steer his tractor semi-trailer back to its initial course. The steering angle can directly affect the controllability of the tractor semi-trailer. Figure 39 demonstrates that although both tractor semi-trailer 1 *(T1)* and tractor semi-trailer 2 *(T2)* can be properly controlled within 4 seconds, tractor semi-trailer 1 *(T1)*

performs better than the tractor semi-trailer 2 *(T2)* because the steering angle for tractor semi-trailer 1 (T1) is smaller than that of the tractor semi-trailer 2 (T2); stability time for the tractor semi-trailer 1 (T1) is also shorter than that for the tractor semi-trailer 2 (T2). The driver can make use of an optimization action to achieve the greatest safe control action.

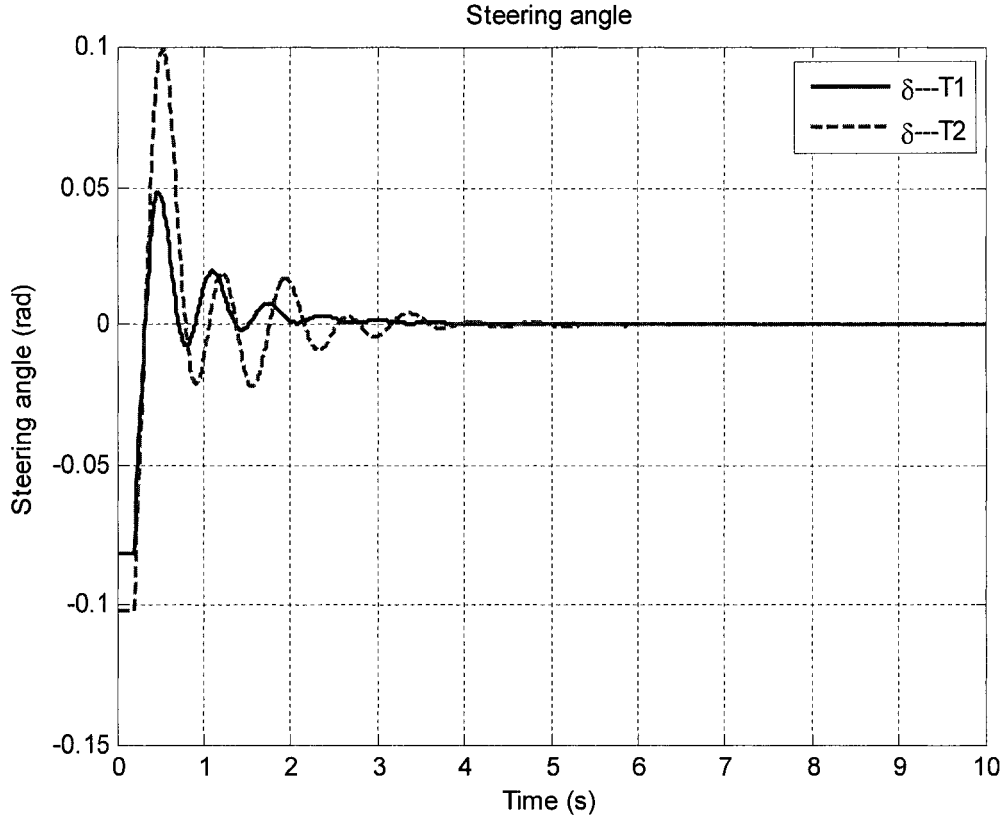

Figure 39 Steering angles for the two tractor semi-trailers

5.5.3 Responses to lateral displacement and lateral velocity

Figure 40 represents the tractor's lateral displacement as a function of time, with a 0.2-second control lag time. The graph confirms that the two tractor semi-trailers have the same traces in response to lateral displacement.

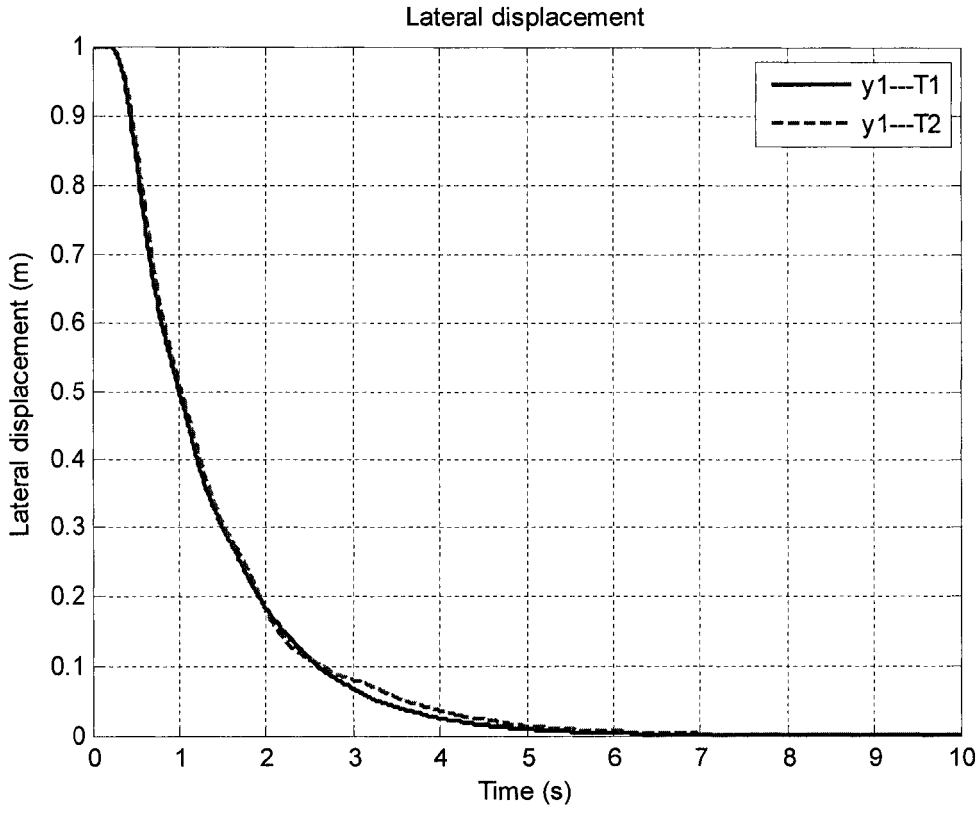

Figure 40 Response to lateral displacement

From outset up to second *two*, both tractors have identical traces and both reach 0.2 m displacement at the same time. From second *two* to second *six*, both tractor semi-trailer 1 (T1) and tractor semi-trailer 2 (T2) travel along their initial courses more slowly than before, and tractor semi-trailer 2 exhibits fewer disturbances than does tractor semi-trailer 1. Stability time is nearly six seconds; both types of tractor semi-trailer are nearly at a steady state at this time. One can conclude that lateral displacement is an important state for vehicle stability. Accordingly, when an automobile company designs its tractor semi-trailers, it will choose similar dynamic characteristics for the displacement state. Equation (2.36) shows that lateral velocity will follow the same path as lateral displacement. This is proven in Figure 41. Of course, lateral velocity is also an important state for vehicle stability.

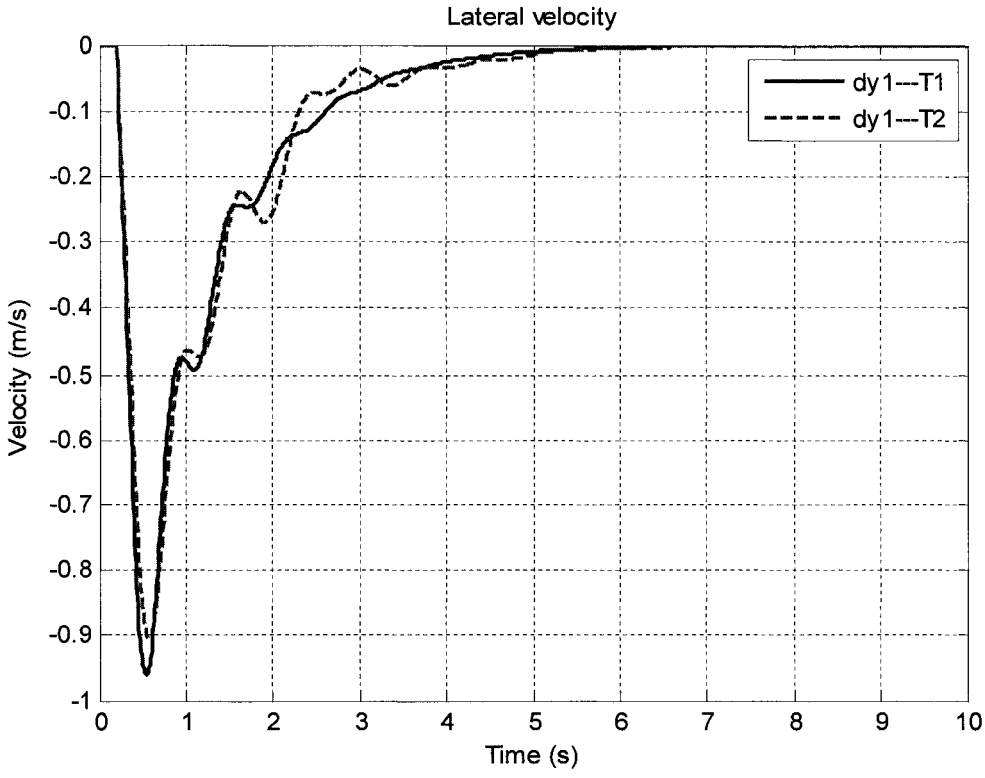

Figure 41 Response to lateral velocity

Figure 41 shows that tractor semi-trailer 1 *(T1)* responds more rapidly than does tractor semi-trailer 2 *(T2)*. In emergency situations, tractor semi-trailer1 *(T1)* has more sensitivity and stability than tractor semi-trailer 2 *(T2)*.

5.5.4 Responses to yaw angle and yaw velocity

Figures 42, 43, 44 and 45 show the responses of both tractor semi-trailers to yaw angle and yaw velocity. Figures 42 and 43 show that yaw angle is not as important as lateral displacement and lateral velocity in the tractor semi-trailer/driver optimal control system. Automobile companies may choose these dynamic characteristics themselves, because the yaw angle of the tractor semi-trailer 1 *(T1)* varies more widely than that of the tractor

semi-trailer 2 *(T2)*. For both the tractor and the semi-trailer, cost function (***J***) is nearly the same. Comparing Figures 42 and 43, one can conclude that for both tractor semi-trailers, the yaw angle of the semi-trailer lags behind the yaw angle of the tractor; it is also smaller than the tractor's yaw angle.

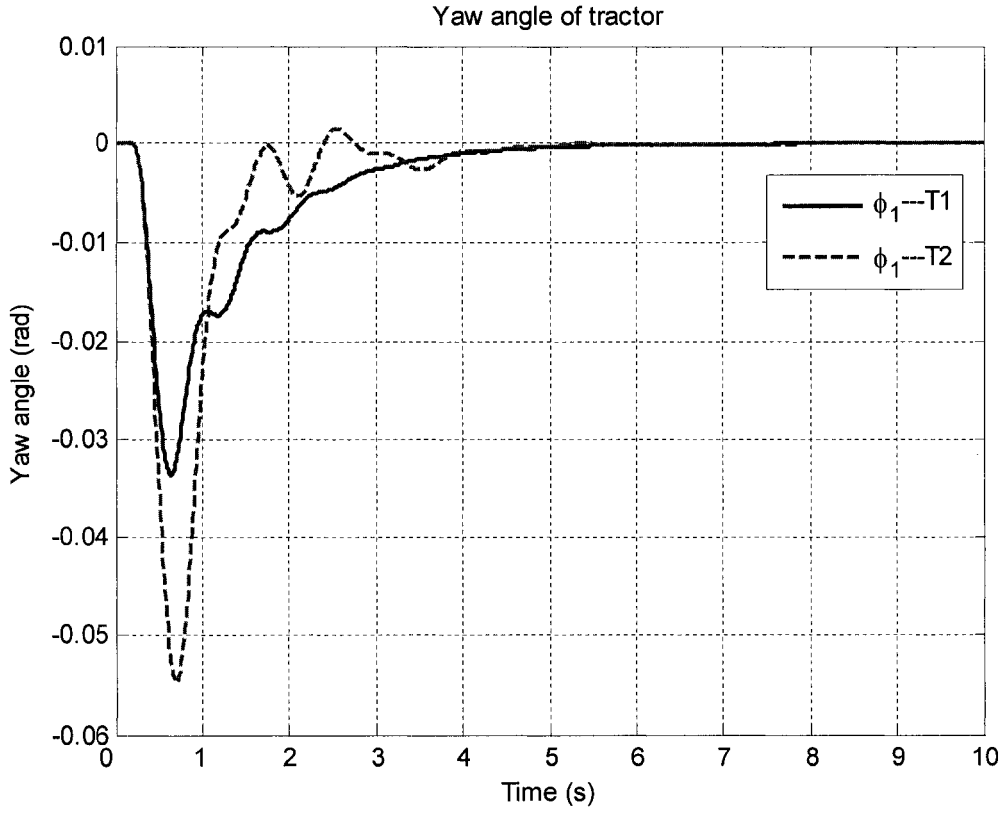

Figure 42 The tractor's response to yaw angle

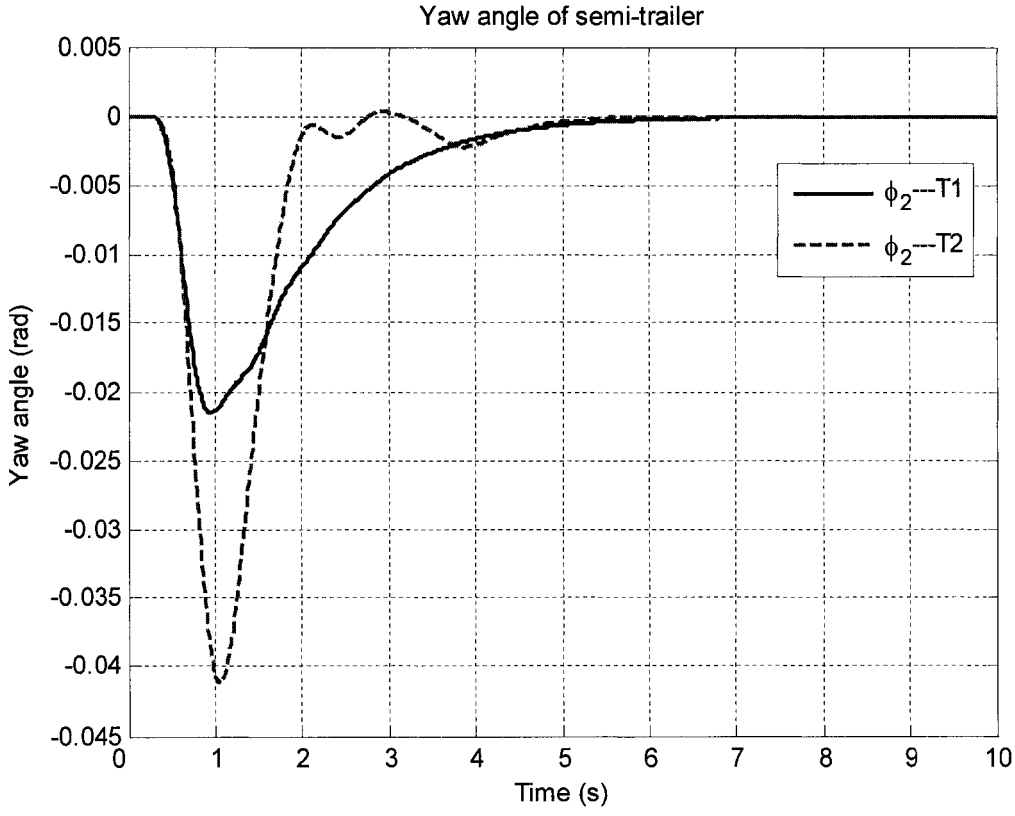

Figure 43 The semi-trailer's response to yaw angle

According to equations (2.6) and (2.8), the values for yaw velocity of two tractor semi-trailers have the same characteristics as do the values for their yaw angle. Moreover, yaw velocity is less crucial than are the states of lateral displacement and lateral velocity.

A comparison of Figures 42, 43, 44 and 45 illustrates that tractor semi-trailer 1 *(T1)* has a better trace than tractor semi-trailer 2 *(T2)*, because the state vector for tractor semi-trailer 1 *(T1)* changes smoothly, and the peak value of tractor semi-trailer 1 *(T1)* is smaller than the peak value of tractor semi-trailer 2 *(T2)*. The four state variables show that tractor semi-trailer 1 *(T1)* lends itself to better control than does tractor semi-trailer 2 *(T2)*.

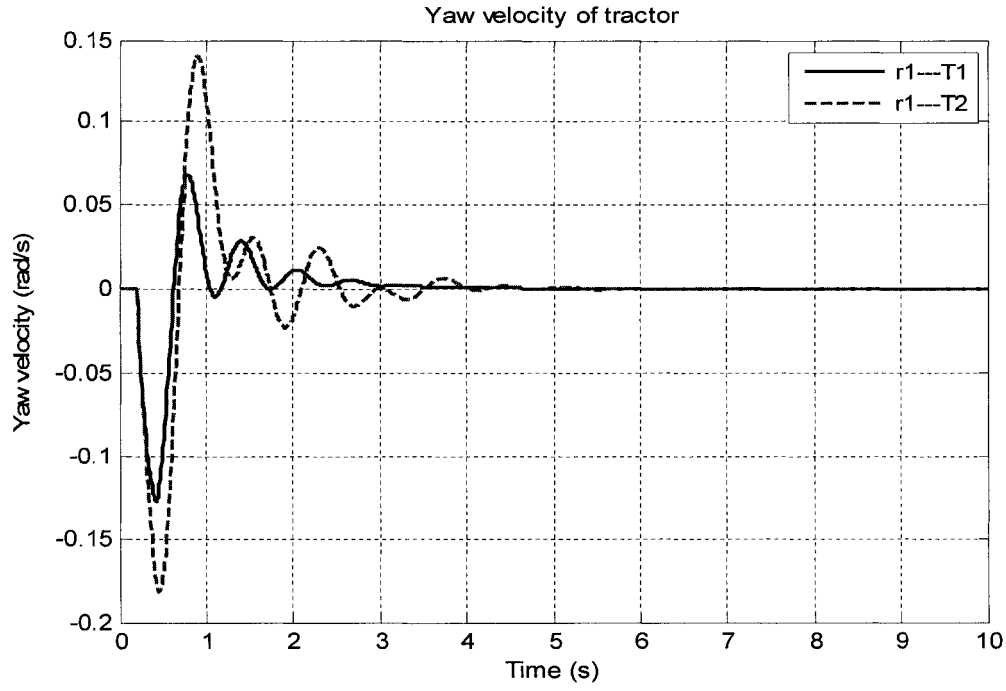

Figure 44 The tractor's response to yaw velocity

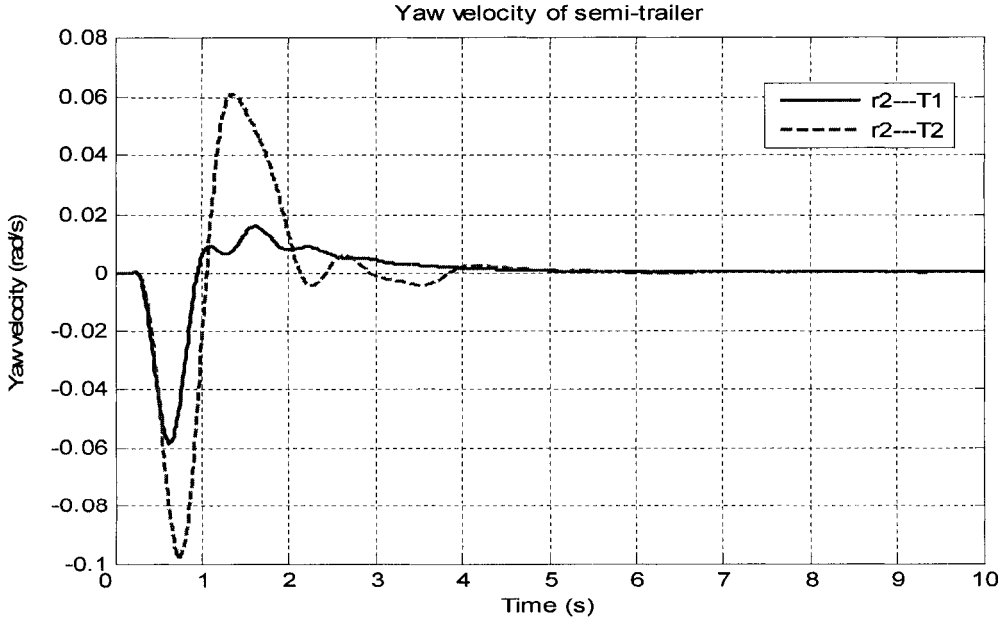

Figure 45 The semi-trailer's response to yaw velocity

5.6 Summary

In this chapter, dynamic responses were simulated using optimal control vector *H*. From the dynamic responses, we were able to conclude that a human driver will always steer his tractor semi-trailer back to its initial course by minimizing lateral displacement. The tractor unit and the semi-trailer unit affect each other. From the responses to various velocities, semi-trailer loads and time delays, we can conclude that within certain ranges of forward speed, semi-trailer load and human time delay, the tractor semi-trailer system can maintain a stable motion. A driver can improve the degree of safety by reducing forward speed or by reducing time delay. In the last part of this chapter, we compared two types of tractor semi-trailer in order to find the stablest tractor semi-trailer; we also noted some design ideas displayed in the tractor semi-trailer.

CHAPTER 6

PREVIEW DRIVER MODEL SAFE VISIBILITY DISTANCE

In this chapter, the preview driver model is arrived at by simplifying the previous driver model (3.39). This simplification is based entirely on Figure 46, which shows that the coefficients of state variables y_1 and $\dot{y}_1$ are the relatively important elements of control vector H. Using the preview driver model, the closed-loop tractor semi-trailer/driver control model is written in Laplace form. Closed-loop gain K, lead-time T_a and safe visibility distance L, all of which can help the driver improve his degree of driving safety, are calculated using the SA method under various conditions.

6.1 Evaluating the most important elements in control vector H

In cost function J (4.1), a weighting matrix Q_w is defined and then used to evaluate the most important elements in control vector H. In Chapter 5, Q_w was defined as a unit matrix: this means that all the elements in control vector H are equally important. Here, for the purpose of evaluating the most important elements in control vector H, the values found along the diagonal of weighting matrix Q_w will be presumed to increase.

Figure 46 illustrates variations in cost function while matrix Q_w changes. The X axis is the importance level, while the Y axis is the value of the cost function. First of all, we will explain the ways in which weighting matrix Q_w varies. For example, when the importance level is 5, the values along the diagonal of the weighting matrix are changed to 5. This means that at every importance level, six cost-function values can be obtained using the values along the diagonal of the weighting matrix. Figure 46 shows that the first and fourth values of the cost function are greater than the others on each importance level. Thus, the control vector's first and fourth elements are more important than are the others. These situations are identical to those mentioned in the previous chapter. The

control vector's control parameters for yaw velocity and yaw angle have little effect on the steering angle.

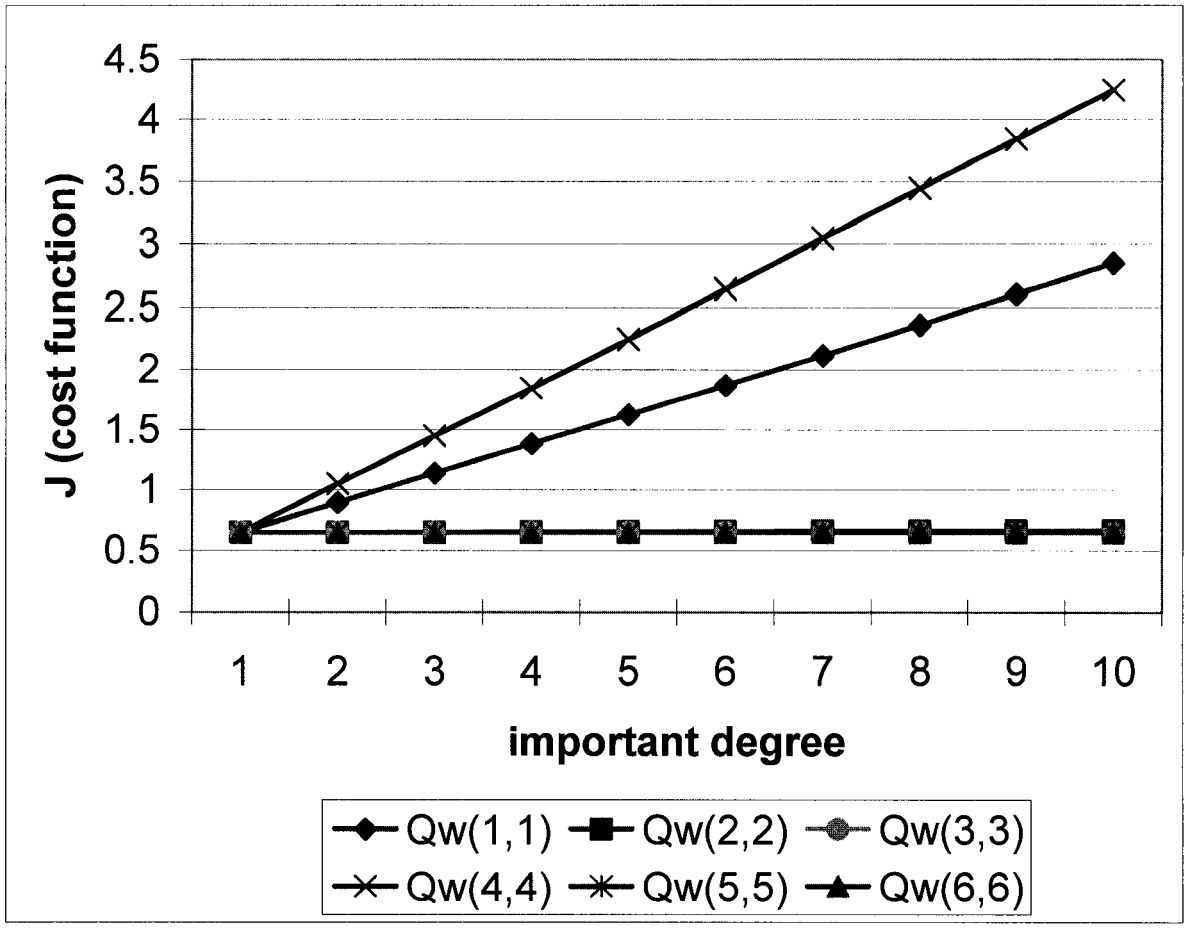

Figure 46 Cost function at various weight matrixes Q_w

6.2 The preview closed-loop control model

In light of Section (6.1), the previous driver model (3.39) can now be written as

$$\delta(t) = h_1 \dot{y}_1(t - T_r) + h_4 y_1(t - T_r) \tag{6.1}$$

where h_1 , h_4 are the optimal control values.

According to T.Legouis *et al.* [36], lateral velocity can be simplified as follows

$$\dot{y}_1(t) \approx u\phi_1(t) \tag{6.2}$$

where u is the constant forward speed; $\phi_1(t)$ is the tractor's yaw angle; and $\dot{y}_1(t)$ is the tractor's lateral velocity. If L denotes the visible distance from the tractor's centre of gravity to a point (x,*y)* in front of the driver, the lateral distance $\tilde{y}$ (see Figure 47) can be expressed as

$$\tilde{y}(t) = y_1(t) + L\phi_1(t) \tag{6.3}$$

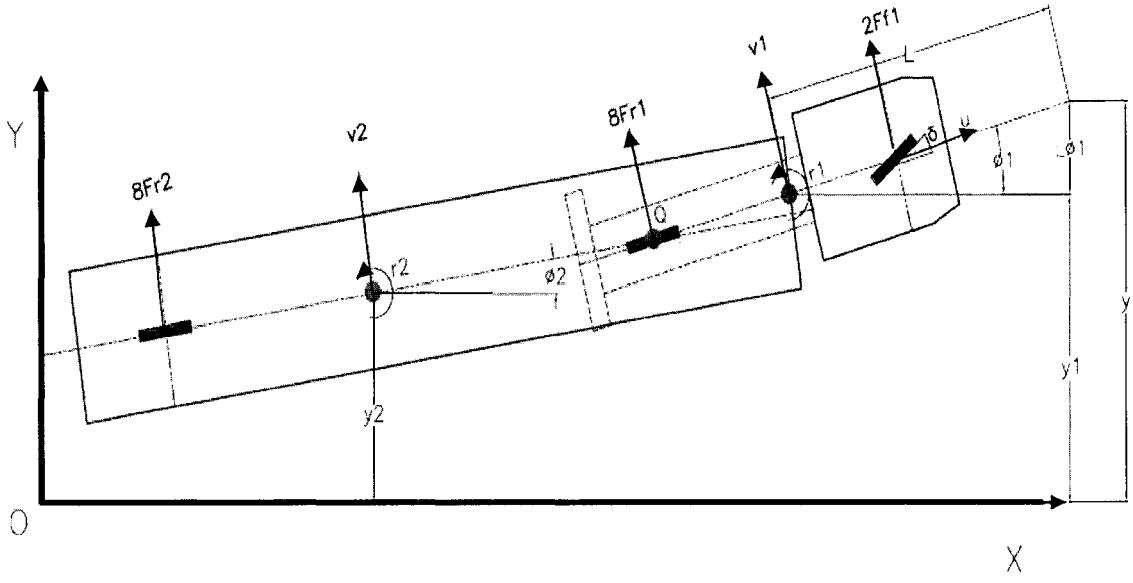

Figure 47 Lateral distance for a simple bicycle model

Combining (6.2) and (6.3), the lateral distance $\tilde{y}$ can be written as

$$\tilde{y}(t) = y_1(t) + \frac{L}{u}\dot{y}_1(t) = y_1(t) + T_a\dot{y}_1(t) \tag{6.4}$$

where L is the visibility distance, and $T_a = \frac{L}{u}$ is defined as the lead time. Thus the preview driver model (6.1) can be written as follows:

$$\begin{aligned} \delta(t) &= h_1\dot{y}_1(t-T_r) + h_4 y_1(t-T_r) \\ &= Ky(t-T_r) \\ &= K(T_a\dot{y}_1(t-T_r) + y_1(t-T_r)) \end{aligned} \tag{6.5}$$

Using the preview driver model, the tractor semi-trailer control model may be expressed in Laplace form, with K the closed-loop gain and T_a the lead-time. Figure 48 illustrates that the lateral displacement y_1(s) is the single state requiring control, and that the preview driver model can be considered as a PD (proportional-differential) controller.

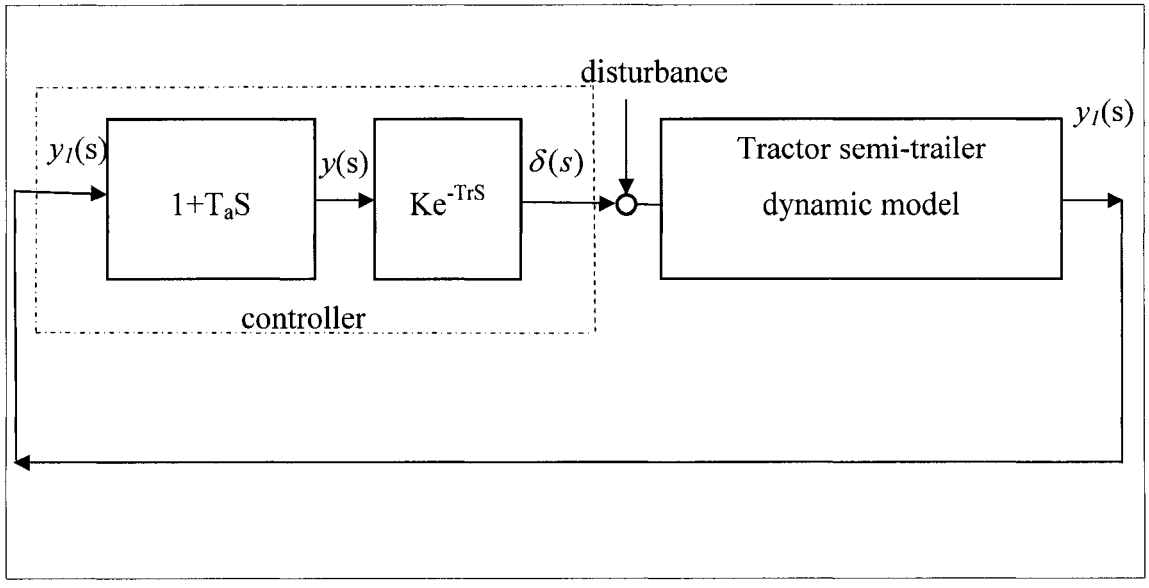

Figure 48 The closed-loop control system expressed in Laplace form

6.3 Visibility distance of the tractor semi-trailer/driver system

The dynamic responses of the tractor semi-trailer/driver system have been discussed in Chapter 5. In this section, the SA method is used to calculate closed-loop gain K and lead-time T_a for the preview driver model in order to calculate visibility distance L_v under various driving conditions.

6.3.1 Visibility distance at various forward speeds

Chapter 5.2 demonstrated that the tractor semi-trailer is safer at relatively lower forward speeds. In this section, visibility distance L is used to evaluate degree of safety for a given forward speed. Using the improved SA method to search the optimal control parameters of the preview driver model, the same assumptions hold true as in Chapter 5.2. They are listed below:

- an initial step lateral displacement $y = 1m$, $(t = 0)$;
- there are no external forces other than road-tire forces;
- constant forward speed is between $u = 80\ km/h$ and $u = 120\ km/h$;
- lag time $T_r = 0.2s$;
- the aim of optimization control is steering the tractor semi-trailer back to its initial course $y = 0$;
- The parameters of the tractor semi-trailer and the parameter settings for the SA method have been presented in Chapter 4.

Table VIII demonstrates optimal control parameters for the preview of the tractor semi-trailer model at various forward speeds. Whenever the tractor semi-trailer's forward speed is higher, lead-time T_a, cost function J and visibility distance L increase. The driver needs a longer visibility distance L_i in order to keep the tractor semi-trailer under

control. In general, forward speed within a range of $u = 80\ km/h$ to $u = 120\ km/h$ is defined as the safest forward speed on the highway, due to fact that the driver has enough time to deal with the disturbance.

Table VIII

Optimal control parameters at various forward speeds

forward speed	$K(rad/m)$	$T_a(s)$	$J(m^2s)$	$L(m)$
80km/h	-0.072	1.361	0.6577	30.24
100km/h	-0.058	1.397	0.6677	38.81
120km/h	-0.05	1.42	0.6749	47.33

6.3.2 Visibility distance at various semi-trailer loads

In Chapter 5.3 we demonstrated that the tractor semi-trailer can be controlled quite easily under rated loads. In this section, visibility distance L is used to evaluate degree of load safety. Using the improved SA method to search the optimal control parameters for the preview driver model, the same assumptions hold as those in Chapter 5.3: these are listed below:

- an initial lateral displacement $y = 1m$, $(t = 0)$;
- there are no external forces other than road-tire forces;
- constant forward speed is $u = 100\ km/h$;
- testing the loads of semi-trailers from $5\ \ tons$ to $25\ \ tons$;
- lag time is $T_r = 0.2s$;

- optimization control is aimed at steering the tractor semi-trailer back to its initial course; $y = 0$
- The parameters for the tractor semi-trailer and the parameter settings for the SA method have been presented in Chapter 3.

Table IX demonstrates optimal control parameters for the preview tractor semi-trailer model under various loads. When the semi-trailer's load increases, lead-time T_a, cost function J and visibility distance L increase. As shown in Chapter 5.3, cost function undergoes little change. Visibility distance L also remains substantially the same. This demonstrates once again that the tractor semi-trailer has near-identical operating characteristics under various rated loads.

Table IX

Optimal control parameters at various loads

loads (*Tons*)	*K*(*rad/m*)	T_a(*s*)	$J(m^2s)$	*L*(*m*)
5	-0.057	1.404	0.6690	39
15	-0.057	1.421	0.6720	39.47
20	-0.056	1.429	0.6744	39.69

6.3.3 Visibility distance for various time delays

In Chapter 5.4 we demonstrated that the tractor semi-trailer's stability is greatly affected by the driver's delays in reaction time. In this section, visibility distance L is used to evaluate the degree of time delay. Using the SA method to search the optimal control parameters for the preview tractor semi-trailer/driver control system, assumptions identical to those found in Chapter 5.4 are listed below:

- an initial step lateral displacement $y = 1m$, $(t = 0)$;

- there are no external forces other than road-tire forces;
- constant forward speed is $u = 100\ km/h$;
- testing the lag time T_r from $0.2\ s$ to $1\ s$;
- optimization control is aimed at steering the tractor semi-trailer back to its initial course $y = 0$;
- the parameters of the tractor semi-trailer and parameter settings for the SA method have been presented in Chapter 3.

Table X demonstrates optimal control parameters for the preview tractor semi-trailer model at various time delays. Cost function J is greatly affected by time delays, as shown in Chapter 5.4. Lead-time T_a, and visibility distance L are greatly affected by time delay as well. The driver needs a very long visibility distance L in order to keep the tractor semi-trailer under control. Thus, the tractor semi-trailer becomes uncontrollable due to physiological limitations. The driver must improve upon his reaction time.

Table X

Optimal control parameters at various time delays

Time delay (s)	K(rad/m)	Ta(s)	J(m^2s)	L(m)
0.2	-0.058	1.397	0.6677	38.81
0.6	-0.024	1.792	0.8465	49.78
1	-0.013	2.308	1.0376	64.11

6.4 Summary

In this chapter, we obtained a preview driver model by evaluating the importance of control vector H. The tractor semi-trailer/driver control system was written in Laplace form, in which closed-loop gain K and lead-time T_a are defined. Visibility distance L was introduced in order to assess the degree of safety of the tractor semi-trailer. The same conclusions were obtained as in Chapter 5. In particular, when visibility distance becomes shorter, for example in bad weather, the driver must reduce forward speed in order to maintain safe conditions for vehicle operation.

CONCLUSION

In this thesis, lateral dynamics and parameters were identified for a closed-loop tractor semi-trailer/driver system. These were then studied in a tracking situation. A lateral dynamic model was proposed based on Newton's 2nd law. The parameters to be identified were the inherent coefficients of the driver model, or a quasi-linear function of the vehicle's instantaneous feedback state with time delay. The results of convergence and annealing speed demonstrated that the Simulated Annealing approach can be employed successfully in order to search these parameters while minimizing the cost function.

The simulations showed that, using proper control parameters, a tractor semi-trailer subjected to a lateral impulse disturbance can eliminate lateral displacement without oscillation. Variations in forward speeds, loads and time delay which may affect the dynamic responses of the tractor semi-trailer vehicle were discussed. The results of the simulation demonstrate that within a certain range of forward speeds, semi-trailer loads and human reaction-time delays, the tractor semi-trailer system can maintain a stable motion. Drivers can improve degree of safety by reducing forward speed or decreasing reaction time. Visibility distance L and lead-time T_a have been defined in a preview tractor semi-trailer/driver model in order to study the effects of human physiological limitations on safety and on optimal driving. The results illustrate that a long visibility distance is needed in cases of high forward speed or long delays in reaction time.

The major contributions made by this research project are:

- An improved Simulated Annealing approach has been applied to the study of the tractor semi-trailer/driver control systems;
- The dynamic response of a tractor semi-trailer/driver system has been studied in order to improve driver behaviour during his attempts to control the tractor semi-trailer;

- We have worked on assessing the importance of control elements in establishing a preview driving model and in finding the safe visibility distance;

Future research related to this project could analyze the tractor semi-trailer/driver system within Laplace's S-field, in order to study the vehicle's stability. Such work would allow for research into the stability of the closed-loop system and systematically determine the vehicle's critical speed in terms of both vehicle and driver parameters.

REFERENCES

[1] J. P. Wideberg, *Simplified method for evaluation of the lateral dynamic behaviour of a heavy vehicle.* Heavy Vehicle Systems, Int. J. of Vehicle Design, 2004. **11**(2).

[2] M. Tai., M. Tomizuka, *Modelling of multi-unit heavy vehicle systems for automated guidance.* Heavy Vehicle Systems, Int. J. of Vehicle Design, 2004. **11**(1).

[3] C. Chen, M. Tomizuka, *Lateral control of commercial heavy vehicles.* Vehicle System Dynamics, 2000. **33**: p. 391-420.

[4] D. H. Wu, J. H. Lin, *Analysis of dynamic lateral response for a multi-axle-steering tractor and trailer.* Heavy Vehicle Systems, Int. J. of Vehicle Design, 2003. **10**(4).

[5] Y. He, A. Khajepour, J. McPhee and X. Wang, *Dynamicm modelling and stability analysis of articulated frame steer vehicles.* Int. J. of Vehicle systems, 2005. **12**(1).

[6] R. V. Dukkipati, S. Narayanaswamy, *Improved compatibility between the lateral stability and curving behaviour of modified truck designs.* Heavy Vehicle Systems, Int. J. of Vehicle Design, 2004. **11**(1).

[7] X. Yang, S. Rakheja and I. Stiharu, *Structure of the driver model for articulated vehicles.* Heavy Vehicle Systems, Int. J. of Vehicle Design, 2002. **9**(1).

[8] A. Y. Ungoren and H. Peng, *An adaptive lateral preview driver model.* Vehicle System Dynamics, 2005. **43**(4): p. 245-259.

[9] K. Guo, H. Ding, J. Zhang, J. Lu and R. Wang, *Development of a longitudinal and lateral driver model for autonomous vehicle control.* Int.J. Vehicle Design, 2004. **36**(1).

[10] C. Brunet, R. Gonzalez-Rubio and M. Tetreault, *A multi-agent architecture for a driver model for autonomous road vehicles.* IEEE, 1995. **0-7803-2766-7-9**.

[11] B. Tutuianu, R. Baldick and M. S. Johnstone, *Nonlinear driver models for timing and noise analysis.* IEEE, 2004. **0278-0070004**.

[12] C.-K. Tsai and M. Marek-Ssdowska, *An interconnect insensitive linear time-varying driver model for static timing analysis.* IEEE. **0-7695-2301-3/05**.

[13] P. Antos and J. A. C. Ambrosio, *A control strategy for vehicle trajectory tracking using multibody models.* Multibody System Dynamics, 2004. **11**: p. 365-394.

[14] Y. Lin, P. Tang, W. J. Zhang, Q. Yu, *Artificial neural network modelling of driver handing behaviour in a driver-vehicle-environment system.* Int.J. Vehicle Design, 2005. **37**(1).

[15] F. F. Alhimdani, *Steering analysis of articulated tracked vehicles.* Journal of Terramechanics, 1982. **19**(3): p. 195-209.

[16] E. Velenis, P. Tsiotras, C. Canudas-de-Wit and M. Sorine, *Dynamic tire friction models for combined longitudinal and lateral vehicle motion.* Vehicle System Dynamics, 2005. **43**(1): p. 3-29.

[17] S. Jimenez, A. Luciani and C. Laugier, *Simulating physical interactions between an articulated mobile vehicle and terrain.* Robotics and Autonomous Systems, 1993. **11**: p. 97-107.

[18] O. Mokhiamar, M. Abe, *Simultaneous optimal distribution of lateral and longitudinal tire forces for the model following control.* Journal of Dynamic Systems, Measurement and Control, 2004. **126**.

[19] J. Wang, L. Alexander and R. Rajamani, *Friction estimation on highway vehicles using longitudinal measurements.* Journal of Dynamic Systems, Measurement and Control, 2004. **126**: p. 265-275.

[20] P. Hingwe, M. Tai and M. Tomizuka, *Modeling and robust control of power steering system of heavy vehicles for AHS.* IEEE, 1999(0-7803-5446-X).

[21] M. Tai, P. Hingwe and M. Tomizuka, *Modeling and control of the steering system of heavy vehicles for automated highway systems.* IEEE, 2004(1083-4435/04).

[22] K., Moriwaki, *Autonomous steering control for electric vehicles using nonlinear state feedback H control.* Nonlinear Analysis, 2005.

[23] J. Sainte-Marie, S. Mammar, L. Nouveliere, V. Rouault, *Sub-optimal longitudinal control of road vehicles with capacity and safety considerations.* Transactions of the ASME, 2004. **126**: p. 26-35.

[24] M. A. Sotelo, *Lateral control strategy for autonomous steering of Ackerman-like vehicles.* Robotics and Autonomous Systems, 2003. **45**: p. 223-233.

[25] K. Park, S.-J. Heo, I. Baek, *Controller design for improving lateral vehicle dynamic stability.* JSAE Review, 2001. **22**.

[26] M. Harada, H. Harada, *Analysis of lateral stability with integrated control of suspension and steering systems.* JSAE Review, 1999. **20**: p. 465-470.

[27] O. Mokhiamar, M. Abe, *Effects of model response on model following type of combined lateral force and yaw moment control performance for active vehicle handing safety.* JSAE Review, 2002. **23**: p. 473-480.

[28] J. Ryu, J. C. Gerdes, *Integrating inertial sensors with Global Positioning System for vehicle dynamics control.* Journal of Dynamic Systems, Measurement and Control, 2004. **126**: p. 243-254.

[29] D. M. Bevly, *Global Positionling System: A low-cost velocity sensor for correcting inertial sensor errors on ground vehicles.* Journal of Dynamic Systems, Measurement and Control, 2004. **126**: p. 255-264.

[30] R. White and M. Tomizuka, *Autonomous following lateral control of heavy vehicles using laser scanning radar.* Proceedings of the American Control Conference Arlington, 2001.

[31] M. Abe, Y. Kano, K. Suzuki, Y. Shibahata, Y. Furukawa, *Side-slip control to stabilize vehicle lateral motion by direct yaw momennt.* JSAE Review, 2001. **22**: p. 413-419.

[32] Y. Tan, A. Robotis, I. Kanellakopoulos, *Speed control experiments with an automated heavy vehicle.* IEEE, International Conference on Control Applications, 1999.

[33] X. Yang, S. Rakheja and I. Stiharu, *Identification of lateral dynamics and parameter estimation of heavy vehicles.* Mechanical Systems and Signal Processing, 1998. **12**(5): p. 611-626.

[34] M. Kosaka and H. Shibata, *An identification method with direct acquisition of reduced order model from a steplike response.* Transactions of the ASME 2004. **126**: p. 746-752.

[35] N. Ayland and P. Davies, *Automatic vehicle identification for heavy vehicle monitoring.*

[36] T. Legouis, A. Laneville, P. Bourassa and G. Payre, *Vehicle/pilot system analysis: A new approach using optimal control with delay.* Vehicle System Dynamics, 1987. **16**: p. 279-295.

[37] *http://www.zhongka.com/newsimg/8350-1.jpg.*

[38] Karnopp, D., *Vehicle Stability*, New York: Marcel Dekker 2001.

[39] M. Heinkenschloss and L. N. Vicente, *An interface between optimization and application for the numerical solution of optimal control problem.* ACM Transactions on Mathematical Software, 1999. **25**(2): p. 157-190.

[40] S. Nahar, S. Sahni and E. Shragowitz, *Simulated annealing and combinatorial optimization.* 23rd Design Automation Conference, 1986. **16.1**: p. 293.

[41] P. P. Mutalik, L. R. Knight, J. L. Blanton and R. L. Wainwright, *Solving combinatorial optimization problem using parallel simulated annealing and parallel genetic algorithms.* ACM 1992.

[42] P. Siarry, G. Berthiau, F. Durbin and J. Haussy, *Enhanced simulated annealing for globally minimizing functions of many continuous variables.* ACM Transactions on Mathematical Software, 1997. **23**(2): p. 209-228.

[43] G. Thomas , *Fundamentals of Vehicle dynamics.* Warrendale, Pa.: Society of Automotive Engineers, 1992.

[44] W. R. Garrott, *Closed loop automobile maneuvers using describing function models.* SAE paper 820360.

[45] J. C. Butcher, *The numerical analysis of ordinary differential equations.* 1987.

[46] M.Tai and M. Tomizuka, *Experimental study of lateral control of heavy vehicles for automated highway systems.* Proceedings of the American Control Conference, 2002.

[47] P. J. M. van Laarhoven and E. H. L. Aarts, *Simulated Annealing: Theory and Applications* , Kluwer Academic Publishers Group, 1988